Four component Ton-Complex in *Sphingobium fuliginis* ATCC 27551: Role of Organophosphate hydrolase in the transport of Ferric Enterobactin

Thesis submitted for the degree of Doctor of Philosophy

In

Animal Biology

By
Hari Parapatla
(13LAPH11)

Supervisor **Prof. S. Dayananda**



Department of Animal Biology School of Life Sciences University of Hyderabad Hyderabad – 500 046 INDIA 2020



University of Hyderabad (A Central University established in 1974 by an act of Parliament) Hyderabad – 500046, INDIA

CERTIFICATE

This is to certify that the thesis entitled "Four component Ton-Complex in Sphingobium fuliginis ATCC 27551: Role of Organophosphate hydrolase in the transport of Ferric Enterobactin" submitted by Mr. Hari Parapatla, bearing registration number 13LAPH11 in partial fulfillment of the requirements for award of Doctor of Philosophy in the Department of Animal Biology, School of Life Sciences is a bonafide work carried out by him under my supervision and guidance.

This thesis is free from plagiarism and has not been submitted previously in part or in full to this or any other University or Institution for award of any degree or diploma.

Publications

- 1. J. Biol. Chem. 291(14): 7774-7785 (2016) (PMID: 26861877)
- 2. FEMS Microbiol Lett. 2017;364(19) (PMID: 28957456).
- 3. Genome Biol Evol. 275; 77-81 (2016) (PMID: 28175269).

Further, the student has passed the following courses towards the fulfillment of course work required for the award of Ph.D

Course Code	Name	Credits	Pass/Fail
AS 801	Seminar 1	1	Pass
AS 802	Research Ethics & Management	2	Pass
AS 803	Biostatistics	2	Pass
AS 804	Analytical Techniques	3	Pass
AS 805	Lab Work	4	Pass

Research Supervisor

Head of the Department

Dean of the school



University of Hyderabad
(A Central University established in 1974 by an act of Parliament)
Hyderabad – 500046, INDIA

DECLARATION

This is to declare that the work embodied in this thesis entitled "Four component Ton-Complex in *Sphingobium fuliginis* ATCC 27551: Role of Organophosphate hydrolase in the transport of Ferric Enterobactin" has been carried out by me under the supervision of Prof. S. Dayananda, Department of Animal Biology, School of Life Sciences. The work presented in this thesis is a bonafide research work and has not been submitted for any degree or diploma in any other University or Institute. A report on plagiarism statistics from the University Librarian is enclosed.

Hari Parapatla (13LAPH11)

Prof. S. Dayananda (Research supervisor)

Date:

Acknowledgements

I express my deep sense of gratitude to my supervisor, **Prof. Dayananda Siddavattam**, for his guidance, suggestions, constant help and support scientifically and financially throughout the entire tenure of my research.

I thank my doctoral committee members Prof. S. Manjula Sritharan, Prof. Kota Arun Kumar for their critical assessment, discussions and advise during my research work.

I thank the current and former Deans, School of Life Sciences, Prof. S. Dayananda, Prof. K.V.A Ramaiah, Prof. Reddanna, and Prof. A.S Raghavendra, for providing all the facilities in the school.

I thank Prof. Anita Jagota, Head, Dept. of Animal Biology, and former Head's Prof. Jagan Pongubala, and Prof. B. Senthil kumaran for allowing me to use the Department facilities.

I would like to extend my sincere thanks to Prof. H.N Nagarajaram, Prof. Manjula sritharan and Prof. S. Rajagopal for their guidance in silico work, iron uptake study and Fluorescence emission spectroscopy analysis.

I would like to thanks to Dr. Arati Ramesh, Reader-F and her students from, NCBS, Bangalore, for allowing me to perform crystallization experiments in their laboratory and for making my stay at the laboratory a memorable one.

I am thankful to Dr. Rajan Sankaranarayanan, Group leader, CCMB for valuable suggestion and advise during my research work.

I specially thank Dr. Manjula Reddy, Principal Scientist, CCMB for providing Keio collection strain.

I thank the help and suggestions of all the faculty members in the School of Life Science, and for allowing me to use their laboratory facilities at different stages of my work.

I also extend my acknowledgements to late Prof. P. S. Sastry for his intellectual interactions and constant motivation.

I am thankful to Guru Prasad, Anirudh and Elsin Raju for helping me in bioinformatics, crystallization work and fluorescence emission spectroscopy analysis.

My research work would have not been complete without the never-ending help and valuable suggestions by my seniors Dr. Emmanuel Paul, Dr. Devi prasanna, Dr. Swetha kamireddy, Dr. Sujana, Dr. Sunil parthasarathy, Dr. Ashok Madikonda and Dr. Venkateshwar Reddy.

Huge thanks to my lab mates, Dr. Devyani, Dr. Ramurthy Gudla. Dr. Harshitha, Aparna, Annapoorni, Ganeshwari, Jay Prakash, Sandhya, Akbar, Thanu, sunil and project students for their support and enjoyable company.

Stay in the department was made fun and memorable by my friends Ananda Rao, Dr. Dhanunjay, Ramgopal Reddy, Ashok Kumar, Suresh Gandham, Krishna Nacharam, Dr. Sita Rami Reddy.

I specially thank Dr. Rajesh Kamindla, Dr. Vinod Kumar Chauhan, Dr. Y.N.G. Verma, Dr. Papa Rao, Dr. Maruthi, Dr. Rameshwar, Dr. Geethavani for their guidance and encouragement.

I specially thank Mr. Krishna, Mr. Rajendra Prasad and Mr. Upendra sir for technical help in the lab which helped me devote more time on research in the lab than with the paperwork.

Special thanks to all friends from the school of life sciences for their support in my research and for the numerous fun-filled discussions at the school canteen.

I am thankful to Dr. Praveen, Dr. Chenna Reddy, Mrs. Monika kannan, and Mrs. Kalpana for their help in SPR analysis and Ultracentrifugation at proteomics facilities.

I thank Mr. Jagan, Mr. Ankineedu, Mr. Gopi, Mr. Seenu, Mr. Mallesh, Mr. Rangaswamy, Mrs. Vijay Lakshmi and Mrs. Jyothi the office staff of Dept. of Animal Biology for always helping me with clerical work and help of all the non-teaching staff is greatly acknowledged.

The financial support provided by BBL Fellowship, DST-SERB, and CSIR is greatly acknowledged.

I thank DBT, ICMR, UGC, UPE-II, UGC-SAP and DBT-CREBB, Aurobindo pharma and Biological E limited, for providing financial support to lab and for the infrastructural facility of the school.

I am grateful for my parents Sri. Ramana Parapatla, Smt. Narasamma Parapatla, my sister Mrs. Saraswathi Parapatla, my brother and sister in law Mr. and Mrs. Haritha Ramesh. P for their love, help, caring, affection and inspiring me to carry out my studies.

I am grateful to my wife K. Vijaya Durga for her support, patience and Love.

I thank Almighty for filling my life with such wonderful people around and also for giving me the patience needed to endure every difficulty encountered.

DEDICATED TO MY PARENTS & MY SISTER

Table of Contents

1 Introduction	1-13
1.1 Organophosphate hydrolase (OPH)	1
1.2 Evolution of OPH	2
1.3 OPH is a Tat substrate	3
1.4 Tat substrates	5
1.5 OPH is a Lipoprotein	6
1.6 OPH exists as part of multiprotein complex.	6
1.7 Outer membrane transport components interact with OPH	8
1.8 TonB-Dependent Transport (TonBDT) system	9
1.9 Outer membrane transporter (TBDT)	9
1.10 The Ton Complex	10
1.11 Siderophores: Chemistry and Biology	11
1.12. Objectives	14
2 General Materials and Methods	
2.1 Antibiotic and Chemical stock solutions	
2.2 Growth Media	
2.2.1 Luria-Bertani (LB) medium	
2.2.2 Terrific broth (TB) medium	
2.3 Preparation of iron-free media and solutions	
2.4 Solutions & buffer for DNA modifications	21
2.5 Agarose gel electrophoresis	
2.6 Plasmid isolation by alkaline lysis method	
2.7 DNA Quantification	23
2.8 Polymerase Chain Reaction (PCR)	23
2.9 Site-Directed Mutagenesis	
2.10 Restriction digestion of a DNA molecule	24
2.11 DNA ligation	24
2.12 Preparation of competent cells	24
2.13 Bacterial Transformation	25
2.14 Protein Methods	25
2.14.1 Solutions for SDS-Polyacrylamide gel electrophoresis	25

2.14.2 Solutions used for Western blotting	27
2.14.3 Solutions for Protein Estimation	27
2.15 Protein estimation by Bradford's method	27
2.16 Polyacrylamide gel electrophoresis	28
2.17 Semi-dry western blotting	29
2.18 Subcellular fractionation	30
2.19 Enzyme assays and preparation of reagents	30
2.19.1 Reagents for Glucose-6-phosphate dehydrogenase assay	30
2.19.2 Reagents for Nitrate reductase assay	31
2.19.3 Reagents for Methyl parathion activity	31
2.20 Glucose-6-phosphate dehydrogenase (G6PD)-Cytoplasmic marker	31
2.21 Nitrate Reductase-Membrane enzyme	32
2.22 Parathion Hydrolase Assay	32
2. Charatan I. Ouranan harribata badanlara and Entanabantin international	24.40
3. Chapter I. Organophosphate hydrolase and Enterobactin interactions	
3.1 Objective Specific Methodology	
3.1.1 Expression and Purification of mature form of OPH (mOPH)	
3.1.2 Expression and purification of moral	
3.1.4 Preparation of enterobactin (Ent) solution	
3.1.5 Thin Layer Chromatography (TLC)	
3.1.6 High-Performance Liquid Chromatography (HPLC) analysis	
3.1.7 Blue Native –PAGE (BN-PAGE)	
3.1.8 Surface Plasmon Resonance (SPR) Analysis	
3.1.9 Fluorescence emission measurements	
3.2 Results and Discussion	
3.2.1 Expression and purification of mOPH	
3.2.2 Ent hydrolase activity	
3.2.3 HPLC analysis of Ent incubated with OPH	
3.2.4 OPH-Ent interactions	
3.2.5 Native PAGE	
3.2.6 OPH interacts with enterobactin.	
3.2.7 OPH interacts strongly with Ferric Enterobactin (Fe-Ent)	
3.2.8 Measurement of Fluorescence Emission Maximum	
1/10404101110111 Of 1 140100001100 L/HH0010H 1/14ΛHH4HH	,,,,,,,,,,,,,,,,,,,, ,,,,,,,,,,,,,,,,

3.3 Discussion	46
4. Chapter II. Identification of Enterobactin binding site in OPH	50-70
4.1 Objective Specific Methodology	50
4.1.1 Generation of OPH variants	50
4.1.2 Site-Directed Mutagenesis (SDM)	52
4.1.3 Generation of expression plasmid pMD301A	52
4.1.4 Generation of expression plasmid pMD301N	53
4.1.5 Generation of expression plasmid pMK82A	53
4.1.6 Expression of OPH variants	53
4.1.7 Measurement of Triesterase Activity	54
4.1.8 Purification of OPH variants	54
4.1.9 Circular Dichroism (CD) Spectroscopy	54
4.1.10 Fluorescence emission measurements	55
4.2 Identification of Ent/Fe-Ent binding site- in silico predictions	55
4.2.1 Prediction and investigation of a potential secondary binding site	55
4.3 Results and Discussion	55
4.3.1 OPH with reduced active site volume (OPHD301N)	56
4.3.2 Purification of OPH variant (OPH ^{D301N})	57
4.3.3 OPH ^{D301N} retains native conformation	58
4.3.4 OPH with increased active site volume (OPHD301A)	59
4.3.5 Purification of OPH variant (OPH ^{D301A})	60
4.3.6 Structural stability of OPH ^{D301A}	61
4.3.7 Ent/Fe-Ent binding ability is independent of triesterase activity	62
4.3.8 Measurement of Fluorescence Emission Maximum	63
4.4 In silico prediction of Ent binding site	64
4.4.1 OPH variant OPH ^{K82A} retains native structure and triesterase activity	65
4.4.2 Purification of OPH ^{K82A}	66
4.4.3 Lysine residue is critical for interacting with Fe-Ent	68
4.5 Discussion	69
5 Chapter III. Role of triesterase and Ent binding activities of OPH in iron upt	ake.71-90
5.1 Objective Specific Methodology	71
5.1.1 Interactions of OPH variants with ExbD-Pull-down assays	73

5.1.2 Generation of preOPH variants	73
5.1.3 Generation of expression plasmid pPD301A	74
5.1.4 Generation of expression plasmid pPD301N	74
5.1.5 Generation of expression plasmid pPK82A	75
5.2 Expression of OPH variants	75
5.2.1 Co-expression of preOPHD301A and ExbDN6xHis and subcellular localization	ion of
preOPHD301A	75
5.2.2 Co-expression of preOPHD301N and ExbDN6xHis and subcellular localizate	tion of
preOPH ^{D301N}	75
5.2.3 Co-expression of preOPH ^{K82A} and ExbD ^{N6xHis} and subcellular localization	on of
preOPH ^{K82A}	76
5.3 Reconstitution of SyTonBDT system with OPH variants	76
5.3.1 Preparation of ⁵⁵ Fe-enterobactin	77
5.3.2 Uptake of ⁵⁵ Fe-enterobactin	77
5.4 Results and Discussion	78
5.4.1 OPH variant OPH ^{D301A} interacts with ExbD	78
5.4.2 OPH variant OPH ^{D301N} interacts with ExbD	79
5.4.3 Generation of OPH variants with signal sequence (preOPHD301A and	
preOPH ^{D301N})	80
5.4.4 OPH variants targets to the membrane in the presence of ExbD	81
5.4.5 OPH ^{K82A} fails to interact with ExbD	82
5.4.6 The preOPH ^{K82A} retains native structure and triesterase activity	83
5.4.7 preOPH ^{K82A} fails to target to the membrane	84
5.5 Both triesterase and Ent binding activities are critical for increased iron upta	ıke85
5.6 The <i>opd</i> negative mutants of <i>S. wildii</i> show retarded growth in iron limiting	medium 87
5.7 Discussion	88
6. Conclusions	91-92
7. References	93-104
8. Publications	
9 Anti-Plagiarism Cartificata	

Abbreviations

ATCC : American type culture collection

°C : Degrees Celsius

CD : Circular dichroism

DDM : n-dodecyl-β-D maltoside

dNTP : deoxynucleoside triphosphate

DSS : Disuccinimidyl suberate

Ent : Enterobactin

Fe-Ent : Ferric-enterobactin

gm : gram h : hour

IPTG : Isopropyl β-D-1-thiogalactopyranoside

Kb : Kilobase

kDa : kilo Dalton

μM : Micro molar

M : Molar

mOPH : mature form of OPH

MP : Methyl Parathion

OP : Organophosphate

OPH : Organophosphate hydrolase

PCR : Polymerase Chain Reaction

PMF : Proton Motive Force

PTE : Phosphotriesterase

RT : Room temperature

SDM : Site-Directed Mutagenesis

SPR : Surface plasmon resonance

Sec : Secretory

SfTonBDT : Sphingobium fuliginis TonB dependent Transport System

TonBDT : TonB dependent transport system

SRP : Signal Recognition Particle

Tat : Twin Arginine Translocase

TBDT : TonB dependent transporter

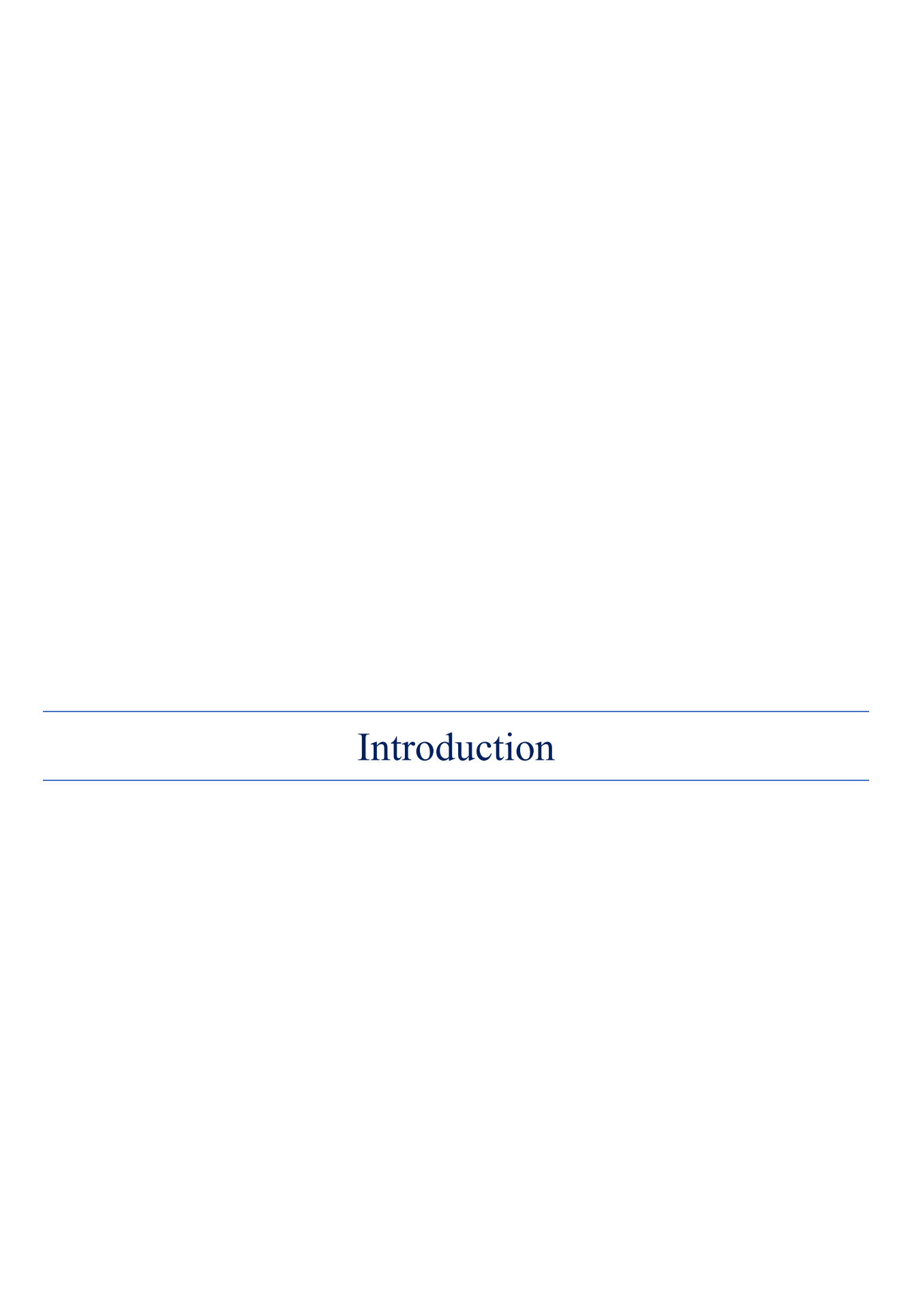
List of Tables

		Page No.
Table 2. 1	List of Antibiotics	15
Table 2. 2	List of Chemicals	15
Table 2. 3	List of Resins used in this study	17
Table 2. 4	List of Restriction endonucleases and DNA modifying enzymes	17
Table 2. 5	Standard PCR cycling conditions	23
Table 2. 6	Resolving gel composition for the SDS-PAGE	28
Table 2. 7	Stacking gel composition for the SDS-PAGE	29
Table 3.1	The association and dissociation constants of OPH with Ent and	46
	Fe-Ent	
Table 4. 1	Primers used in chapter II	51
Table 4. 2	Plasmids used in chapter II	51
Table 4. 3	Strains used in chapter II	52
Table 4. 4	The association and dissociation constants of OPH ^{D301A} and	64
	OPH ^{D301N} with Fe-Ent	
Table 5. 1	Plasmids used in chapter III	71
Table 5. 2	Strains used in chapter III	72
Table 5. 3	Primers used in chapter III	72

List of Figures

Fig 1. 1	Crystal structure of Organophosphate hydrolase (OPH)	2
Fig 1. 2	Schematic representation showing various stages involved in membrane	
	transport of Tat substrates	5
Fig 1. 3	The signal peptide sequence of OPH	6
Fig 1. 4	Affinity purification of OPH complex	7
Fig 1. 5	Tricine-PAGE analysis of OPH-complex	8
Fig 1. 6	Structural organization of outer membrane transporter (TBDT)	10
Fig 1. 7	Model showing the transport of vitamin B ₁₂ via TonB-dependent transport	
	system	11
Fig 1. 8	Classical nature of different siderophores and their natural producers	12
Fig 3. 1	SPR-analysis	39
Fig 3. 2	Purification of mOPH	40
Fig 3. 3	Thin Layer Chromatography (TLC) analysis of Ent hydrolase activity	41
Fig 3. 4	HPLC analysis of Ent incubated with OPH	42
Fig 3. 5	OPH-Ent interactions	43
Fig 3. 6	SPR analysis of OPH-Ent interactions	44
Fig 3. 7	SPR analysis of OPH and Fe-Ent interactions	45
Fig 3. 8	Fluorescence emission spectra of OPH with enterobactin/ferric-	
	enterobactin	46
Fig 3. 9	Structural basis for natural lactonase and promiscuous	
	phosphotriesterase activity	47
Fig 3. 10	Structures of enterobactin and its ferric complex	49
Fig 4. 1	Schematic diagram showing alteration of active site architecture by	
	substituting active site aspartate with alanine and asparagine	56
Fig 4. 2	Generation of OPH variant OPH ^{D301N}	57
Fig 4. 3	Purification of OPH ^{D301N}	58
Fig 4. 4	CD spectroscopy of OPH and OPH ^{D301N}	59
Fig 4. 5	Generation OPH ^{D301A}	60
Fig 4. 6	Purification of OPH ^{D301A}	61
Fig 4. 7	CD spectroscopy of OPH and OPH ^{D301A}	62
Fig 4. 8	OPH ^{D301A} and Fe-Ent interactions	62

Fig 4. 9	OPH ^{D301N} and Fe-Ent interactions	63
Fig 4. 10	Fluorescence emission spectra of OPH variants OPH ^{D301A} and OPH ^{D301N}	64
	with ferric-enterobactin	
Fig 4. 11	The Fe-Ent binding site in OPH	65
Fig 4. 12	Generation of OPH ^{K82A}	66
Fig 4. 13	Purification of OPH ^{K82A}	67
Fig 4. 14	CD spectroscopy of OPH and OPH ^{K82A}	68
Fig 4. 15	OPH ^{K82A} -Fe-Ent interactions	69
Fig 5. 1	Interactions between OPH ^{D301A} and ExbD ^{N6xHis}	79
Fig 5. 2	Interactions between OPH ^{D301N} and ExbD ^{N6xHis}	80
Fig 5. 3	Generation of preOPH variants preOPH ^{D301A} and preOPH ^{D301N}	81
Fig 5. 4	Membrane localization of OPH variants (preOPHD301A and preOPHD301N)	82
Fig 5. 5	Interactions between OPH ^{K82A} and ExbD ^{N6xHis}	83
Fig 5. 6	Generation of preOPH ^{K82A}	84
Fig 5. 7	Membrane localization of preOPH ^{K82A}	85
Fig 5. 8	Shows growth of E. coli GS27 cells complemented with sfTonBDT system	
	reconstituted with OPH and its variants under iron limiting conditions	86
Fig 5. 9	Iron Uptake	87
Fig 5. 10	Growth curve and uptake of ⁵⁵ Fe by <i>S. wildii</i> cells	88
Fig 5. 11	Ferric-enterobactin structure and its coordination shift from catecholate to	89
	salicylate	
Fig 5. 12	Proposed model showing the role of OPH in protonation of Fe-Ent	90



1. Introduction

1.1 Organophosphate hydrolase (OPH)

Organophosphate hydrolases (OPHs), also known as phosphotriesterases (PTEs), are initially identified in soil bacteria, isolated from agricultural soils polluted with organophosphate insecticides (Sethunathan and Yoshida, 1973; Munnecke and Hsieh, 1974; Serdar et al., 1982; Chaudhry et al., 1988; Mulbry and Karns, 1989a & Somara and Siddavattam, 1995). They hydrolyze third ester linkage found in a wide range of organophosphate (OP) compounds and nerve agents (Dumas et al., 1989, 1990). Although OPH exists in a number of soil bacteria, much of the information pertaining to its structure and catalytic properties came from the OPH purified from Brevundimonas diminuta MG and Flavobacterium sp. ATCC 27551, the soil isolates recently reclassified as Sphingopyxix wildii (Parthasarathy et al., 2016) and Sphingobium fuliginis ATCC 27551 (Kawahara et al., 2010). Both of them contain identical OPH coding organophosphate degradation (opd) genes on a large, self-transmissible indigenous plasmids. Interestingly, despite of having identical opd genes, these native plasmids shared no homology outside opd region. Subsequent studies have shown that this conserved region containing opd gene has structural features of a complex transposon (Siddavattam et al., 2003). Genome sequences are available for these two OP degrading soil bacteria. The genome sequences and experimental evidences gathered using the indigenous plasmids of these soil isolates delineated their role in lateral mobility of opd genes among soil bacteria (Pandeeti et al., 2012; Parthasarathy et al., 2017; Azam et al., 2019 & Siddavattam et al., 2019).

Membrane associated OPH is a homo-dimeric metallo-protein, and each monomer contains an active site with two zinc ions (Omburo et at., 1992; Benning et al., 1994). High resolution X-ray structure showed each subunit of dimer folds into a TIM barrel, with 8 strands of parallel β-sheet (Benning et al, 2000). The conserved histidines (His 55, His 57, His 201, and His 230) and aspartate (Asp 301), serve as ligands to keep the bivalent metal ions together (Fig. 1.1. Panel B) (Benning et al., 2001). The two zinc metal ions are separated by ~ 3.4 Å and bridged together via a carbamylate functional group of Lys 169, and hydroxide ion from the solvent (Fig. 1.1. Panel B). Though Zn²⁺ ions serve as natural cofactors at active site of protein, it can be replaced with 2 equivalents of Co²⁺, Mn²⁺, Ni²⁺, or Cd²⁺ ions without affecting the catalytic properties of the enzyme (Omburo et al., 1992).

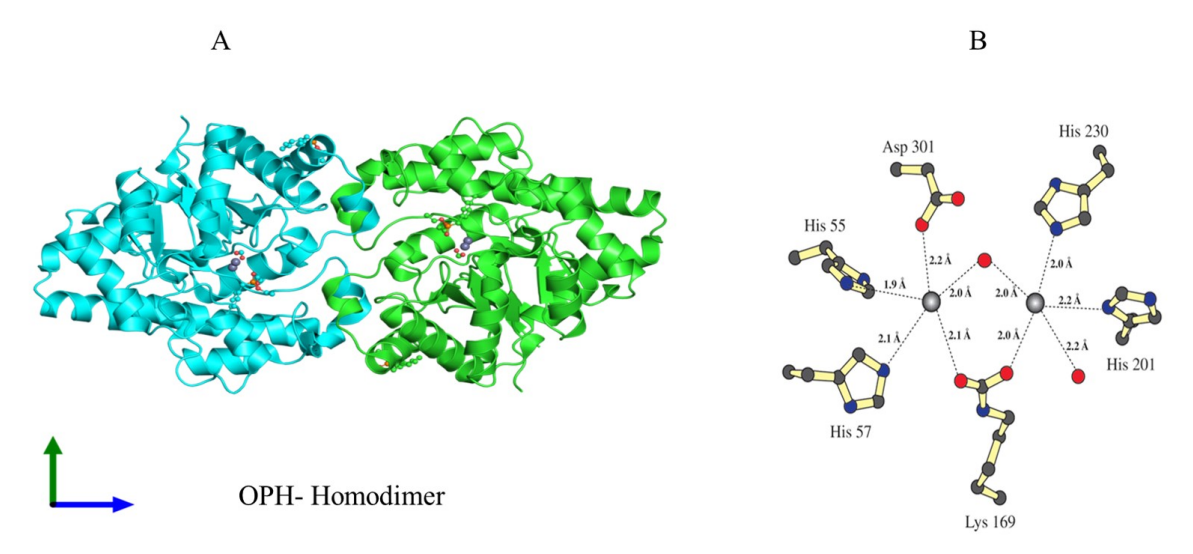


Fig. 1.1 Panel A shows the ribbon diagram for the homodimer structure of organophosphate hydrolase from *pseudomonas diminuta*. Panel B shows the close-up view of the active site region of the Zn²⁺/Zn²⁺ containing enzyme (the crystal structure is taken from Benning et al., 2001).

1.2 Evolution of OPH

OPH hydrolyzes a broad range of OP compounds (LeJeune et al., 1998; Prokop et al., 2006; Singh and Walker, 2006; Karpouzas and Singh, 2006; Theriot and Grunden, 2011 & Bigley and Raushel, 2013). It catalyzes some of them with a rate that matched close to substrate diffusion limit (Dumas et al., 1989; Omburo et al., 1992). OP compounds are aliens to soil bacteria, for that matter to the natural ecosystem (Singh et al., 1999; Raushel and Holden, 2000 & Singh, 2009). They are synthesized during second world war and released as insecticides only in 1950s as substitutes to more persistent organochloride insecticides (Singh et al., 1999; Raushel and Holden, 2000; Singh and Walker, 2006 & Singh, 2009). Prior to 1950s there is no scope for the soil microbial enzymes to have access to these compounds. Existence of an enzyme like OPH with such precision and speed in catalysis attracted the attention of biochemists working on evolution of new catalytic activities.

Promiscuous activities of enzymes have been proposed to play a key role in the evolution of enzymatic activities. It provides a starting point for evolution of novel activities (James and Tawfik, 2001). OPH homologues are classified into three groups based on the structural differences in the loops (1, 7 and 8) involved in substrate binding sites (Parthasarathy et al., 2017). The first group, designated as phosphotriesterases (PTE), show more than 86 % identity to PTE isolated from *B. diminuta*. The *EcPTE* (*E. coli*-Phosphotriesterase) is in the second group of OPH homologues, they contain shorter substrate binding loops. The third group of enzymes have one loop (loop 7) shorter than PTE. The PTE family shows less than 35 % homology to the second and third classes. These proteins annotated as putative parathion

hydrolase (PPH) in the database, include PPH from *M. tuberculosis*, Acyl homoserine lactonase (AhlA) from *R. erythropolis*, and SsoPox of *Sulfolobus solfataricus* and have been characterized as phosphotriesterase-like lactonases (PLLs) (Afriat et al., 2006), essentially based on their fairly limited homology to _{Bd}PTE (*B. diminuta*-Phosphotriesterase). OPH shows structural similarities with quorum quenching lactonases, involved in hydrolysis of quorum sensing signaling molecules like homoserine lactone (Afriat et al., 2006). Considering these structural similarities, the quorum quenching lactonases are designated as phosphotriesterase like lactonases (PLL). Although structural similarities are apparent between these two molecules, there exists difference in substrate-binding loop, and it is in fact the main structural difference between phosphotriesterases (PTEs) and phosphotriesterase-like lactonases (PLLs) (Afriat et al., 2006). In addition to the structural similarities these two enzymes show existence of reciprocal promiscuity, the OPH has weak lactonase activity, likewise the PLLs show weak triesterase activity (Afriat et al., 2006; Elias and Tawfik, 2012). Considering structural and functional similarities, the lactonases are considered as progenitors of organophosphate hydrolases (Afriat et al., 2006; Afriat et al., 2012 & Elias and Tawfik, 2012).

1.3 OPH is a Tat substrate

As stated before, the OPH is a membrane associated protein (Gorla et al., 2009). It contains 24 amino acids long signal peptide which is unique in a number of ways. It contains a Twin Arginine Transport (TAT) motif with a consensus sequences of MQTRRVVLK at the N-terminus (Gorla et al., 2009). It also contains a lipobox (LAGC) motif at the signal peptidase cleavage site (Parthasarathy et al., 2016). The TAT motif is an absolute requirement for OPH to target membrane (Gorla et al., 2009). Amino acid substitutions of invariant arginine residues found in the TAT motif (TRRVVL) affected the processing and membrane localization of OPH (Gorla et al., 2009). The Tat (twin-arginine translocation) pathway itself is unique in number of ways. It is the only transport machinery available in gram-negative bacteria for transporting/targeting prefolded proteins across the membrane (Berks et al., 2003; Palmer and Berks, 2012 & Berks, 2015). Originally it is discovered in plants, especially in nuclear encoded proteins targeting to subcellular organelles (Mould and Robinson, 1991; Chaddock et al., 1995; Creighton et al., 1995; Berks, 1996 & Weiner et al., 1998) and subsequently its presence is identified in bacteria and archaea (Mori et al., 2001 & Muller and Klosgnn, 2005). Unlike in Sec pathway, where the unfolded proteins pass through a SecY/E (Wickner et al., 1991; Keyzer et al., 2003 & Osborne et al., 2005), the TAT pathway translocates or targets across/into the membrane only fully folded proteins (Berks et al., 1996). The TAT pathway contains three

significant proteins encoded by an operon called *tat* operon, *tatABC* (Berks, 1996; Robinson and Bolhuis, 2004; Berks et al., 2005; Strauch and Georgiou, 2007 & Palmer and Berks 2012).

The TatA is the most abundant protein of all Tat-translocases and is roughly found 20 times more copious than TatB and TatC (Sargent et al., 2001; Jack et al., 2001). TatA is a 9.6 kDa polypeptide with 89 amino acids and has a structure similar to TatB, with a hydrophobic α -helix towards N-terminal followed by a short hinge region and a longer amphipathic α -helix region (Leeuw et al., 2001; Hu et al., 2010). The TatA forms tetrameric homo-oligomers in the cytoplasmic membrane producing an intramolecular pore (Alami et al., 2003). TatB is a 18.5 kDa protein and it is important for the transport of endogenous substrates in E. coli (Sargent et al., 1999). TatC is the largest and most highly conserved Tat system component in bacteria and chloroplasts and it having 258 amino acids with a molecular mass of 29kDa (Bogsch et al., 1998). As predicted by its secondary structure, this protein contains six trans membrane helices, possessing an N-in C-in topology (Punginelli et al., 2007) and it forms an initial complex which recognizes the Tat substrates (Eijlander et al., 2009). Initially, the recognition of the cognate substrate by the SRP bound to the RR motif is initiated by the TatC protein. The TatB and TatC then form an initial association complex with several copies of each of the constituent subunits (Orriss et al., 2007). Subsequently, the TatBC complex in association with TatA makes the active translocation site (Oates et al., 2005; Barrett and Robinson 2005). In Tat system, the homo-oligomeric ring-like structures are comprising of TatA forms the protein translocating channels (Fig. 1.2). The proton motive force generated across the membrane drives the transport prefaded proteins (Delisa et al., 2002). Finally, as a result of a series of co-ordinated events, the prefolded proteins successfully translocate to the periplasmic compartment (Berks, 1996; Berks et al., 2003, 2005; Lee et al., 2006 & Palmer and Berks 2012).

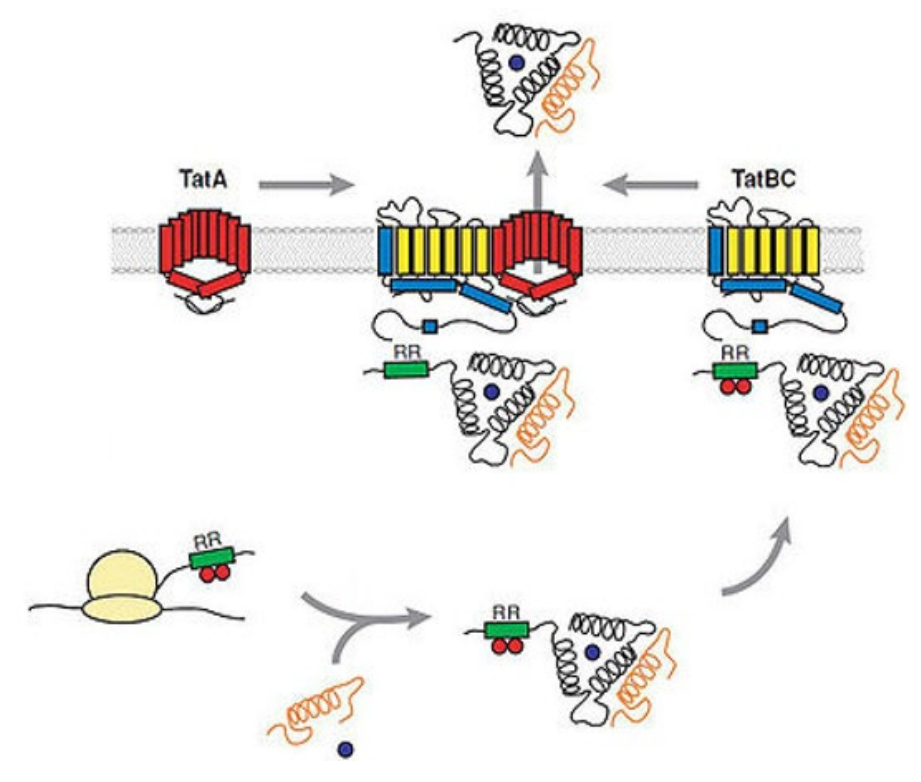


Fig. 1.2: Schematic representation showing various stages involved in membrane transport/targeting of Tat substrates in *E. coli* (Philip et al., 2006).

1.4 Tat substrates

The novelty of the Tat pathway is its ability to transport fully folded proteins and the proteins with a consensus twin arginine (S/TRRxFLK) invariant motif in its signal peptides (Berk et al., 2005). Before export, the bacterial Tat substrates interact with cofactors like FAD, NADP, molybdopterin, iron-nickel and iron-sulphur clusters, coppers and others and acquire active conformation before translocating across /targeting the inner membrane (Berks, 1996; Berks et al., 2003, Berk et al., 2005 & Palmer and Berks, 2012).

Three types of proteins follow Tat pathway to target /translocate across the membrane. The first group belongs to proteins that requires a large cofactor for activity. As the required large cofactors fail to cross the inner membrane, the active protein with the cofactor is formed in the cytoplasm before translocating/targeting the cytoplasmic membrane (Berks, 1996 & Palmer et al., 2005), (2) it transport hetero-oligomeric protein complexes, that acquire folded confirmation while still in the cytoplasm (Berks et al., 2003; Palmer and Berks, 2012), (3) The Tat pathway also facilitates transport of folded proteins across the membrane in the halophilic archaea, as their folding is affected in unfavourable extracellular environments (Rose et al., 2002; Bolhuis, 2002 & Pohlschroder et al., 2004).

1.5 OPH is a Lipoprotein

As stated before, the OPH has a 24 amino acids long TAT specific signal peptide. Our lab has also shown existence of lipo-box motif with an invariant cysteine residue generally seen in membrane anchored proteins in the signal peptide of OPH (Fig. 1.3). Our previous studies have shown requirement of this invariant cysteine for membrane anchoring of OPH. Substitutions of this invariant cysteine residue with serine facilitated translocation of otherwise inner membrane anchored OPH into periplasmic space (Parthasarathy et al., 2016). A diacyl glycerol moiety linked to invariant cysteine residues helps OPH to anchor the inner membrane of OPH (Parthasarathy et al., 2016). The PEG-Mal (methoxypolyethylene glycol maleimide) labelling experiments have revealed existence of entire OPH in the periplasmic space of the inner membrane (Parthasarathy et al., 2017).

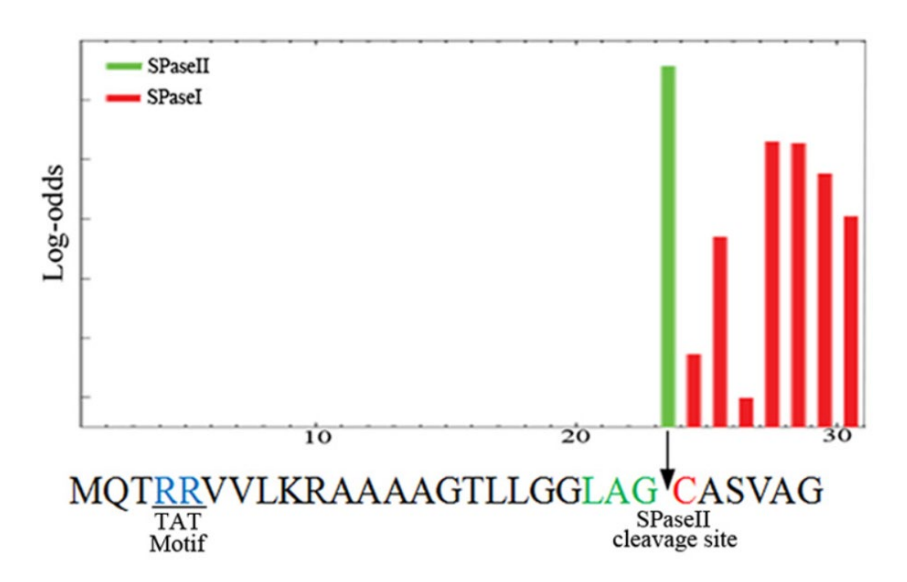


Fig. 1.3: The signal peptide sequence of OPH. The green bar indicates the predicted SPaseII cleavage site, lipobox (green letters), and the invariant cysteine residue (red letter) found at the junction of the SPaseII cleavage site are shown. The red bar indicates the potential SPaseI cleavage sites. The twin arginines of the Tat signal peptide are underlined (blue letters) (Parthasarathy et al., 2016).

1.6 OPH exists as part of multiprotein complex

Previously our laboratory has purified OPH complex by using the Ni-charged immobilized metal affinity chromatography (IMAC). The membrane isolated from *B. diminuta* DS010 (pOPH141HIS) cells coding OPH^{10xHis} (created by introducing an internal His10 tag at the loop region of OPH), were detergent solubilized and the soluble protein complexes were then passed through IMAC. The affinity purified OPH^{10xHis} complex was subjected to gel filtration and BN-PAGE (Fig. 1.4. Panel A & Panel B). Both the techniques have shown existence of OPH as part of the protein complex with a molecular mass of around 294 kDa

(Parthasarathy et al., 2016). This was the first study that indicated existence of OPH as membrane associated multi-protein complex. Therefore, an independent study was performed to obtain supporting evidence by following immune-purification using anti-OPH antibody cross-linked protein A/G-agarose beads. The membranes isolated from the formaldehyde cross-linked *B. diminuta* wild type and *B. diminuta* DS010 (pOPH141HIS) cells were extracted with chloroform: methanol (1:3) to delipidate the sample. The delipidated membrane proteins were then resolubilized and used to purify by OPH immune-affinity column (Fig. 1.4. Panel C). and nickel-affinity column (Fig. 1.4. Panel C). Again, these two independent techniques have shown existence of OPH as part of multiprotein complex (Parthasarathy et al., 2016). The mass spectrometry (LTQ-Orbitrap XL ETD mass spectrometer) data of affinity purified OPH complexes showed the OPH interacting proteins belong to efflux pump components AcrB and TolC and subunits of the F_1F_0 -ATP synthase (α , β , γ). The phosphate ABC transporter substrate-binding protein (PstS) was also found among the OPH interacting proteins (Parthasarathy et al., 2016).

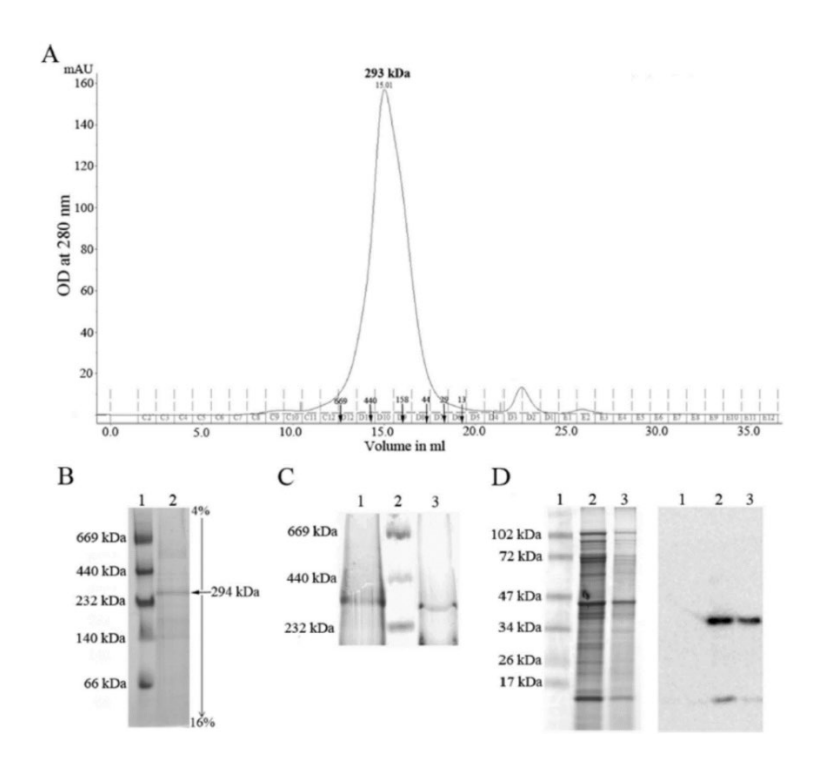


Fig. 1.4: Affinity purification of OPH complex. Panel A shows the molecular mass determination of OPH complex using gel filtration chromatography. The native mass determined by using BN-PAGE, is shown in panel B. The affinity purified OPH complex using anti-OPH antibody column (Lane 1) and metal ion (Lane 3) chromatography were analyzed on BN-PAGE (4–16% acrylamide) to gain better comparison of molecular mass is shown in panel C. Resolution of IMAC (Lane 3) and anti-OPH antibody column (Lane 1) purified OPH complex on SDS-PAGE and its corresponding western blots developed using anti-OPH antibodies is shown in Panel D. Reproduced from the published work done in our laboratory (Parthasarathy et al., 2016).

1.7 Outer membrane transport components interact with OPH.

Further studies performed to identify OPH interacting proteins revealed interesting aspects and played a key role in suggesting a physiological role to OPH. The outer membrane transport components, otherwise known as TonB dependent Transport (TonBDT) system components got co-purified along with OPH. In fact, the TonB dependent transporter (TonR), energy transducing component (TonB), proton motive force (PMF) components (ExbB/ExbD) and outer membrane component OmpW were among the OPH co-purified proteins (Gudla et al., 2019). Out of these copurified proteins (Fig. 1.5), OPH physically interacted with TonB and ExbD to form a four component Ton-complex (Gudla et al., 2019). In fact, formation of a cytoplasmic complex involving OPH and energy producing PMF components ExbB/ExbD is a prerequisite for membrane targeting of OPH. In the absence of ExbB/ExbD the heterologously expressed OPH remained in cytoplasm in *E. coli*. Such physical interactions with TonBDT system components suggest a role for OPH in outer membrane transport.

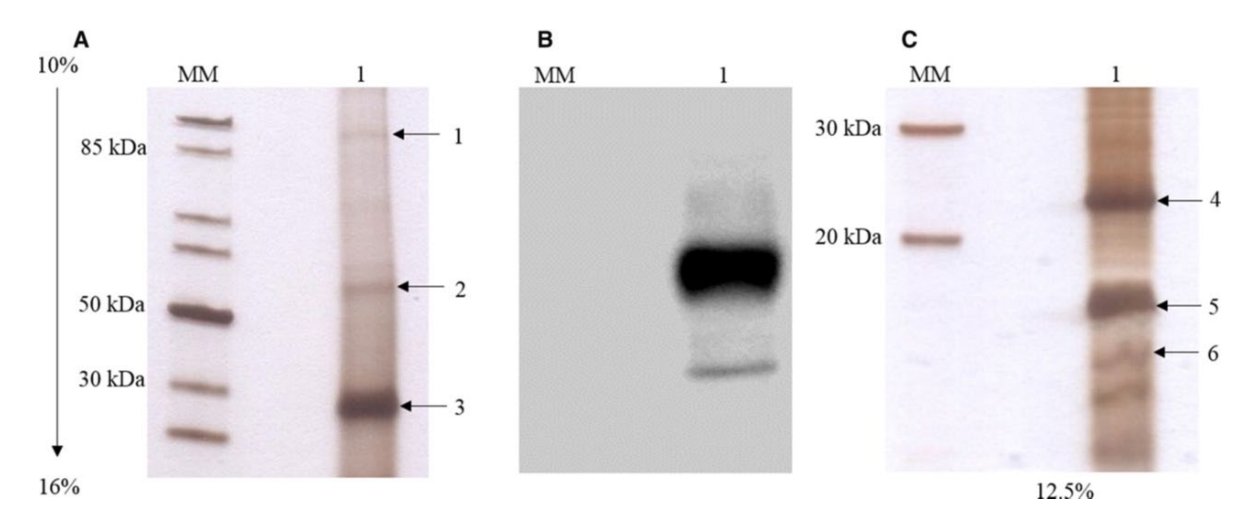


Fig. 1.5: Represents Tricine-PAGE analysis of OPH-complex. Panels A and C shows the profile of OPH-associated proteins obtained on Tricine PAGE. Lane 1, immune-purified OPH complex. The independent protein bands resolved on tricine PAGE (Panel A, C) were identified as TonR (band 1), TonB (band 3), ExbB (band 4), outer membrane porin, OmpW (band 5) and ExbD (band 6). Panel B shows the cross-reaction of a 52 kDa protein (band 2) with OPH-specific antibodies. The figure is reproduced from the work done in our laboratory (Gudla et al., 2019).

1.8 TonB-Dependent Transport (TonBDT) system

All Gram-negative bacteria contain an outer membrane (OM) and existence of such barrier is considered advantageous to the cell (Ferguson and Deisenhofer, 2004; Wiener, 2005; Schauer et al., 2008 & Noinaj et al., 2010). The outer membrane is an asymmetric lipid bilayer with an outer leaflet containing of lipid-anchored oligosaccharides, and a lower leaflet of phospholipids (Postle and Larsen, 2007). It provides the diffusion barrier and restricts the

passage of lipophilic toxins permeable in a typical membrane, yet the outer membrane still permits the small hydrophilic nutrients and allows the solutes of molecular mass ~600 Da or lower via passive diffusion through transmembrane porins (Wiener, 2005; Postle and Larsen, 2007 & Noinaj et al., 2010). The main disadvantage of outer membrane of Gram-negative bacteria is that it doesn't have any known source of energy. In order to overcome this problem, Gram negative bacteria have developed a mechanism to harness energy generated by the inner membrane localized proton motive force (PMF). The energy thus harnessed is transduced to the outer membrane localized transporter known as TonB dependent transporter (TBDT). (Krewulak and Vogal, 2011; Noinaj et al., 2010). Therefore, the outer membrane transport system contains two components, the outer membrane located TonB dependent transporter (TBDT) and the inner membrane associated Ton-complex. The entire transport system is designated as TonB Dependent Transport (TonBDT) system. The Ton-complex is formed by the three integral polytopic proteins present in the inner membrane: PMF components ExbB/ExbD and energy transducer TonB (Celia et al., 2016). The ExbB is unstable in absence of ExbD (Held and Postle, 2002). There are about five copies of ExbB proteins in a Ton Complex (Higgs et al., 2002). It contains three transmembrane spanning helices with a large cytoplasmic domain. About two copies of ExbD and one copy of TonB exists in Ton complex (Celia et al., 2016). The ExbB/ExbD complex generate energy via proton motive force. The generated energy is then transduced to TonB dependent transporter (TBDT) through TonB. The carboxy-terminal domain of energized TonB (amino acids 103-239) interacts with OM transporter, TBDT (Sean et al., 2005). Upon ligand binding to the TBDT, the TonB-box of the TBDT gets exposed to periplasmic space facilitating its interaction with TonB. Such interaction leads to conformational changes in TBDT and facilitates the release of substrate into periplasmic space (Wiener, 2005).

1.9 Outer membrane transporter (TBDT)

As stated, before the TonBDT system contains an inner membrane associated PMF components ExbB/ExbD and an energy transducer TonB and outer membrane transporter, TBDT. The outer membrane transporter, TBDT has a unique structural feature. It contains a C-terminal membrane-spanning barrel domain with 22 antiparallel β-strands and is bigger than the barrel domain of porins (Krewulak and Vogel, 2008). The N-terminal region of TBDT contains a plug domain, which blocks the barrel and stops the passage of solutes. It also interacts with inner membrane-localized energy transducer, TonB through an eight-amino acid sequence

motif called as the 'TonB box'. These interactions are indeed critical for facilitating the solute bound to the transporter.

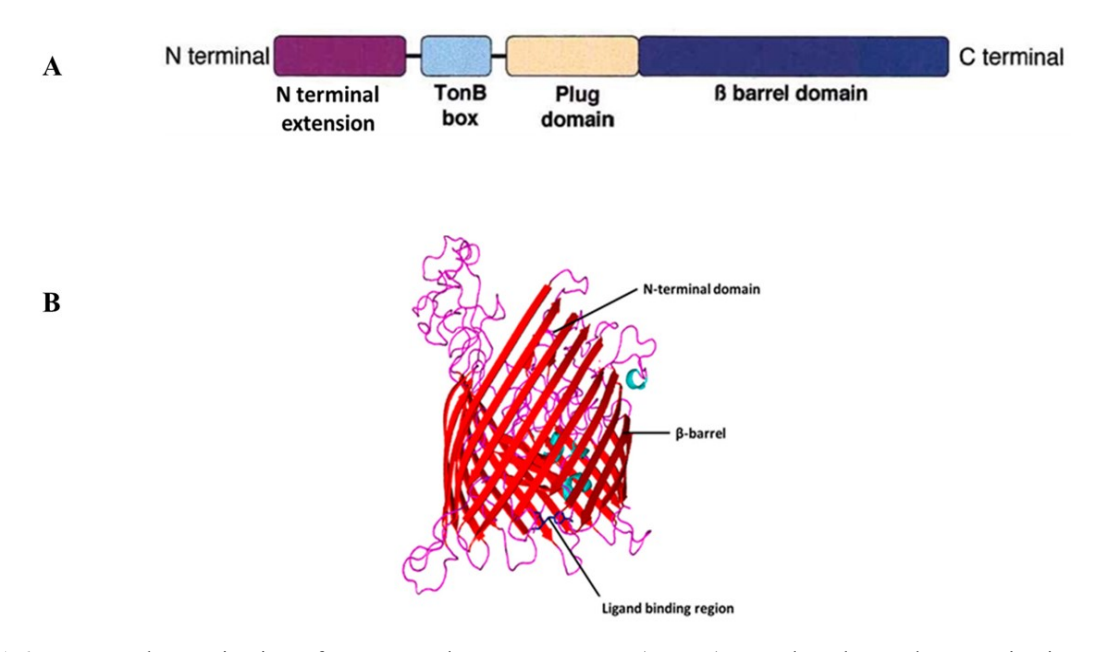


Fig. 1.6: Structural organization of outer membrane transporter (TBDT). Panel A shows the organization of the domains in TBDT (the figure is taken and modified from Folschweiller et al., 2000). Panel B shows the typical structural features in the outer membrane transporter (TBDT), N-terminal plug domain, 22 β-barrel structure, and ligand binding motif are indicated with an arrow (Samantarrai et al., 2020).

1.10 The Ton Complex

The inner membrane associated ExbB/ExbD and TonB interact in a ratio of 7:2:1 (Higgs et al., 2002; Maki-Yonekura et al., 2018) and together this complex is called Ton-complex (Celia et al., 2016). The ExbB/ExbD complex generate energy via proton motive force and the generated energy is then transduced to TonB dependent transporter through TonB. TonB interacts with the outer membrane located TBDT by establishing physical contact with a conserved consensus pentapeptide motif (ETVIV) known as TonB-Box (Tuckman and Osburne, 1992; Krewulak and Vogel, 2011). The TonB-Box is located at the N-terminus of all TonB dependent transporters (Noinaj et al., 2010). Upon ligand binding to the TBDT, the N-terminally located TonB-box gets exposed facilitating its interaction with TonB. These interactions lead to conformational changes in TBDT and facilitates the release of substrate into periplasmic space (Wiener, 2005). In fact, the novel transport system was originally identified with transport of phage T one (T1) therefore the outer membrane transport system is designated as TonB dependent Transport (TonBDT) system (Killmann et al., 1995). Subsequently, it is shown to transport a number of nutrients including iron complexes, vitamin B₁₂ and Heme, Nickel complexes (Ferguson and Deisenhofer, 2004; Wiener, 2005; Schauer et al., 2008 & Noinaj et al., 2010).

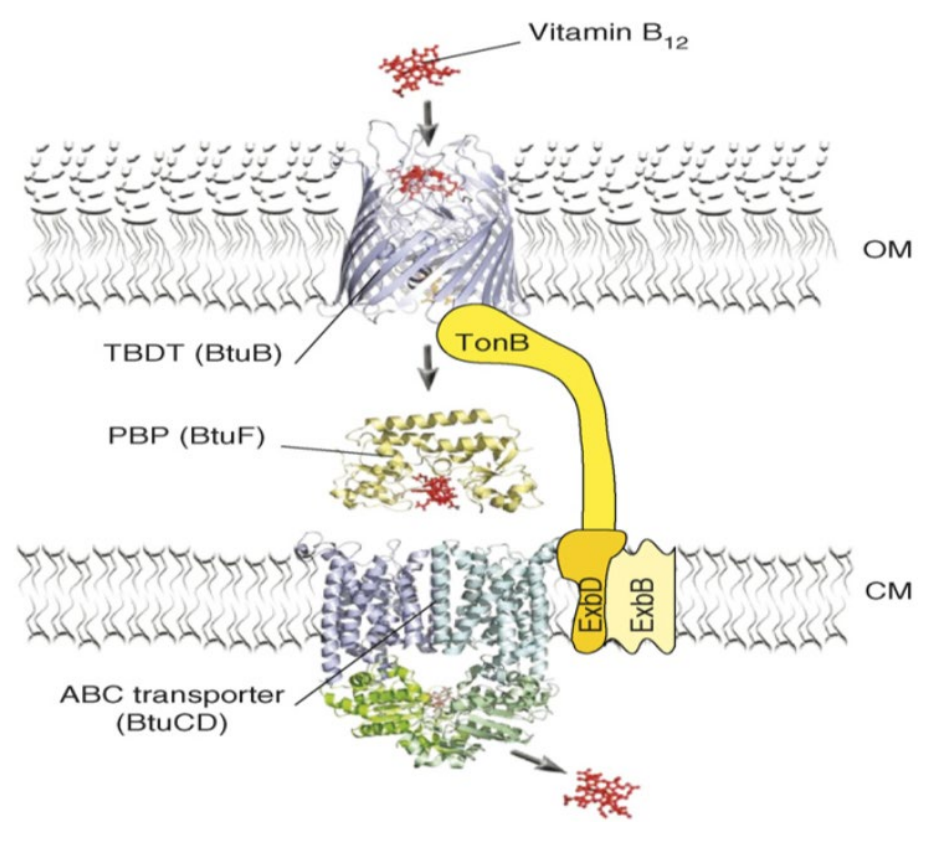


Fig. 1.7: Model showing the transport of vitamin B_{12} via TonB-dependent transport system. The transport of essential micronutrients (such as iron-siderophores and vitamin B_{12}) across the outer membrane of Gram-negative bacteria proceeds via TonB Dependent Transport (TonBDT) system. Upon binding to vitamin B_{12} (red) to the specific TBDT, BtuB (blue ribbon) present in the outer membrane it interacts with the TonB (yellow) present in Ton-complex (TonB-ExbB-ExbD). The TonB transduces energy, generated by proton motive force components ExbB/ExbD (light yellow) to TBDT. The conformational change induced in TBDT facilitates release of bound B_{12} into periplasmic space. After translocation into the periplasmic space the vitamin B_{12} binds to BtuF (yellow ribbon) and before crossing through inner membrane via ABC transporter BtuCD (Schauer et al., 2008).

1.11 Siderophores: Chemistry and Biology

During evolution, bacteria have developed an active-uptake method by which they make low-molecular-weight molecules (generally <1 kDa), called as siderophores, which chelate Fe^{3+} ions with strong affinity, organizing into soluble complexes (Hider and Kong, 2010). Siderophore mediated iron acquisition pathways exist in a wide range of prokaryotes and eukaryotes (and also in higher plants) and produces the siderophores (Fig. 1.4) when iron concentration within the cells fall below the threshold of about 10^{-6} M, which is crucial for growth and survival of microorganisms (Miethke and Marahie, 2007). Based on the chemical nature of the moieties donating the oxygen to form coordinating ligands with Fe (III), siderophores are classified into three main classes. (I) catecholates: catecholate type, phenolate type (II): hydroxamates, or (α -hydroxy-) carboxylates (III) mixed-type of siderophores (Miethke and Marahie, 2007). As of now, over 500 siderophores of various kinds have been established (Krewulak and Vogel, 2008).

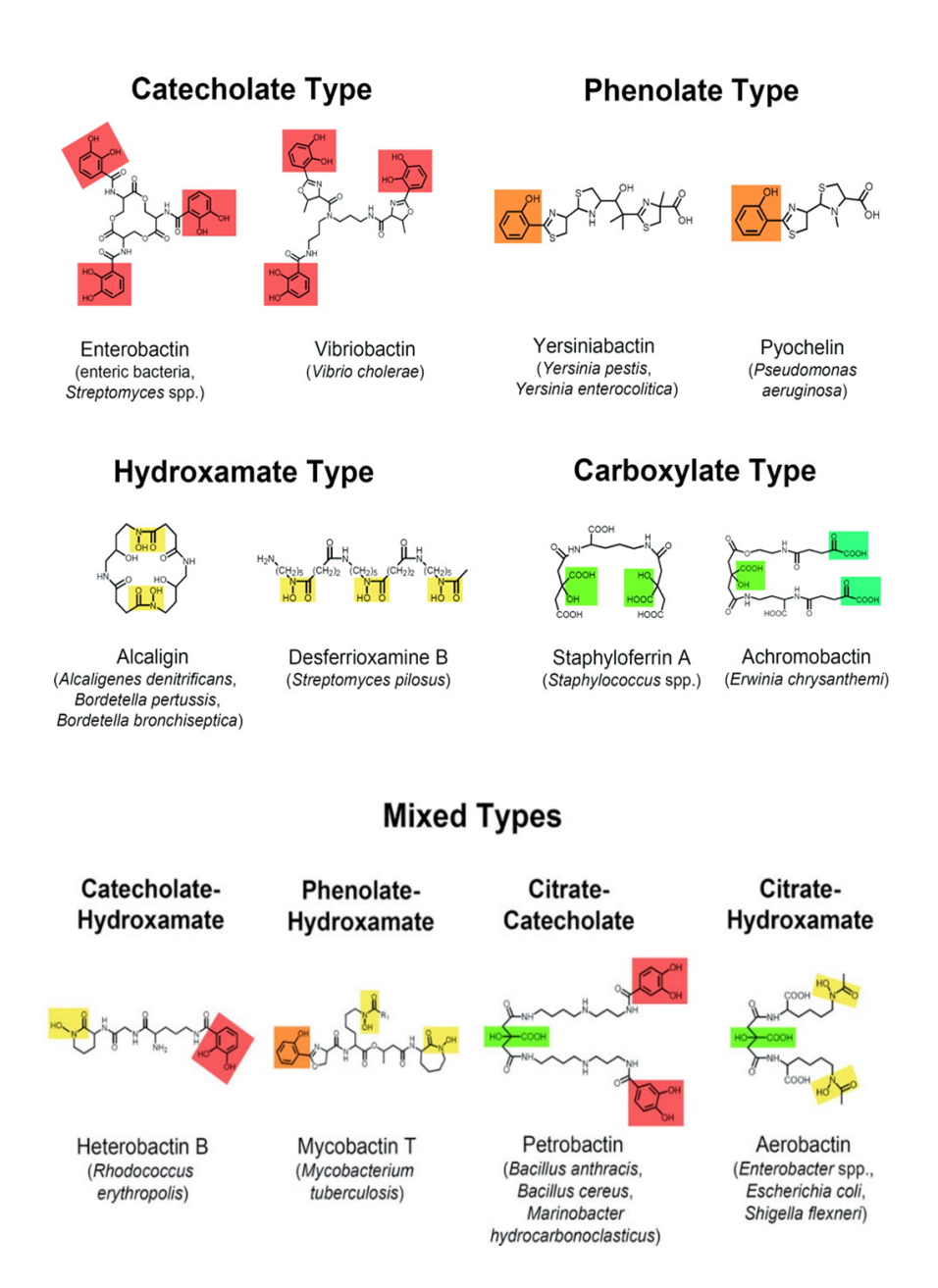


Fig. 1.8: Classical nature of different siderophores and their natural producers. Moieties involved in iron coordination are highlighted: catecholates are shown in red, phenolates are in orange, hydroxamates are in pale yellow, α-hydroxy-carboxylates are in light green, and α-keto-carboxylates (deriving from 2-oxo-glutarate units) are in blue-green (Miethke and Marahie 2007).

Enterobactin (enterochelin) is a standard catecholate type of siderophore produced and secreted by the bacterial family Enterobacteriaceae. It was first found in *E. coli* (O'Brien and Gibson, 1970) and in *Salmonella typhimurium* (Pollack et al., 1970). Since then, it has been identified in most other enterobacteria genera, such as *Klebsiella*, *Shigella*, *Enterobacter*, *Serratia* (Perry and San Clemente, 1979; Lawlor et al., 1984). The biosynthesis of siderophore is regulated by the availability of iron concentration in the cell. Therefore, when the iron concentration is below the (0.1-1μm) the production of enterobactin is observed. Enterobactin [tri-(N-(2,3-1))]

dihydroxybenzoyl)-L-serine)-ester] is a cyclic trilactone, where 3dihydroxybenzoylserine residues are linked through an ester linkage and as high-affinity for ferric iron Fe (III) (Raymond et al., 2003). The produced Ents are secreted out of the cell and capture iron atoms with a stoichiometry of 1:1 and high efficiency (Ka=10⁵²) (Raymond and Carrano, 1979; Harris et al., 1979). Three 2, 3-dihydroxybenzovl moieties of Ent play a role in the coordination of an iron atom (Karpishin and Raymond, 1992; Raymond et al., 2003) and the ferric-enterobactin (Fe-Ent) bears three negative charges. The Fe-Ent is recognized by the outer membrane transporter TBDT (FepA) in E. coli (Buchanan et al., 1999) and actively transported into the periplasm. In the periplasm the strongly bound iron is released from Fe-Ent either by hydrolyzing the tri-lactone backbone of Ent or by weakening the interactions between Ent and Fe³⁺ by reducing Fe-Ent complex (Loomis and Raymond 1991; Lin et al., 2005; Abergel et al., 2006 & Zeng et al., 2013).

Hypothesis

As stated in the aforementioned sections, our laboratory has shown OPH as part of the membrane associated multiprotein complex (Parthasarathy et al., 2016; Gudla et al., 2019). The outer membrane transport components TBDT, TonB, ExbB/ExbD and OmpW are found to be part of OPH complex (Gudla et al., 2019). The OPH exists as part of Ton complex by establishing physical contact with PMF components (ExbB/ExbD) and energy transducer TonB (Gudla et al., 2019). The OPH containing syTonBDT system reconstituted in E. coli showed enhanced iron uptake by an unknown mechanism. One hypothesis is that the OPH, through its weak lactonase activity, hydrolyzing the trilactone ring of Fe-enterobactin (Fe-Ent), or protonating Fe-Ent complex to facilitate the release of bound iron. The present study with the following objectives is designed to address these questions.

1.12. Objectives

- i) To identify the role of OPH in TonB dependent Transport (TonBDT) system.
- ii) To assess if enterobactin (Ent) serves as a physiological substrate for OPH.
- iii) To evaluate if the triesterase activity OPH has any role in OPH dependent enhanced iron uptake.



2. MATERIALS AND METHODS

Table 2.1: List of Antibiotics

Antibiotic	Supplier name
Ampicillin sodium salt	HiMedia
Chloramphenicol	HiMedia
Kanamycin Sulphate	HiMedia
Gentamycin	HiMedia
Streptomycin	HiMedia
PolymyxinB	HiMedia
Tetracycline hydrochloride	HiMedia

Table 2.2: List of Chemicals

Name of the Chemical	Name of the Company
Absolute Ethanol	CH Fine Chemical
Acetic Acid, Glacial	Fisher Scientific
Acetonitrile	Qualigens Fine Chemical
Acrylamide	Sigma- Aldrich
Agar	HiMedia
Agarose	Lonza
Ammonium persulphate	Ameresco
Ammonium sulphate	SRL
Bis-Tris	Ameresco
Bovine serum albumin	HiMedia
Bromophenol blue	Fisher Scientific
Butanol	SRL
Calcium chloride	Fisher Scientific
Calcium nitrate	Qualigens
Dimethyl sulfoxide (DMSO)	Sigma- Aldrich
EDTA Disodium salt dihydrate	SRL
Enterobactin	Sigma- Aldrich
Ferric Chloride Hexahydrate	HiMedia
Ferrous sulphate	Fisher Scientific

Glycine	SRL
Glycerol	SRL
Hydrochloric acid	SRL
4-(2-hydroxyethyl)-1-piperazine ethane sulfonic acid	Fisher Scientific
(HEPES)	
Imidazole	SRL
Isopropanol	SRL
Isopropyl β-D-1-thiogalactopyranoside (IPTG)	G-biosciences
Lysozyme	G-biosciences
Lithium Chloride	SRL
Methyl parathion	Sigma Aldrich
Manganese chloride	SRL
Magnesium sulphate	SRL
Methanol	SRL
β-mercaptoethanol	Sigma Aldrich
Nickel sulphate	Sigma Aldrich
N, N'-Methylenebis (acrylamide)	Sigma Aldrich
Phenol water-saturated	Fisher Scientific
Phenylmethyl sulfonyl fluoride (PMSF)	G-biosciences
Peptone	HiMedia
Potassium chloride	SRL
Potassium dihydrogen orthophosphate (KH ₂ PO4)	SRL
Potassium phosphate dibasic anhydrous (K ₂ HPO4)	SRL
Protease inhibitor cocktail	G-biosciences
SERVA Blue G	SERVA
Sodium dodecyl sulfate	SRL
Sodium Hydroxide	SRL
Skimmed milk powder	HiMedia
N, N, N', N'-Tetramethylethylenediamine (TEMED)	Sigma Aldrich
Tricine	Ameresco
Tryptone	HiMedia
Trishydroxymethylaminomethane (Tris-base)	SRL
Tween 20	Ameresco

5-Bromo-4-chloro-3-indolyl β-D galactopyranoside	Sigma Aldrich
(X- Gal)	
Yeast Extract	HiMedia

Table 2.3: List of Resins used in this study

Name of the Resin	Name of the Company
SP Sepharose Fast Flow	GE Healthcare
DEAE Sepharose Fast Flow	GE Healthcare
HiLoad Superdex 200 pg	GE Healthcare

Table 2.4: List of Restriction endonucleases and DNA modifying enzymes

Enzyme	Supplier name
BamHI	Thermo Fisher Scientific
BgIII	Thermo Fisher Scientific
EcoRI	Thermo Fisher Scientific
HindIII	Thermo Fisher Scientific
NdeI	Thermo Fisher Scientific
PstI	Thermo Fisher Scientific
XhoI	Thermo Fisher Scientific
T4 DNA Ligase	Thermo Fisher Scientific
PfuDNA polymerase	Thermo Fisher Scientific
Phusion® High-Fidelity DNA polymerase	New England Biolabs
TaqDNA polymerase	Thermo Fisher Scientific
DNase	Sigma Aldrich
RNase A	Thermo Fisher Scientific
HyperLadder 1kb DNA Ladder	G-biosciences
Unstained Protein Ladder, 10-200 kDa,	Genetix

2.1 Antibiotic and Chemical stock solutions

2.1.1 Ampicillin

Ampicillin stock solution was prepared by dissolving 500 mg of ampicillin in 5 ml of autoclaved milli-Q water. The ampicillin solution was then sterilized by passing it through a $0.22~\mu m$ filter (Millipore PVDF membrane) and the stock solution was aliquoted and stored

at -20°C until further use. When necessary 50μl of stock solution was added to the 50 ml of sterile and warm (50°C) culture medium to obtain a final concentration of 100μg/ml.

2.1.2 Chloramphenicol

Chloramphenicol stock solution was prepared by dissolving 150 mg of chloramphenicol in 5 ml of 70 % (v/v) absolute ethanol. The chloramphenicol solution was then sterilized by passing it through a 0.22 μ m filter (Millipore PVDF membrane) and the stock solution was aliquoted and stored at -20°C until further use. When necessary 50 μ l of stock solution was added to the 50 ml of sterile and warm (50°C) culture medium to obtain a final concentration of 30 μ g/ml.

2.1.3 Gentamycin

Gentamycin stock solution was prepared by dissolving 100 mg of gentamycin in 5 ml of autoclaved milli-Q water. The gentamycin solution was then sterilized by passing it through a 0.22 µm filter (Millipore PVDF membrane) and the stock solution was aliquoted and stored at -20°C until further use. When necessary 50µl of stock solution was added to the 50 ml of sterile and warm (50°C) culture medium to obtain a final concentration of 20µg/ml.

2.1.4 Kanamycin

Kanamycin stock solution was prepared by dissolving 150 mg of kanamycin in 5 ml of autoclaved milli-Q water. The kanamycin solution was then sterilized by passing it through a 0.22 μm filter (Millipore PVDF membrane) and the stock solution was aliquoted and stored at -20°C until further use. When necessary 50μl of stock solution was added to the 50 ml of sterile and warm (50°C) culture medium to obtain a final concentration of 30μg/ml.

2.1.5 Tetracycline

Tetracycline stock solution was prepared by dissolving 100 mg of tetracycline in 5 ml of 70 % (v/v) absolute ethanol. The tetracycline solution was then sterilized by passing it through a 0.22 μ m filter (Millipore PVDF membrane) and the stock solution was aliquoted and stored at -20°C until further use. When necessary 50 μ l of stock solution was added to the 50 ml of sterile and warm (50°C) culture medium to obtain a final concentration of 20 μ g/ml.

2.1.6 Isopropyl-β-D-thio-galactoside (IPTG)

IPTG stock (1M) solution was prepared by dissolving 238 mg of IPTG in 1 ml of autoclaved milli-Q water. The IPTG solution was then sterilized by passing it through a 0.22 μ m filter (Millipore PVDF membrane) and the stock solution was aliquoted and stored at -20°C until further use. When necessary 50 μ l of stock solution was added to the 50 ml of sterile and warm (50°C) culture medium to obtain a final concentration of 1mM.

2.1.7 5-bromo-4-chloro-indolyl-β-D-galactopyranoside (X-Gal)

X-Gal stock (4%) solution was prepared by dissolving 200 mg of X-Gal in 5 ml of N, N' – dimethylformamide and the stock solution was aliquoted and stored at -20°C until further use. When necessary 50µl of stock solution was added to the 50 ml of sterile and warm (50°C) culture medium to obtain a final concentration of 0.004%.

2.2 Growth Media

All media used for growing bacterial cultures were sterilized by autoclaving for 15 minutes at 15lbs pressure and 121°C. When required the autoclaved media was brought to 40° C and appropriate amounts of stock solutions of antibiotics polymyxin B (10μ g/ml), chloramphenicol (30μ g/ml), tetracycline (20μ g/ml), ampicillin (100μ g/ml), streptomycin (20μ g/ml), gentamycin (20μ g/ml) and kanamycin (20μ g/ml) were added to the growth media.

2.2.1 Luria-Bertani (LB) medium

LB medium was made by dissolving 10gm peptone, 5gm yeast extract and 10gm NaCl in 900ml of double-distilled water. The contents were thoroughly mixed before adjusting its pH to 7.0 by adding (approx. 0.5ml) of 2N NaOH solution. The contents were then adjusted to 1000ml with double distilled water and sterilized as described above. While preparing LB plates agar (2%) was added prior to proceeding for sterilization.

2.2.2 Terrific broth (TB) medium

TB medium was made by dissolving 12gm tryptone, 24gm yeast extract, 3.12gm KH₂PO₄, 12.5gm K₂HPO₄ and 5ml glycerol in 900ml of double-distilled water. The contents were thoroughly mixed before adjusting its pH to 7.0 by adding (approx. 0.5ml) of 2N NaOH solution. The contents were then adjusted to 1000ml with double distilled water and sterilized as described above. While preparing TB plates agar (2%) was added prior to proceeding for sterilization.

2.3 Preparation of iron-free media and solutions

Iron free minimal salts solutions and other solutions containing essential micronutrients supplemented in minimal salts medium were prepared by passing them via the Chelex® 100 resin (Bio-Rad) following manufacturers protocols. Briefly, the chelex resin was washed with iron-free Milli-Q water to remove 0.5M sodium acetate buffer (pH 5.6) used as storage buffer.

The chelex resin was then transferred onto a metal free glass column and left it at room temperature for 2-3 hours to settle the resin particles in the column. The minimal salts and other stock solutions used in preparation of minimal salts medium were passed at a flow rate of 1ml/minute through the column to remove the trace metals. After passing each solution through the Chelex® 100 column the column was regenerated by passing 2 bed volumes of 1N HCl followed by 5 bed volumes of Milli-Q water and 2 bed volumes of 1N NaOH followed by 5 bed volumes of Milli-Q water. After regeneration, the chelex resin was stored in 0.5M sodium acetate buffer (pH 5.6) at 4°C until further use.

A) Minimal salts medium for E. coli

Minimal salts solution was made by dissolving 4.8gm of K₂HPO₄, 1.2gm of KH₂PO₄ in 1000ml of double-distilled water. The contents were then autoclaved and stored at room temperature until further use. While preparing minimal salts medium sterile stock solutions of Ca (NO₃)₂. 4H₂O, FeSO₄, MgSO₄.7H₂O and Glucose were added to a final concentration of 0.04gm of CaNO₃ 4H₂O, 0.001gm of FeSO₄, 0.2gm of MgSO₄.7H₂O and 1gm of Glucose per 1000ml of minimal salts solution. The freshly prepared minimal slats medium was used to growth *E. coli* cultures.

B) Minimal salts medium for sphingopyxis wildii

Minimal salts solution was made by dissolving 4.8gm of K₂HPO₄, 1.2gm of KH₂PO₄ and 1gm of NH₄NO₃ in 1000ml of double-distilled water. The contents were then autoclaved and stored at room temperature until further use. While preparing minimal salts medium sterile stock solutions of MgSO₄.7H₂O, FeSO₄ and Ca (NO₃)₂. 4H₂O were added to a final concentration of 0.2gm of MgSO₄.7H₂O, 0.001gm of FeSO₄ and of 0.04gm of CaNO₃. 4H₂O per 1000ml of minimal slats solution. Subsequently, the medium was made complete by adding filter sterilized essential amino acid mixture (0.07mM), biotin (0.001mg), pantothenate (0.5mg), vitamin B-12 (0.001mg) and sodium acetate (2%) as carbon source to get complete minimal salts medium.

C) Preparation of high iron solution.

FeSO₄ (1%) stock solution was prepared by dissolving 1gm of FeSO₄.7H₂O in 100ml of iron-free Milli-Q water. The contents were sterilized by autoclaving following procedures described above and the sterile FeSO₄ stock solution was stored at room temperature until further use. When required 100μl of this solution was added to 100ml of iron-free minimal salts medium to attain a final concentration of 10μg Fe/ml.

D) Preparation of low iron solution

FeSO₄ ($2\mu g/ml$) stock solution was prepared by adding $20\mu l$ of iron stock solution (1% FeSO₄) into the 20ml of iron-free Milli-Q water to give a final concentration of $2\mu g/ml$ concentration. The contents were sterilized by autoclaving following procedures described above and the sterile FeSO₄ stock solution was stored at room temperature until further use. When required 1ml this solution was added to 100ml of iron-free minimal salts medium to attain a final concentration of $0.02\mu g$ Fe/ml.

E) Preparation of iron-free glassware

All glassware was made iron-free by initially soaking overnight in 2% methanolic KOH. They were rinsed for 4 to 5 times with Milli-Q water and then soaked for one day in 6N HCl. Again, the glassware was washed 4 to 5 times with Milli-Q water and autoclaved to obtain sterile iron free glassware.

2.4 Solutions & buffer for DNA modifications

A) TAE buffer

The 50x TAE (Tris-Acetate-EDTA) buffer was prepared by dissolving 242gm of Tris base in 800ml of double-distilled water. After dissolving the salt completely, 100ml of 0.5M EDTA (pH 8.0) and 57.1ml of glacial acetic acid were added and the final volume was adjusted to 1000ml with double distilled water. When needed the stock (50x TAE) was diluted to get a working concentration of 1x TAE.

B) 6x Gel loading dye

The (6x) DNA loading dye was prepared by dissolving 25mg of xylene cyanol FF, 25mg of bromophenol blue and 1.5gm of Ficoll 400 in 8ml of Milli-Q water. After complete dissolution of the contents, the final volume was adjusted to 10ml and stored at room temperature until further use.

C) Ethidium bromide stock solution

Ethidium bromide (100mg) was added to 10ml of sterile water taken in an amber colour bottle. The contents were kept stirring overnight to facilitate complete dissolution of added ethidium bromide. After solubilization of ethidium bromide, the solution was further diluted to get a final working stock solution of 1 mg/ml. While preparing agarose gel 2.5μl of working stock solution was added to 50ml of gel solution to attain a final concentration of 0.05μg/ml (Sambrook et al., 1989).

2.5 Agarose gel electrophoresis

Agarose gels (0.8-2%) were prepared by weighing appropriate amounts of agarose in 100ml of 1x TAE buffer and the contents were boiled until the added agarose was completely dissolved. Then the molten agarose was cooled to approximately 45 to 50°C and supplemented with 0.5μg/ml of ethidium bromide. The ethidium bromide supplemented molten agarose was then poured into the casting tray. An appropriate comb was placed in casting tray before the solidification of agarose solution. After solidification, the casting tray was placed in the buffer tank and the comb was carefully removed from the agarose gel. The wells formed in agarose gel were flushed with tank buffer to remove air bubbles. The DNA samples were mixed with required volumes of 6x loading dye and loaded into the wells of an agarose gel immersed in 1x TAE buffer. Electrophoresis was performed at constant voltage (100V) for about 20 minutes. After electrophoresis, the migration of DNA fragments was visualized and the results were documented using UVTech gel imaging system. The size of resolved DNA fragments was determined by comparing its migration with that of a DNA standard (1Kb ladder; Fermentas) loaded.

2.6 Plasmid isolation by alkaline lysis method

A single colony containing the desired plasmid was inoculated into 3ml LB medium supplemented with required antibiotic and was incubated for overnight at 37°C with shaking. Cells were harvested from 1 ml overnight culture by centrifugation at 6000rpm for 5 minutes. The obtained cell pellet was resuspended in 100µl of ice-cold TEGL solution-I (10mM EDTA, pH 8.0; 50mM glucose; 25mM Tris-HCl, pH 8.0; 50mM lysozyme). The above cell suspension was mixed with 200µl of freshly prepared solution-II (freshly prepared by mixing equal volume of 2% SDS and 0.4 N NaOH) and the cells were incubated on ice for 3 minutes to facilitate the cell lysis. The cell lysate was then neutralized by addition of 150µl ice-cold solution-III (3M Sodium acetate, pH 8.0). The contents were mixed by inverting the tubes for 4-5 times and left on the bench for 5 minutes to complete the neutralization process. The degraded genomic DNA and denatured cellular proteins were removed by centrifuging the contents at 13,000rpm for 10 minutes. The supernatant containing plasmid DNA was collected into a fresh 1.5ml Eppendorf tube and is subjected to phenol: chloroform (1:1) and later with chloroform: isoamyl alcohol (24:1) extraction to remove proteins leftover in the aqueous phase. The clear aqueous phase containing plasmid DNA was precipitated by addition of 1/10th volume of 3M CH₃COONa (pH 3.8) and 2 volumes of ice-cold ethanol and incubating the tubes at -20°C for 20 minutes.

The precipitated plasmid DNA was collected by centrifugation at 10000rpm for 30 minutes at 4°C. The obtained plasmid pellet was then washed with ice-cold 70 % ethanol to remove traces of salts in the plasmid. The plasmid was further air-dried and redissolved in an appropriate volume of TE buffer (10mM Tris, 1mM EDTA).

2.7 DNA Quantification

The concentration of nucleic acid samples was quantified spectrophotometrically using a NanoDropTM 1000 spectrophotometer (Thermo Scientific). About 2μl of sample was pipetted on to the sample pedestal and the absorbance peak of nucleic acid in the sample was measured at 260nm. The software calculated the nucleic acid concentration following the Beer-Lamberts Law with an extinction coefficient of 0.030 (ng/μl)⁻¹ cm⁻¹ and 0.020 (ng/μl)⁻¹ cm⁻¹ for single-stranded and double-stranded DNA, respectively. The extent of protein contamination in a nucleic acid sample was estimated by the ratio of absorbance measured at 260 and 280nm or by the ratio measured at 260 and 230nm respectively.

2.8 Polymerase Chain Reaction (PCR)

PCR amplification reactions (20μl) were performed in 200μl reaction tubes containing 2.5mM MgCl₂, 200μM dNTP mix containing all the individual deoxynucleotides dATP, dGTP, dCTP and dTTP at equal concentrations, 10 picomoles of both forward and reverse primers, 1 Unit *Taq* polymerase or high fidelity Phusion DNA polymerase, 5-20ng of genomic or plasmid DNA was used as a template. The PCR reaction was performed in a thermal cycler (Bio-Rad), programmed according to the amplicon size and Tm of the primers (Table 2.5). The PCR reaction the reaction mix was analyzed on 0.8% agarose gel electrophoresis.

Table 2.5: Standard PCR cycling conditions

Cycling Step	Temperature	Time	No of cycles
Initial denaturation	94-98°C	5 min	1
Denaturation	94-98°C	15-30 sec	
Annealing	55-65°C	45 sec	30
Elongation	72°C	1Kb/ min	
Final Elongation	72°C	5-10 min	1
Hold	12°C	infinite	-

2.9 Site-Directed Mutagenesis

Site-Directed Mutagenesis was performed by using Q5 SDM Kit (New England Bio Labs) following manufacturer's protocols. Initially, the region of the gene sequence to be mutated is identified and complementary oligos were designed by introducing the required alteration in the sequence of the primer. The plasmid containing the gene of interest was used as a template and the PCR reaction was performed using appropriate primers having a mutation at the desired position. The PCR product generated was treated with KLD (Kinase, Ligase and DpnI) enzyme mix provided along with the kit and the resulting KLD treated PCR product was the transformed into the NEB-alpha competent cells of *E. coli* strain. The insertion of the desired mutation at the desired position was confirmed by sequencing the plasmid.

2.10 Restriction digestion of a DNA molecule

A typical 20 to 30µl reaction mix contained 0.5 to 1µg of vector or insert DNA, 1 Unit of restriction endonuclease enzyme/1µg of DNA and 1x digestion buffer. The reaction mix was incubated at 37°C for one hour and the digestion of DNA samples were ascertained by analyzing on agarose gel.

2.11 DNA ligation

The ligation reactions were carried out in a 20µl reaction containing 1x ligase buffer. About 100ng of total DNA having vector and insert in a molar ratio of 1:3 was taken for performing ligation reaction. The vector and insert ratio was calculated following the formula given below:

$$mass_{insert}[ng] = \frac{mass_{vector}[ng] \times size_{insert}[bp]}{size_{vector}[bp]} \times 3$$

The ligation reactions were incubated at 22°C for three hours or at 4°C for overnight. Prior to proceeding for the transformation of the ligation reaction into the bacterial cells, the ligase enzyme was heat-inactivated at 65°C for 20 minutes.

2.12 Preparation of competent cells

A single colony of *E. coli* DH5α was picked from a fresh overnight LB plate and inoculated into a 3ml of LB broth. The culture was incubated for 16hrs at 37°C with shaking at 180rpm.

The above culture (1%) was inoculated into 250ml of LB broth and incubated at 37°C for 4 to 5 hours with moderate shaking. The culture was allowed to grow till the cell density reaches to 0.5 (A₆₀₀) when measured at 600nm. The cells were harvested by centrifuging at 3500rpm for 10 minutes at 4°C. The obtained cell pellet was gently resuspended in 75ml of ice-cold 20mM CaCl₂-80mM MgCl₂. The cell suspension was incubated on ice for 30 minutes and subsequently harvested. Finally, the cell pellet was resuspended in 10ml of 100mM CaCl₂ and 2ml of DMSO and kept on ice for 10 minutes. Quickly, this cell suspension was distributed into 100µl aliquots into chilled sterile eppendorf tubes and immediately snap-freezed in liquid nitrogen and stored at -80°C until further use.

2.13 Bacterial Transformation

The frozen competent cells were thawed by keeping the tubes on ice for 5-10 minutes. Once thawed, 20µl of ligation mixture or 40-50 ng plasmid of interest was added and incubated on ice for 30 minutes. Following the incubation, the cells were subjected to a thermal shock for exactly 1 minute 30 seconds at 42°C and immediately chilled on ice for 2 minutes. Further, 1 ml of fresh LB broth was added and incubated for 60 minutes at 37°C with shaking at 180rpm. The cells were harvested by centrifugation at 6000rpm for 5 minutes. The obtained cell pellet was resuspended in 100µl of LB broth and plated on required selective LB agar plates. When needed 1mM IPTG and 2% X-gal was added with preferred antibiotics. The plates were then incubated for 12-16 hours at 37°C for colonies to appear.

2.14 Protein Methods

2.14.1 Solutions for SDS-Polyacrylamide gel electrophoresis

A) Acrylamide solution

Acrylamide (30%) stock solution was prepared by mixing 150gm of acrylamide and 4gm of N, N'- methylene-bis-acrylamide in 300ml of Milli-Q water. The contents were left overnight to ensure complete dissolution of acrylamide. Finally, the volume was adjusted to 500ml and stored at 4°C until further use.

B) Resolving gel buffer

Tris (1.5M) pH 8.8 was made by dissolving 18.17gm of Tris base in 80ml of Milli-Q water and pH of the buffer was adjusted by adding require amount of concentrated 2N HCl. Finally, the volume of the buffer was adjusted to 100ml using Milli-Q water before autoclaving the solution. After sterilization SDS (0.3%) was added and stored at room temperature until further

use. When required, appropriate amounts of the stock solution was added to the gel components to get a working concentration of 0.39M Tris-HCl with a pH of 8.8.

C) Stacking gel buffer

Tris (0.5M) pH 6.8 was made by dissolving 12.14gm of Tris base in 80ml of Milli-Q water and pH of the buffer was adjusted by adding required amounts of concentrated 2N HCl. Finally, the volume of the buffer was then adjusted to 100ml with Milli-Q water before autoclaving the solution. After sterilization SDS 0.3% was added and stored at room temperature until further use. When required, appropriate amounts of the stock solution was added to the gel components to get a working concentration of 0.13M Tris-HCl with a pH of 6.8.

D) Tris glycine electrophoresis buffer

The 10X Tris glycine buffer was made by mixing 30gm of Tris base, 10gm of SDS and 140gm of Glycine in 800ml of double-distilled water. After dissolving the salts completely, the final volume was adjusted to 1000ml with double-distilled water and stored at room temperature until further use. When needed the stock (10X Tris glycine buffer) was diluted to get working concentration of 1X Tris glycine buffer containing 25mM Tris base, 0.1% SDS and 250mM Glycine.

E) SDS gel loading dye (2X)

A 2x stock solution of SDS gel loading dye was prepared by mixing 5ml of 0.5M Tris-HCl, pH 6.8, 0.045gm of bromophenol blue, 0.5gm of SDS and 5ml of glycerol in 20ml of Milli-Q water and kept for 10 minutes at 45°C to achieve complete solubilization of SDS. To this reagent, 0.349ml of β-mercaptoethanol was added and finally made up to 25ml with Milli-Q water. The loading dye was stored in 5ml at -20°C until further use. The resulting solution contains 0.1M Tris-HCl (pH 6.8), 0.2% (w/v) bromophenol blue, 4% (w/v) SDS and 20% (v/v) glycerol. When required equal amount of this buffer was added to the protein samples and boiled for 5-10 minutes prior to loading on to the SDS-PAGE.

F) Staining solution

Coomassie brilliant blue R-250 was (0.25gm) dissolved in 50ml of CH₃OH after solubilization of dye 30ml of acetic acid was added and volume was finally adjusted to 100ml using double-distilled water. The content was filtered using Whatman paper and stored at room temperature in a brown bottle until further use.

G) Destaining solution

The detaining solution was prepared by mixing 30ml of methanol in 10ml of acetic acid before making up to the 100ml using double-distilled water. The resulting destaining solution was stored at room temperature until further use.

2.14.2 Solutions used for Western blotting

A) Towbin buffer

Towbin buffer (25mM Tris, 192mM glycine, pH 8.3) was made by mixing 3.03gm of tris-base and 14.4gm of glycine in 700ml of double- distilled water. After dissolving salts completely, 200ml of methanol was added and the final volume was adjusted to 1000ml with double-distilled water. The resulting Towbin buffer was stored at room temperature until further use.

B) TBST buffer

TBST buffer was made by mixing 10ml of 1M Tris-HCl (7.6), 4gm of NaCl and 0.5ml of Tween-20 in 400ml of double-distilled water. After dissolving salts completely, the final volume was adjusted to 500ml. The resulting TBST buffer was stored at room temperature until further use.

C) Blocking reagent

Blocking solution (10%) was prepared by dissolving one gram of skimmed milk powder in 10ml of TBST buffer and used for blocking PVDF membrane.

D) Ponceau S reagent

Ponceau S reagent (0.1%) was prepared by dissolving 100mg of Ponceau salt in 80ml of 5% acetic acid. After dissolving salt completely, the final volume was adjusted to 100ml with 5% acetic acid and stored at room temperature until further use.

2.14.3 Solutions for Protein Estimation

A) Standard BSA

BSA (10mg) was dissolved in 1ml of 0.17M NaCl to prepare 10mg/ml stock solution and was stored at -20°C. 1mg/ml BSA solution was prepared by diluting the stock and used for the generating standard graph.

B) Bradford's reagent

The Bradford's reagent was prepared by dissolving 0.01gm of coomassie brilliant blue G-250 in 80ml of 95% ethanol. After dissolution of dye 10ml of 85% (w/v) orthophosphoric acid was added and the contents were made up to 100ml with Milli-Q water. The contents were filtered using Whatman filter paper and stored in an amber colour bottle at 4°C until further use.

2.15 Protein estimation by Bradford's method

Protein standard graph was prepared by using readings obtained from a reaction mix containing 10µl of solution having BSA in the concentration range of 2, 4, 6, 8, 10µgs and 990µl of Bradford's reagent. The contents were incubated in dark for 10-20 minutes and a

standard graph was plotted for the values obtained by measuring absorption at 595nm. The obtained standard graph was used to estimate protein in an unknown sample.

2.16 Polyacrylamide gel electrophoresis

The protein samples were separated on SDS-Poly acrylamide gels by performing electrophoresis following the standard procedures (Laemmli, 1970). Mini-PROTEAN II Bio-Rad system was used to prepare gels and to perform SDS-PAGE. The spacer plates and thin glass plates were assembled into the casting unit. Initially, 12.5%-15% resolving gel mixture was prepared and poured between two glass plates containing 1 mm spacers to form a slab. The resolving gel was covered with water saturated n-butanol and allowed to polymerize for 20 minutes at room temperature. After polymerization of resolving gel, the butanol was removed by repeated washing and the traces of water was removed by wiping with filter paper strips. Subsequently, 4.5% stacking gel mixture was made and poured on top of resolving gel to the top edge of short plate. A required size of comb was inserted immediately to create the wells. The stacking gel was allowed to polymerize for 20 minutes. After solidification, the comb was removed and the wells were washed with distilled water. The polymerized gels between the glass plates were placed into the buffer tank with the electrode assembly and the buffer tank was filled with 1X Tris-glycine buffer. The protein samples were prepared by mixing with equal volume of 2X sample loading dye and boiled for 5-10 minutes in hot water both. The samples were given a short spin before loading into the wells. The electrophoresis was performed at 120 volts till the tracking dye reached to the anode end of the gel. After completing the electrophoresis, the gels were removed from the glass plates and the protein bands were stained with Coomassie stain for 30-60 minutes. The gels were then destained by using destaining solution.

Table 2.6: Resolving gel composition for the SDS-PAGE

Solution	12.5% for 10ml	15% for 10ml
H ₂ O	3.40ml	2.50ml
Solution II (1.5 M Tris, pH 8.8)	2.50ml	2.50ml
Acrylamide mix (30%)	4.00 ml	5.00ml
APS (10%)	100μ1	100μl
TEMED	10μ1	10μ1

Table 2.7: Stacking gel composition for the SDS-PAGE

Solution	7.5% for 5ml
H_2O	2.50ml
Solution III (0.5 M Tris, pH 6.8)	1.25ml
Acrylamide mix (30%)	1.25ml
APS (10%)	50μl
TEMED	5μ1

2.17 Semi-dry western blotting

After protein samples resolved by SDS-PAGE, the gel was soaked in Towbin buffer for 5-10 minutes. Meanwhile, PVDF membrane was soaked in methanol for 5-10 minutes to activate the membrane. The methanol activated PVDF membrane and filter pads were equilibrated separately in the Towbin buffer for 10-15 minutes. These pre-wetted filter pads act as ion source to facilitate the electrophoretic transfer of the proteins onto the PVDF membrane. Initially, the filter pads were placed on the top of the anode plate of the TransBlot Semi-dry transfer cell (Bio-Rad). The PVDF membrane was then placed appropriately onto the filter pad and later gel was carefully positioned on the top of the membrane and additional filter pads were placed above it. The cathode plate of the apparatus was assembled according to the instructions by the manufacturer and the electrophoretic transfer was performed at 16V for 45 minutes.

Following the transfer process, the membrane was blocked in 10% skimmed milk solution made in TBST for an hour at room temperature. After blocking, the membrane was rinsed thrice for 5 minutes using TBST. The washed membrane was incubated with primary antibody solution at the appropriate dilution for 1 hour at room temperature. The membrane was washed three times with TBST for 5 minutes. The membrane was then incubated for 1 hour with the HRP conjugated secondary antibody containing buffer in a correct dilution. Finally, membrane was given 5 minutes rinse for 3-5 times before proceeding to develop the membrane using ECL Prime Western Blotting detection reagent following manufacturer's instructions. The resulting chemiluminescence was captured by ChemiDocTM imager (Bio-Rad).

2.18 Subcellular fractionation

The cells having expression plasmid were induced with the 1M IPTG and incubated for 10h at 18°C with shaking at 180rpm. The cells were harvested by centrifugation at 6000rpm for 5 minutes. The cell pellet obtained was washed twice with wash buffer (50mM Tris-HCl pH 8.0, 100mM NaCl and 3% glycerol) and each gram of pellet obtained was resuspended in 10ml of lysis buffer (50mM Tris-HCl pH 8.0, 100mM NaCl, 3% glycerol, 1mM PMSF and 50 μg lysozyme). The cells were lysed by sonication with 20 sec on and 40 sec off sonic cycles for 10 min. Unbroken cells and cell debries were removed from the cell lysate by centrifugation at 13000rpm for 30 minutes. The clear supernatant obtained was then subjected to the ultracentrifugation at 40,000rpm for 1 hour 30 minutes to separate the subcellular fraction. The supernatant containing cytoplasmic faction was collected and stored at -20°C until further use. The pellet containing membrane fraction was resuspended in 1ml of 50mM Tris-HCl pH 8.0, 100mM NaCl and 3% glycerol. The resuspended membrane fraction was subjected to recentrifugation at 40,000rpm for 1 hour 30 minutes to remove any traces of cytoplasmic faction. The pure membrane fraction obtained was stored in -80°C until further use. The purity of membrane fraction was assessed by performing marker enzymes assay.

2.19 Enzyme assays and preparation of reagents

2.19.1 Reagents for Glucose-6-phosphate dehydrogenase assay

A) Glycylglycine buffer

Glycylglycine (0.25M) buffer was made by dissolving 3.03gm of Glycylglycine base in 80ml of Milli-Q water and the pH of the buffer was adjusted to 7.4 by adding required amount of concentrated 2N HCl. Finally, the volume of the buffer was adjusted to 100ml with Milli-Q water and the solution was stored at room temperature until further use.

B) D-Glucose-6-Phosphate Solution

D-Glucose-6-Phosphate (0.06M) solution was prepared by dissolving 0.10gm of D-Glucose-6-phosphate in 5ml of Milli-Q water and the solution was stored at -20°C until further use.

C) NADP solution (0.02M)

NADP (0.02M) solution was prepared by dissolving 0.742gm of Nicotinamide Adenine Dinucleotide Phosphate in 50ml of Milli-Q water and the solution was stored at 4°C until further use.

D) Magnesium Chloride (0.3M)

Magnesium Chloride (0.3M) was prepared by dissolving 0.363gm of MgCl₂ in 5ml of Milli-Q water and stored at 4°C until further use.

2.19.2 Reagents for Nitrate reductase assay

A) Methyl viologen

Methyl viologen solution was prepared by dissolving 0.1gm of sodium hydrosulfite in 20ml of 0.01M NaOH and 4% sulfanilamide containing 25% HCL. Further the solution was mixed with 0.08% N-(1-Napthyl) ethylene diamine dihydrochloride. The solution was stored at 4°C until further use.

B) Potassium nitrate (0.1M)

Potassium nitrate (0.1M) was prepared by dissolving 0.101gm of KNO₃ in 10ml of Milli-Q water and stored at 4°C until further use.

C) Phosphate buffer (0.1M, pH 7.2)

Phosphate (0.1M) buffer was prepared by mixing 13.6gm of KH₂PO₄ and 1.74gm of K₂HPO₄ in 800ml of double-distilled water and the pH of the buffer was adjusted to 7.2 by adding required amount of concentrated 2N NaOH. Finally, the volume of the buffer adjusted to 1000ml with double-distilled water and stored at room temperature until further use.

2.19.3 Reagents for Methyl parathion activity

A) CHES buffer (0.2M, pH 9.0)

CHES (0.2M) buffer was prepared by dissolving 4.15gm of CHES in 80ml of Milli-Q water and the pH of the buffer was adjusted to 9.0 by adding required amount of concentrated 2N NaOH. Finally, the volume of the buffer was adjusted to 100ml with Milli-Q water and stored at room temperature until further use.

B) Substrate solution

Methyl parathion (0.1M) stock solution was prepared by dissolving 26.3mg of methyl parathion in 1ml of methanol and stored at 4°C until further use. When needed the stock (0.1M methyl parathion) was diluted to get a working concentration of 100µM of methyl parathion.

2.20 Glucose-6-phosphate dehydrogenase (G6PD)-Cytoplasmic marker

Glucose-6-phosphate dehydrogenase was used as a cytoplasmic marker enzyme. Subcellular fractions were tested for G6PD enzyme activity by monitoring glucose-6-phoaphate dependent reduction of NADP at 340nm. The assay was performed in Tris buffer (50mM Tris-HCl pH 7.5) containing 0.25M NADP⁺ at 37°C. The reaction was initiated by adding 12.5mM glucose-6-phosphate (Sargent et al., 1998). The specific activity was calculated by using the formulae given below.

Activity =
$$\frac{(\Delta A_{340} \text{ nm/min Test} - \Delta A_{340} \text{ nm/min Blank}) (3) (df)}{(6.22) (0.1)}$$

Where,

3 = Total volume (in milliliters) of assay

df = Dilution factor

6.22 = Milli molar extinction coefficient of β-NADPH at 340nm

0.1 = Volume (in milliliters) of enzyme used

2.21 Nitrate Reductase-Membrane enzyme

Nitrate reductase assay was performed by following the method described by Michal & Showe 1968. Initially, the assay was initiated by pre-incubating the subcellular fractions in a 2.4ml volume of the reaction mixture containing 0.1M phosphate buffer (pH 7.2), 0.1M potassium nitrate and 10⁻⁴ M methyl viologen for 5 minutes at 37°C. Before the reaction commences, 50mg of sodium hydrosulfite was dissolved in a 10ml of 0.01M NaOH solution and the reaction was started by adding 0.1ml of sodium hydroxide solution to the reaction mixture. After 10 minutes, the reaction was stopped by shaking the tube to oxidize the remaining hydrosulfite and reduce methyl viologen. While determining nitrite, sulfanilamide (0.75ml) solution was prepared by mixing one part of 0.08% N-(1-Napthyl) ethylene diamine dihydrochloride solution with two parts of 4% sulfanilamide in 25% HCl was added to the 2.5ml of reaction mixture and incubated the reaction for 10 minutes at RT. The absorbance of the reaction mixture was measured spectrophotometrically at 540nm. The specific activity of nitrate reductase was calculated using the following the formulae given below.

Activity =
$$\frac{\text{(OD of the Test at A}_{540} \text{ nm}) \text{ x df x 1000}}{\text{mg of protein from subcellular fraction x time in minutes (10 min) x OD of the standard (A}_{540} \text{ nm/}\mu\text{mol}).}$$

2.22 Parathion Hydrolase Assay

A spectrophotometric assay was adapted to estimate organophosphate hydrolase (OPH) activity. Reaction mixture (1ml) contained the 200mM CHES buffer (pH 9.0), 1μ M CoCl₂ and 100μ M of methyl parathion. The reaction was initiated by adding cellular fractions as source of OPH. The reaction tubes were incubated at 37^{0} C for 10-30 minutes. The formation of p-

nitrophenol (PNP) was measured at 410nm and the amount of PNP released in the reaction was determined using the extinction coefficient of PNP (17500/M/cm). The specific activity of the enzyme was measured by calculating the micromoles of PNP produced/mg of protein/minute (Chaudhry *et al.*, 1988). The specific activity of OPH enzyme was calculated using the following the formulae given below.

Specific activity = Enzyme activity/mg of protein/min

Chapter-I

Organophosphate hydrolase and Enterobactin interactions

As stated in the introduction our laboratory has demonstrated existence OPH as part of inner membrane associated Ton-complex (Gudla et al., 2019). However, the physiological significance of OPH association with Ton complex is not known. The Ton complex consisting of ExbB/ExbD and TonB and an outer membrane transporter also known as TonB Dependent Transporter (TBDT) are part of outer membrane transport system known as TonB dependent Transport (TonBDT) system (Ferguson et al., 2004; Wiener, 2005; Schauer et al., 2008 & Noinaj et al., 2010). The TonBDT system is involved in transport of several nutrients including ferric-enterobactin (Fe-Ent). After crossing outer membrane, the trilactone ring of Fe-Ent is hydrolyzed by a periplasmically bound esterase to facilitate the release of bound iron (Zeng et al., 2013). Since OPH is interacting with Ton-complex components its intrinsic properties were revisited in the light of its interactions with Ton-complex components. The triesterase activity of OPH is very well established and it is shown to hydrolyze organophosphate insecticides and certain nerve agents at a rate close to their diffusion limits (LeJeune et al., 1998; Prokop et al., 2006; Singh and Walker, 2006; Karpouzas and Singh, 2006; Theriot and Grunden, 2011 & Bigley and Raushel, 2012). A number of studies were conducted to understand the evolution of such efficient and novel catalytic properties (Raushel and Holden, 2000; Afriat et al., 2006; Khersonsky and Tawfik 2010; Afriat et al., 2012 & Elias and Tawfik 2012). Such studies have identified a weak lactonase activity in OPH (Afriat et al., 2006). Considering, its weak lactonase activity, together with its association with TonB Dependent Transport (TonBDT) system, further experiments were performed to assess if Fe-Ent serves as a substrate to OPH. The experimental procedures, results and inference drawn from the results are described in the chapter.

3.1 Objective specific methodology

3.1.1 Expression and Purification of mature form of OPH (mOPH)

Performing Fe-Ent hydrolase assays requires pure OPH in sufficient quantities. As mentioned in the introduction section, OPH is a membrane associated protein (Gorla et al., 2009, Parthasarathy et al., 2016). It contains 24 amino acids long signal sequence to facilitate its insertion in the inner membrane, If OPH is expressed in *E. coli* with a signal peptide it either targets to the membrane or remains in cytoplasm as inclusion bodies. Therefore, an expression plasmid was constructed by using the *opd* gene coding OPH in which the region coding signal peptide was deleted. The truncated *opd* gene was then used to fuse to the translational signals of constitutively expressed *lacZ* gene. The construction details of the expression plasmid

coding OPH without its signal sequence (mature form of OPH) is described elsewhere (Mulbry and Karns, 1989a).

A number of studies have been performed to express OPH in *E. coli*. Most of them failed to yield active OPH. The expressed protein filed to acquire native conformation and the misfolded protein remained in the cytoplasm in the form of inclusion bodies. However, when *opd* gene coding mature form of OPH was fused to the 5'end of *lacZ* gene an active, soluble OPH was made in *E. coli* (Mulbry and Karns, 1989a). The recombinant OPH thus expressed contain fist five N-terminal residues of β-galactosidase. The construction details of expression plasmid designated as pUCOPH is described elsewhere (Mulbry and Karns., 1989a).

3.1.2 Expression and purification of mOPH

Expression and purification of mOPH was performed by following established protocols (Mulbry and Karns., 1989b, Omburo et al., 1992). An overnight culture of E. coli DH5α (pUCOPH) was used to inoculate 5 L of terrific broth supplemented with ampicillin (50 μg/ml). After growing the cells for 24 hours, an additional amount of ampicillin (50 μg/ml) was added and the culture was permitted to grow for another 12 hours. The culture was chilled by placing the flasks on ice bath for an hour and the cells were harvested by centrifuging the culture at 8, 000 rpm for 15 minutes. The cell pellet was then suspended by dissolving each gram of the cell pellet in 5 ml of 10 mM potassium phosphate buffer (pH 6.7, 50 µM CoCl₂) before lysing the cells by sonication for 15 min (20 sec ON and 40 sec OFF). The cell lysate was centrifuged at 15,000 rpm for 30 minutes and the clear supernatant obtained was then treated with 1 % streptomycin sulphate to remove nucleic acids. Subsequently, the OPH was precipitated by adding solid ammonium sulphate to the supernatant to a final concentration of 45% (w/v). The ammonium sulphate precipitated OPH was recovered by centrifugation at 15,000 rpm for 30 minutes. Further, the pellet was dissolved in 40 mL of 10 mM potassium phosphate buffer (pH 6.7, 50 µM CoCl₂) and dialyzed against 10 mM potassium phosphate buffer (pH 6.7 supplemented with 50 μM CoCl₂) for 5 times with a time interval of 4 hours.

3.1.3 Ion exchange chromatography

The dialyzed sample was loaded on to an SP Sepharose cation exchange resin (GE Healthcare, India) column equilibrated with the 10 mM potassium phosphate buffer (pH 6.7, 50 µM CoCl₂) at a flow rate of 1 ml/min. The column was washed with the same buffer and the total bound protein was eluted using a linear gradient of 50-500 mM KCl (pH 6.7 adjusted

with KOH) at a flow rate of 1 ml/min. The fractions containing OPH activity were pooled and dialyzed for 20 hours at 4⁰C against 10 mM potassium phosphate buffer (pH 8.3, 50 mM KCl, 50 μM CoCl₂) by exchanging the buffer for every 4 hours.

After dialysis, the protein was applied onto a DEAE Sepharose weak anion exchange (GE Healthcare, India) column equilibrated with 10 mM potassium phosphate buffer (pH 8.3, 50 mM KCl, 50 μM CoCl₂) at a flow rate of 1 ml/min. The pure OPH collected in flowthrough leaving contaminating proteins in the column was concentrated before loading it on gel filtration column to obtain pure OPH. The DEAE eluted fraction was concentrated to a final volume of 2 ml and applied to a HiLoad 16/600 Superdex 200 high-resolution gel-filtration resin (GE Healthcare, India) equilibrated with the 10 mM HEPES buffer pH 8.5, 50 mM NaCl. The same buffer was used to elute the samples and eluted fractions were collected and analyzed for purity on 12.5 % SDS-PAGE gel.

3.1.4 Preparation of enterobactin (Ent) solution

Enterobactin was purchased from Sigma-Aldrich, USA. The 10 mM stock solution of Ent was prepared by dissolving 1 mg of Ent in 150 μl DMSO. The stock solution was store at -20°C until further use. When necessary the stock solution of Ent was mixed with FeCl₃ (10mM in water) at a 1:1 ratio (equimolar ration) and incubated for 10 minutes at RT. The resulting Fe-Ent complex was passed through desalting column to remove unbound Ferric ion and the pure Fe-Ent complex was then used for further studies.

3.1.5 Thin Layer Chromatography (TLC)

While evaluating to test if Ent serves as a substrate for OPH the TLC method described elsewhere was employed with minor modifications (Zeng et al., 2013). Initially, a fixed amount of Ent (6.66µg) dissolved in acetonitrile: water (9:1), was taken into sterile Eppendorf tube and added 1µg of pure OPH. The reaction volume was then adjusted with 100mM sodium phosphate buffer (pH 8.0) to 10µl before incubating the contents at RT for 15 minutes. The reaction mix prepared in similar manner by omitting OPH served as control. Then these two reactions were quenched with 3µl acetonitrile and the contents were analyzed on TLC plate. An aliquot (9µl) taken from each reaction mix was carefully spotted on TLC silica gel 60 F254 plate (Merck Millipore, USA) and carefully kept in a chamber saturated using solvent system prepared by mixing benzene: acetic acid: water in a ratio of 62.5ml: 36ml: 1.5ml (v/v). TLC was performed till the solvent front reached 3/4th of the plate and the plates were

carefully removed and placed in a fume hood to ensure complete drying on the plate. The formation of linear Ent was detected by developing the pale by spraying 1% FeCl₃.

3.1.6 High-Performance Liquid Chromatography (HPLC) analysis

Detection of Ent degradation products formed due to OPH mediated hydrolytic cleavage of Ent was also done using HPLC method described elsewhere (Zeng et al., 2013). The Fe-Ent (6.66 μ g) prepared as described above was incubated with 1 μ g of OPH to assess its ability to hydrolyze lactone ring of Fe-Ent. The reaction volume was made up with phosphate buffer (pH 8.0) to 20 μ l and the constituents were incubated at 37°C for 30 minutes. The contents of the reaction mix was then extracted with 200 μ l of ethyl acetate and the organic phase obtained after centrifuging the sample at 10000 rpm for 15 min at 4°C was collected in a clean open tube and kept it in a fume hood till the ethyl acetate was completely evaporated. Finally, the contents were redissolved in 40 μ l of methanol and briefly centrifuged before injecting 20 μ l of sample in HPLC.

HPLC analysis was performed using Shimadzu (LC-20AT) instrument equipped with photodiode array detector fitted with Phenomenex C18 column (Luna, $5\mu m$, $250\times4.6mm$) following procedures described elsewhere (Mujahid et al., 2011). The mobile phase contained 1% glacial acetic acid and 100% acetonitrile. Initially the column was washed with acetonitrile for 30 minutes using a linear gradient of 0–55%, this wash by step was followed by an additional wash step with 100% acetonitrile for 5 minutes. The column was given a final wash with 1% glacial acetic acid before injecting the sample extracted from the reaction mix (20 μ l). HPLC was performed at a flow rate of 1 ml per minute. The Ent, Fe-Ent were detected at 316 nm.

3.1.7 Blue Native –PAGE (BN-PAGE)

Blue Native PAGE was performed using Novex Bis-Tris 4-16% precast gels from Invitrogen (Schagger and Jagow, 1991). The native Bis-Tris gels with 4-16% polyacrylamide concentrations were assembled as per manufacturer's instructions. The concentration of pure OPH was measured and 10µM of purified OPH was taken into a prechilled eppendorf tube and mixed with either enterobactin or ferric enterobactin (Fe-Ent) at a molar ratio of 1:10 and incubated for 10, 20 minutes at RT. Then the samples were mixed with Novex Tris-glycine native sample buffer from Invitrogen. The protein samples were then loaded onto the wells along with native protein molecular weight markers (HMW Native Marker Kit, GE healthcare). Initially electrophoresis was performed for 30 minutes at 100 V

and then the process was continued for additional 30 minutes at 200 V. After this point, the cathode buffer B (15 mM Bis-Tris pH 7.0, 50 mM Tricine, 0.02% Serva blue) was removed and replaced with a cathode buffer B10 (15 mM Bis-Tris pH 7.0, 50 mM Tricine, 0.002% Serva blue). Under this buffer condition the electrophoresis was performed for 30 minutes at 250 V. Finally, the cathode buffer B10 was removed and replaced with a fresh cathode buffer (15 mM Bis-Tris pH 7.0, 50 mM Tricine) prepared by omitting Serva blue and electrophoresis was performed at a fixed 300 V for 60 min. The gels were initially destained to remove the excess Serva blue G dye and the separated proteins were transferred on to PVDF membrane to perform western blot using anti-OPH antibodies.

3.1.8 Surface Plasmon Resonance (SPR) Analysis

Immobilization of OPH on CM7 sensor chip: The purified OPH protein was covalently immobilized by amine coupling on a carboxymethylated dextran sensor chip CM7 (GE Healthcare) following procedures described elsewhere (Veggi et al., 2012). The amine coupling was done by using pure OPH (50µg/mL of OPH) as a ligand. The pure OPH taken in 10mM sodium acetate pH 5.0 buffer was injected at a flow rate of 30 µl/min with a contact time of 60 seconds. The process was continued until the captured response units (RU) reached approximately to 5340. The blank surface was generated by treating the chip with a buffer (10mM sodium acetate pH 5.0) prepared by omitting the OPH. Further, the background response units (RU) were subtracted from RU generated for the buffer containing 2% DMSO (PBS pH 7.4+ 0.005% P20 + DMSO (2%).

Determination of binding kinetics: Initially, titration experiments were performed by passing increased concentrations of either Ent or Fe-Ent at a flow rate of 30 μl/min over OPH-CM7 chip. The buffers containing Ent and Fe-Ent solutions were prepared by dissolving increasing concentrations (3.12 μM, 6.25 μM, 12.5μM, 25 μM, 50 μM, 100 μM) of either Ent or Fe-Ent. Following each injection, the sensor chip surface was regenerated by washing for 30 seconds with the buffer (PBS pH 7.4+ 0.005% P20 + DMSO (2%) containing 50% DMSO in running buffer. The process was repeated thrice and the binding kinetics pertaining to Ent and OPH were determined by taking the data obtained from three independent experiments. Data were analyzed using Biacore T200 Evaluation software 2.0 version and 1:1 Binding Model (GE Healthcare). Affinity curve was generated manually by plotting the equilibrium binding response (R_{eq}) against analyte concentration. The entire process of immobilization of OPH on CM7 chip and subsequent determination of binding kinetics is shown in Fig. 3.1.

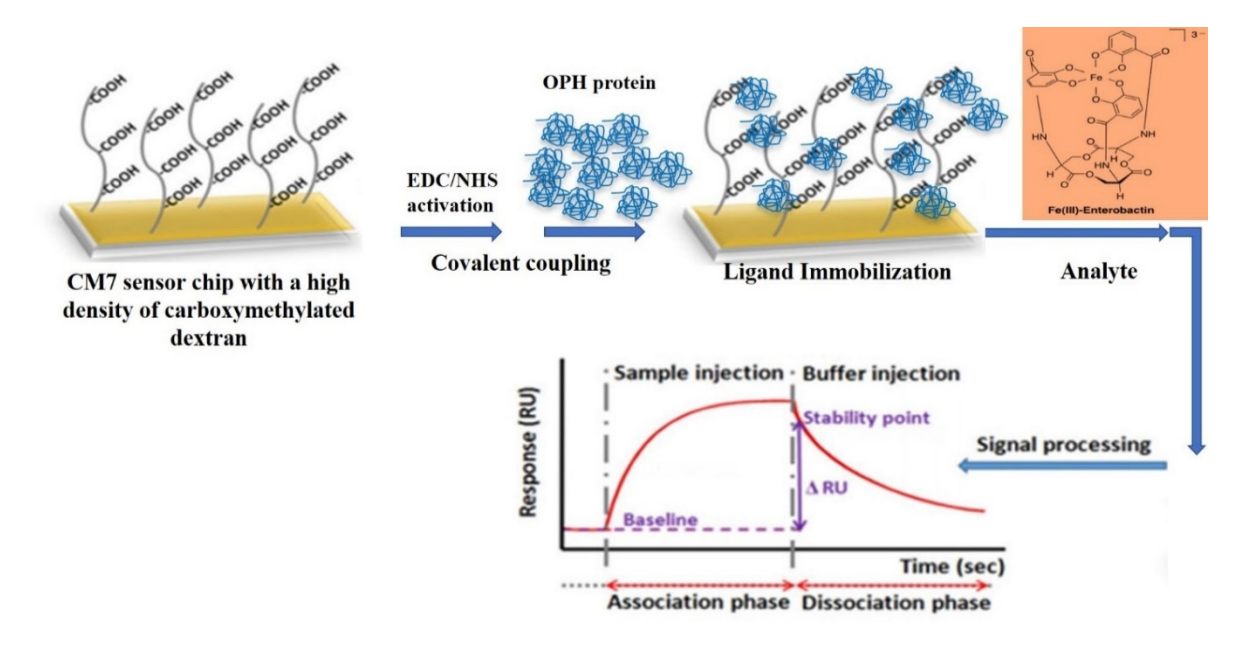


Fig. 3.1: SPR-analysis. Schematic diagram showing OPH immobilization on CM7 chip and subsequent measurement of response units by passing of Fe-Ent/Ent over immobilized OPH.

3.1.9 Fluorescence emission measurements

Room temperature fluorescence emission spectra were recorded with a LS-55 Spectrofluorimeter (PerkinElmer Inc., USA) fitted with 1 cm quartz cuvettes at RT with a wavelength range of 300–450 nm with an excitation wavelength of 280 nm, and slit width of 5.0 nm for both excitation and emission. The sample temperature was kept constant at 25°C. The concentration of OPH was fixed at 1µM, and the concentrations of enterobactin (Ent) and ferric-enterobactin (Fe-Ent) dissolved in 0.01M sodium phosphate buffer (pH 7.4) was varied from 1 to 11µM. Three independent experiments were performed to obtain statistically significant data. The inner filter effect was corrected for absorption of exciting light and re-absorption of the emitted light. The binding constant was measured using the maximum fluorescence intensity value at maximum emission wavelength (335nm). All the spectra were analyzed and plotted by using Microsoft Excel software. The binding constants were calculated following equation:

$$\log(F_0 - F)/F = \log K + n \log[Q]$$

Where n corresponds to the number of binding sites, K is the binding constant and [Q] is the quencher concentration. Log K was calculated from the intercept of the graph $log(F_0-F)/F$ vs. log[Q] and the slope of the graph gave number of binding sites.

3.2 Results and discussion

3.2.1 Expression and purification of mOPH

The mOPH was purified by performing both ion-exchange and gel filtration chromatography. As described in the material and methods section, the cell lysate prepared from E. coli DH5α (pUCOPH) cells were subjected to Ammonium Sulphate (AS) precipitation. Most of the expressed mOPH was precipitated when 25.8 grams of ammonium sulphate was added to the 100 ml cell lysate. At 45% AS concentration substantial amounts of impurities were eliminated (Fig. 3.2. Panel A lane2). The pellet obtained from AS precipitation was dialyzed and passed through SP Sepharose (Cation-exchanger) column and the bound OPH got eluted with increased salt concentration in elution buffer. When buffer concentration reached to 0.5 M KCl, most of the bound OPH got eluted and the fractions with OPH activity were analyzed on SDS-PAGE gel. As expected, the OPH specific band got significantly increased in elution fractions (Fig. 3.2. Panel A). However, a significant number of nonspecific proteins were detected along with OPH (Fig. 3.2. Panel A). The total fractions containing OPH activity were pooled and passed through DEAE Sepharose (Anion-exchanger) column. Most of the contaminating proteins were bound to the DEAE column and the OPH protein was collected in the flowthrough. The collected OPH from DEAE column appears to be 90% pure (Fig. 3.2. Panel B). The remaining contaminated proteins were eliminated by passing the semi pure OPH through gel filtration column. (Fig. 3.2. Panel C).

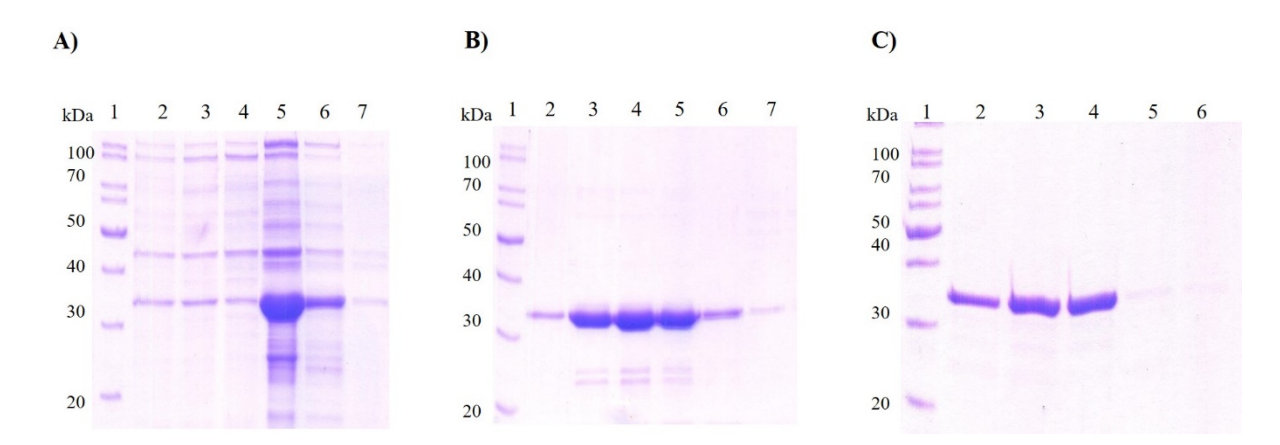


Fig. 3.2: Purification of mOPH. Panel A, B & C represent 12.5 % SDS-PAGE used to determine the purity of mOPH during different stages of purification. Panel A shows the mOPH purified by SP Sepharose column: lane 1 shows the protein molecular weight marker. Proteins found in AS fraction used as input (lane 2), flowthrough (lane 3), wash (lane 4) and elution fractions (lane 5-7) are shown. Panel B shows proteins found in flowthrough fractions collected from DEAE Sepharose column with OPH activity (2-7). The OPH positive elution fractions collected from gel filtrations column are shown in panel C.

3.2.2 Ent hydrolase activity

After purification of OPH the purified OPH was used to test if it has any Ent hydrolase activity. While performing Ent hydrolase activity two independent techniques were employed and both of them were described in detail in materials and methods section. The TLC method was successfully employed to gain prima facie evidence to show Ent hydrolase activity. This method exploits differences in Rf values of Ent and its hydrolytic products (linear and monomeric, dimeric). Ent migrates much faster than its linearized trimers (Furrer et al., 2002; Zeng et al., 2013). Based on these differences it is possible to detect Ent hydrolase activity of OPH. The Ent incubated with and without OPH was extracted and analyzed on TLC as mentioned in materials and methods section. Interestingly there was no difference in Rf profile of Ent incubated with OPH and without OPH. There was no linear species of Ent in reaction mix incubated with OPH (Fig. 3.3). This results clearly suggested that the lactonase activity found in OPH was not serving to hydrolyze Ent.



Fig. 3.3: Thin Layer Chromatography (TLC) analysis of Ent incubated with (lane 1) and without OPH (lane 2). The Ent incubated with either buffer or with OPH was extracted and spotted on TLC plate. The TLC was performed using benzene: acetic acid: water in a ratio of 62.5ml: 36ml: 1.5ml (v/v) as solvent system.

3.2.3 HPLC analysis of Ent incubated with OPH

HPLC method has been successfully employed to detect Ent hydrolase activity of a periplasmically located trilactone esterase, Cee (Campylobacter Enterobactin Esterase). The linear, monomeric and dimeric products of Ent were successfully detected using HPLC (Zeng et al., 2013). Similar analysis was done to detect Ent degradation products in reaction mix incubated with OPH. As revealed in TLC no Ent degradation products were detected in reaction mix incubated with Ent and OPH. The HPLC profile obtained for ethyl acetate extracts prepared from control (buffer+ENT/Fe-Ent) and experimental

(OPH+ENT/OPH+Fe-Ent) reactions were identical (Fig. 3.4. Panel A & C). There was no reduction in either Ent or Fe-Ent peak in reaction mix prepared by including OPH, suggesting that there is no decrease in parent compound (Fig. 3.4. Panel B & D). These two independent studies have clearly suggested lack of Ent hydrolase activity in OPH.

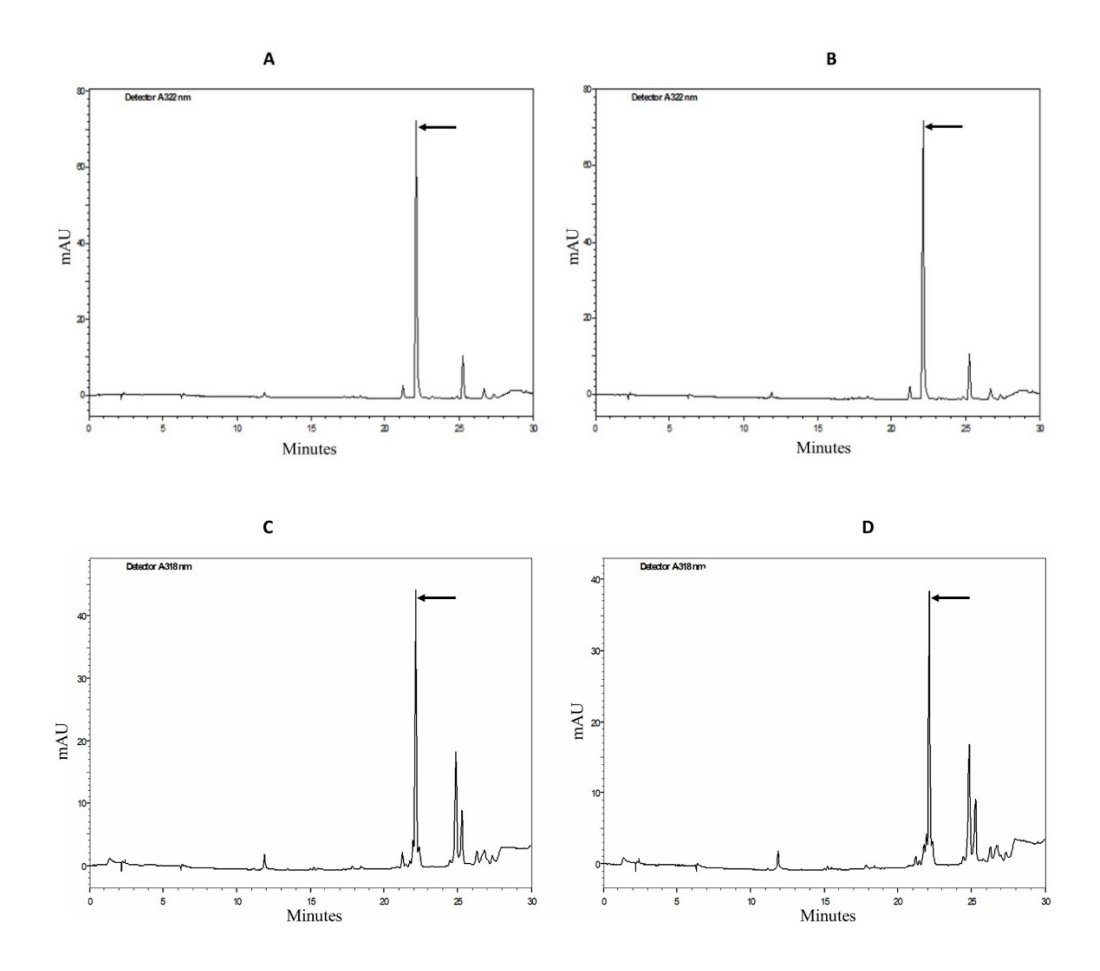


Fig. 3.4: HPLC profile for the etheyl acetate extracts prepared from reaction mix containing Ent +buffer (panel A), Fe-Ent+buffer (panel C), buffer+Ent+OPH (panel B) and buffer+OPH+Fe-Ent (panel D). The peak corresponding to Ent or Fe-Ent is shown with an arrow.

3.2.4 OPH-Ent interactions

The *in vitro* assays clearly demonstrated lack of Ent hydrolase activity in OPH. In certain cases, the Fe-Ent is reduced to weaken the interactions between ferric iron and Ent (Abergel et al., 2006). Such reduction reactions require direct interactions between OPH and Fe-Ent. While assessing such interactions three independent techniques were performed. One of them was BN-PAGE and it provides qualitative data providing prima facie evidence on protein and ligand interactions (Schagger, H. et al., 1991). The BNPAGE was successfully used to study

interactions between Ent and factor H binding protein (Veggi et al., 2012). In the present study the BNPAGE was performed to assess interactions between Ent / Fe-Ent and OPH.

3.2.5 Native PAGE

While performing BNPAGE, pure OPH (10μM) was incubated with 100μM of Ent at RT for 10 and 20 minutes respectively and analyzed on native PAGE to see formation OPH-Ent complex. If compact complex is formed between OPH and Ent, such complex migrates faster than free OPH indicating existence of an additional band on BNPAGE (Veggi et al., 2012). As expected in lanes loaded with reaction mix having both Ent and OPH, an additional faster migrating band was noticed and such band was absent in lanes loaded with only OPH indicating formation of OPH-Ent complex (Fig. 3.5. Panel A Lanes 3 & 4, Fig. 3.5. Panel A Lane 2). Interestingly in lane loaded with the reaction mix containing OPH and Fe-Ent, the intensity of band increased suggesting existing of better affinity between OPH and Fe-Ent (Fig. 3.5. Panel B Lane 3 & 4). Interestingly the Fe-OPH complex formation increased with an increase of incubation time (Fig. 3.5. Panel B Lane 4). The BNPAGE analysis gave a clear indication existence of specific interactions between OPH and Ent/Fe-Ent.

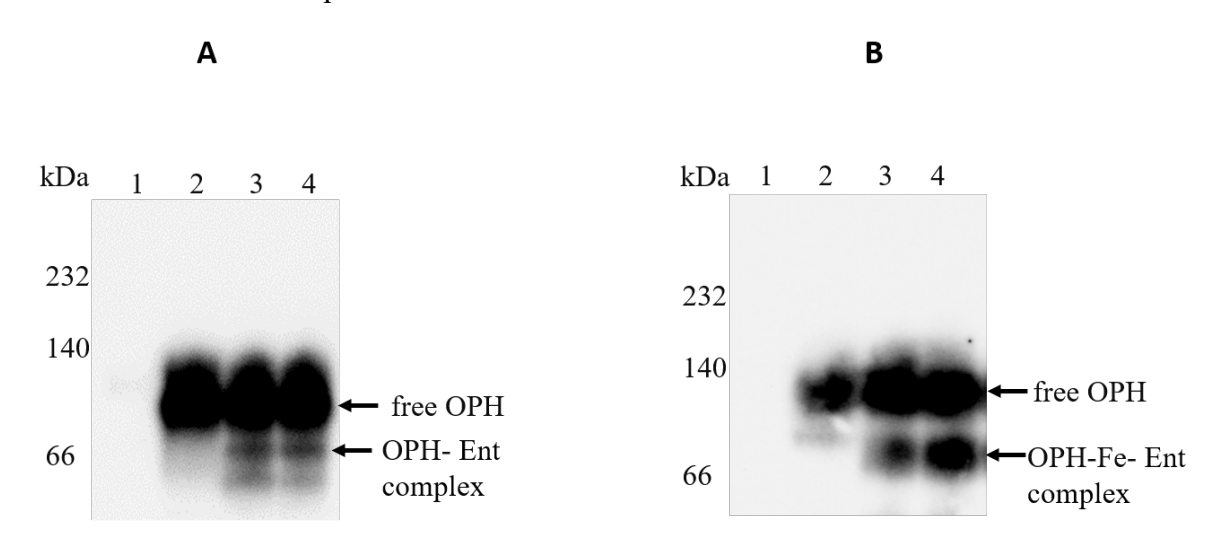


Fig. 3.5: OPH-Ent interactions. Panel-A shows western blot of a BNPAGE developed using anti-OPH antibodies. Formation of OPH-Ent complex is shown with an arrow. Lanes 2-4 indicate reaction mix containing free OPH (2), and OPH+Ent incubated for 10 minutes (lane 3) and 20 minutes (lane 4) respectively. Panel-B shows similar blot of BNPAGE to assess interactions between OPH and (Fe-Ent). Lanes 2, 3 and 4 represent free OPH and OPH-Fe-Ent incubated for 10 and 20 minutes respectively.

3.2.6 OPH interacts with enterobactin

The BNPAGE data clearly showed existence interactions between Fe-Ent and OPH. However, the data is purely qualitative. In order to gain quantitative evidences surface plasmon resonance spectroscopy was performed by using OPH immobilized on CM7 chip. The

sensorgrams were generated by passing increased concentrations of either Ent or Fe-Ent on OPH immobilized on CM7 sensor chip (Fig. 3.6). The values obtained from three independent experiments were used for determining kinetic data (Fig. 3.6. Panel A & B). When Ent or Fe-Ent concentrations ranging from $3.12\mu M$ to $100\mu M$ were passed over OPH-CM7 chip, a gradual increase in response units were observed with a proportionate increase in either Ent or Fe-Ent concentrations. However, in case of Ent the bound Ent suddenly dissociated from OPH. As a result, a sudden dissociation of OPH-Ent complex was observed indicating sudden downfall of sensorgram (Fig. 3.6. Panel A). These typical binding properties are reflected in kinetics data. The association (k_a) and dissociation (k_d) rate constants between OPH and Ent were 249 (1/Ms) and 0.0302 (1/s) respectively. Similarly, a value of 9.10E-04 M was obtained for the equilibrium constant for dissociation (K_D) with a standard error of 1.70E-04M.

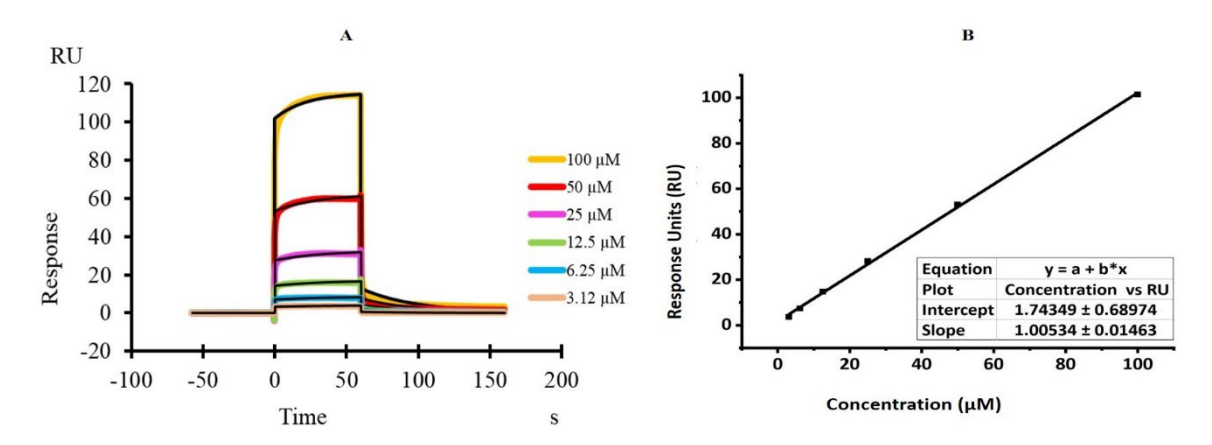


Fig. 3.6: SPR analysis of OPH-Ent interactions. Sensorgrams were generated by Biocore T200 by passing increased concentrations of enterobactin over OPH immobilized on CM7-sensor chip. Panels A and B indicate graphs plotted using response units versus time (Panel A) and response units versus Ent concentration (Panel B).

3.2.7 OPH interacts strongly with Ferric Enterobactin (Fe-Ent)

The OPH-CM7 chip was also used to study interactions between OPH and Fe-Ent. When Fe-Ent was passed with increasing concentration over immobilized OPH-CM7 chip the sensorgrams obtained have shown quite different pattern. The Fe-Ent bound much more strongly than pure Ent (Fig. 3.7. Panel A & B). Unlike Ent, the bound Fe-Ent dissociated slowly from OPH. Such slow dissociation of Fe-Ent indicates functional significance. The k_a , k_d , K_D values obtained for Fe-Ent with OPH are 246 (1/Ms), 0.0073 (1/s) and 3.03E⁻⁰⁵ M with a standard error of 0.069E⁻⁰⁵.

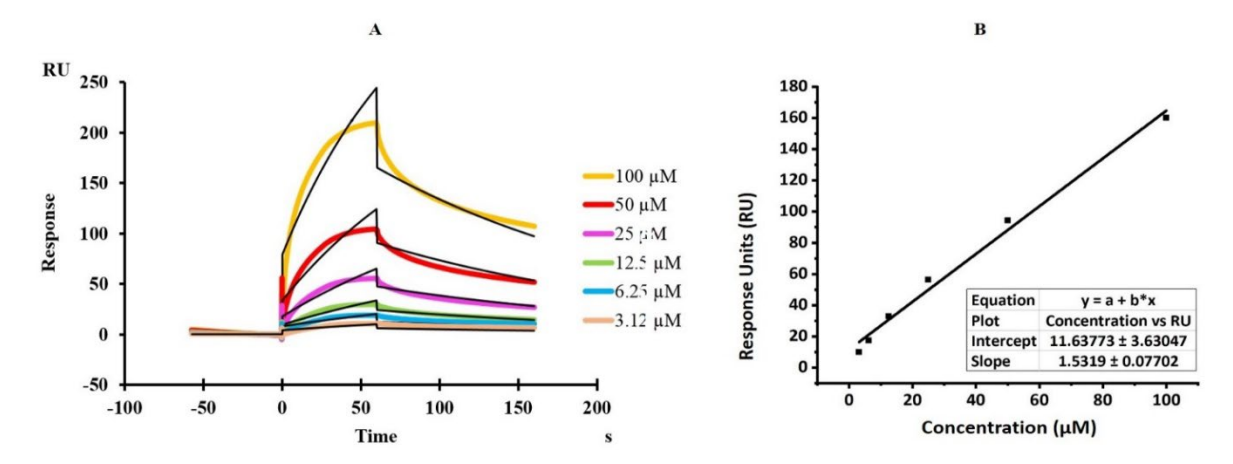


Fig. 3.7: SPR analysis of OPH and Fe-Ent interactions. Sensorgrams were generated by Biocore T200 while by passing increased concentrations of Fe-Ent over OPH immobilized on CM7-sensor chip. Panels A and B indicates graphs plotted using response units versus time (Panel A) and response units versus Fe-Ent concentration (Panel B).

3.2.8 Measurement of Fluorescence Emission Maximum

Both BNPAGE, SPR analysis provided clear evidence on existence of interactions between OPH and Fe-Ent. A supporting evidence was also generated by measuring intrinsic fluorescence emission maxima of OPH in presence of increasing concentrations of Ent and Fe-Ent. Basically, the Ent and Fe-Ent show no fluorescence (Fig. 3.8. Panel A & B). However, when they were are added to OPH in increasing concentrations (0.001-0.011 mM) maximum fluorescence emission obtained at 335 nm was proportionately quenched (Fig. 3.8. Panel A & B). Such decline in fluorescence intensity appears to be due to interaction of excited state fluorophore with its surrounding protein molecules. The Ent and Fe-Ent used in the reaction mix act as fluorophore. If they bind in the vicinity of tryptophan (Trp), it induces conformational changes in OPH bringing changes in Trp emission spectra, a phenomenon commonly observed in proteins upon binding to substrates (Liang et al., 2008). Such changes in Trp emission spectra contributes for the decreased fluorescence emission. Supporting this proposition, a total quench in the fluorescence of OPH was observed at maximum concentrations of Ent and Fe-Ent. Further, a good linear relationship was seen between concentration of Ent and Fe-Ent and fluorescence quenching of OPH (Fig. 3.8. Panel A & B). Likewise, the binding dissociation constants for Ent and Fe-Ent with OPH shown (Table- 1). Interestingly the kinetic values determined by using fluorescence emission showed very good correlation with binding kinetics determined by SPR data (Fig. 3.6. Panel B & Fig. 3.7. Panel B). All three independent studies involving BNPAGE, SPR and fluorescence emission indicated existence of interactions between OPH and Fe-Ent.

TABLE 3.1: The association and dissociation constants of OPH with Ent and Fe-Ent.

Sample	Ка	<i>K</i> d
OPH-Ent	4.98×10 ⁵ M ⁻¹	2.00803E-06 M ± 3.51188E-11 M
OPH-Fe Ent	1.69×10 ⁵ M ⁻¹	$4.31034E-07 M \pm 5.7449E-11 M$

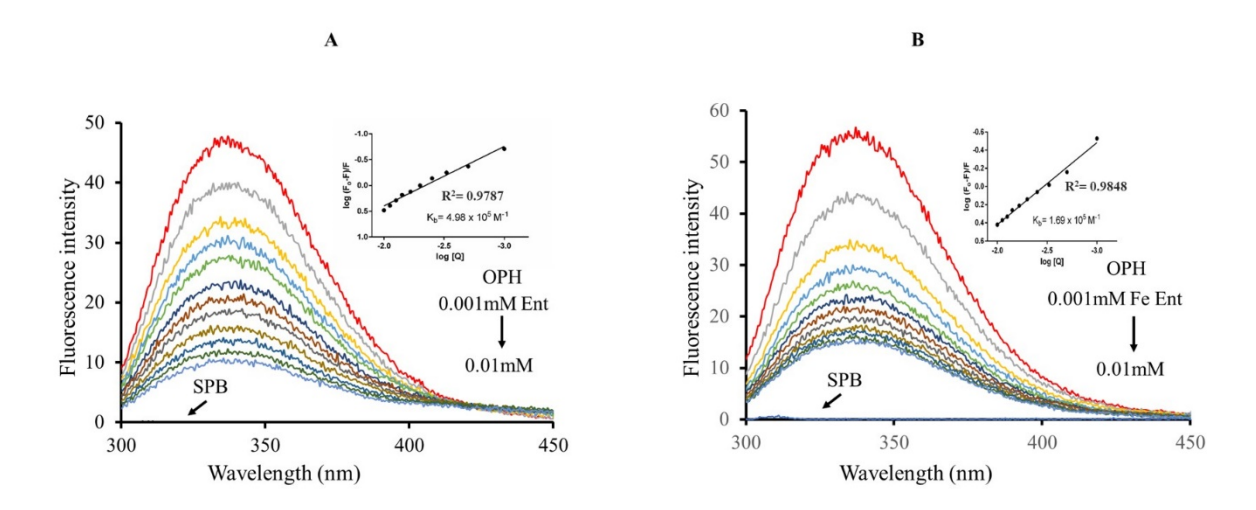


Fig. 3.8: Panels A and B represent fluorescence emission spectra taken for OPH with increasing concentrations of enterobactin (A) ferric-enterobactin (B). The increased fluorescence quenching is observed with increasing concentrations (1 to 11μM) of Ent (A) and Fe-Ent (B). The inset shows modified Stern–Volmer plots obtained by plotting Log [Q] values on X-axis and Log [dF/F] values on Y-axis. Slope of the plot gives number of binding sites. The Y-intercept value gives log K values. The binding constant values were calculated from log K. Lack of fluorescence emission for buffer (SPB) containing either Ent or Fe-Ent is shown with an arrow.

3.3 Discussion

Originally the OPH is purified from soil bacteria capable of degrading organophosphate (OP) insecticides (Serdar et al. 1982; Mulbry and Karns 1989a; Dumas et al., 1989; Singh et al., 1999 & Siddavattam et al., 2003). In view of its catalytic efficiency and broad substrate range a number of studies were performed to exploit its intrinsic properties for detection and decontamination of toxic organophosphate insecticides and nerve agents (LeJeune et al., 1998; Raushel, 2002; Prokop et al., 2006; Singh and Walker, 2006; Karpouzas and Singh, 2006; Theriot and Grunden, 2011 & Bigley and Raushel, 2012). The OPH is a homodimer and each monomer contain an active site with two zinc ions and play a critical role in hydrolyzing third ester linkage found in OP insecticides and nerve agents. The OPH coding *opd* gene exists on indigenous plasmids as part of mobile elements (Mulbry et al., 1986; Harper et al., 1988; Pandeeti et al., 2011; Pandeeti et al., 2012 & Parthasarathy et al., 2016). The mobile elements paly critical role in lateral mobility of *opd* genes. Therefore, identical OPH coding *opd* genes were found in soil bacteria that share a weak or no taxonomic relationship.

The OP insecticides are introduced into environment about 75 years ago as pest control agents (Singh and Walker, 2006). Prior to this there was no scope for bacterial enzymes to gain access to these synthetic molecules. Evolution of microbial enzyme like OPH, with catalytic rate that matches close to the substrate diffusion limit, in such a short span of 75 years caught the attention of biochemists. Numerous studies were conducted on evolution of catalytic function using OPH as model enzyme (Singh, 1999; Yang et al., 2003; Afriat et al., 2006; Singh, 2009; Elias and Tawfik 2012 & Afriat et al., 2012). The structurally the OPH is very similar with quorum quenching lactonases, involved in hydrolysis of lactone ring found in quorum sensing signal molecules homoserine lactone (Afriat et al., 2006). In consistence of structural similarities, the OPH hydrolyzes a number of lactones, including quorum sensing lactonases (Fig. 3.8). Based on promiscuous lactonase activity and structural similarity (Fig. 3.8), the quorum quenching lactonases (QQL), were proposed to be the progenitors of OPH (Afriat et al., 2006; Elias and Tawfik 2012). Interestingly there exists reciprocal promiscuity between two structural homologues suggesting evolutionary relationship between these two enzymes (Afriat et al., 2006; Parthasarathy et al., 2017).

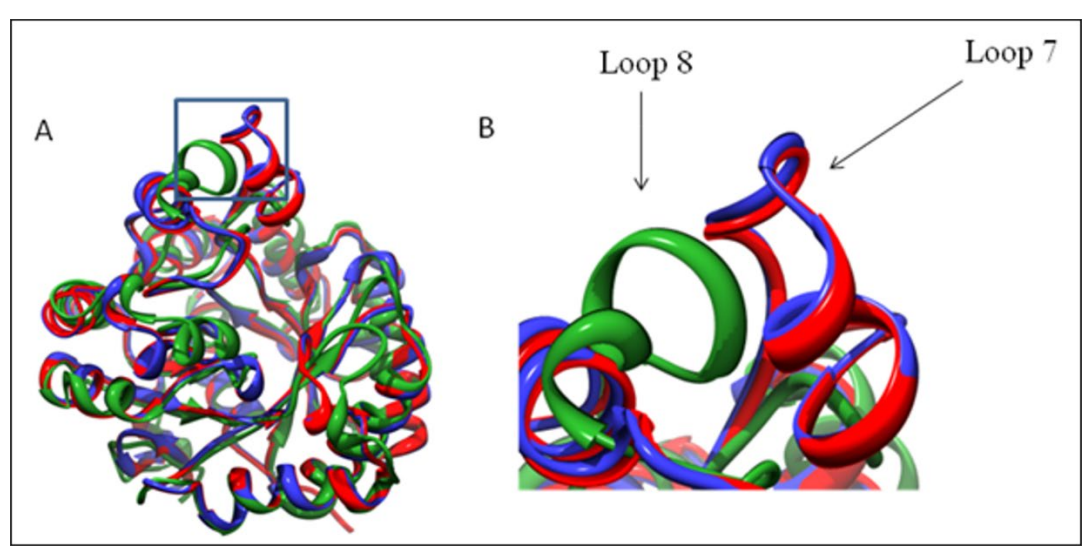


Fig. 3.9: Superimposition of OPH of *B. diminuta* (RED) and *A. radiobacter* (BLUE) with the phosphotriesterase like lactonases PLLs, (green) of *S. solfataricus* (SsoPox), Absence of 15 residue long loop 7 in SsoPox, is shown with arrow mark (Parthasarathy et al., 2017).

Transport of nutrient across energy deprived outer membrane is a major challenge in Gram-negative bacteria (Posey and Gherardini, 2000; Postle and Larsen 2007; Schauer et al., 2007 & Schauer et al., 2008). The TonB dependent transport system plays an important role in the active transport of essential nutrients across the outer membrane (Schauer et al., 2008). As described in introduction section, it consists of two components, the outer membrane located TonB dependent transporter (TBDT) and the inner membrane associated

Ton-complex. The Ton-complex consists of PMF components ExbB/ExbD and energy transducer TonB. TonBDT system is involved in transport of a variety of nutrients including ferric-siderophores. Bacteria produce and release siderophores (iron carriers) in response to iron deficient conditions. Once released into environment, they chelate ferric (Fe⁺³) irons to form a stable Fe-siderophore complex. These complexes are translocated across outer membrane through TonB dependent transport system (Schauer et al., 2008). The siderophores, such as enterobactin (Ent) chelate ferric iron much more strongly than some of synthetic iron chelators like EDTA. Soon after transportation into periplasmic space the interactions between Fe and Ent need to be destabilized to facilitate the release of iron. Enterobactin is a cyclic triester with 2, 3-dihydroxybenzoylserine as a monomer (Raymond et al., 2003). The Gramnegative bacteria follow two independent strategies to destabilize interactions between Ent and ferric ions (Miethke and Marahiel 2007; Abergel et al., 2009). One of them is enzymatic hydrolysis of lactone ring (O'Brien et al., 1971; Greenwood and Luke, 1978; Brickman and McIntosh, 1992 & Lin et al., 2005). A periplasmically located esterases hydrolyzes the lactone backbone of Fe-Ent to weaken the interactions between Ent and Fe. The second strategy is to reduce Fe-Ent soon after reaching periplasmic space. The reduced Fe-Ent cannot hold iron and therefore is released in the periplasmic space. Once reduced, the iron free Ent is sent out of the outer membrane to fetch a fresh batch of iron from the environment (Loomis and Raymond 1991; Abergel et al., 2006). The reduction dependent release of Ent is physiologically favoured as it is more economical than the esterase dependent release of iron from Fe-Ent (Abergel et al., 2006). The esterase destroys one Ent molecules for every ferric ion transported into the periplasmic space. A new Ent molecule has to be made for transport of every single iron atom, which is a physiological burden on the cell. However, both the processes are found in gramnegative bacteria (Zeng et al., 2013).

Fig. 3.10: Structures of enterobactin and its ferric complex (Raymond et al., 2003).

Since OPH interacts with Ton-components of TonBDT system and possesses weak lactonase activity, a hypothesis was generated implicating OPH in Fe-Ent hydrolysis. However, both TLC and HPLC experiments did not support the hypothesis and showed no hydrolysis of either Ent or Fe-Ent in presence of OPH. A wide range of pH and temperature conditions were tested to examine Ent hydrolysis in presence of OPH. None of the conditions indicated existence of Ent hydrolase activity for OPH. However, both BNPAGE, SPR and fluorescence emission experiments suggested existence of interactions between OPH and Ent/Fe-Ent. Surprisingly Fe-Ent bound more strongly than Ent. Such differential affinities indicate physiological significance. An attempt was made to gain meaningful conclusion on these observations and the experimental design and inferences are described in subsequent chapters.



Identification of Enterobactin binding site in OPH

The study is primarily designed to understand the role of OPH in outer membrane transport as it has been shown to associate with outer membrane transport system, otherwise known as TonBDT system. It is involved in transport of several nutrients including ferric-enterobactin (Fe-Ent). Since OPH contains promiscuous lactonase activity, experiments were designed to test if Ent or Fe-Ent serve as substrates for OPH. The experiments designed in the first chapter failed to show Ent hydrolase activity. However, they have provided solid evidence on Ent-OPH interactions. In fact, the Fe-Ent showed better interactions with OPH and the dissociation appears to be very slow. Such unique interactions have suggested physiological relevance. Therefore, further studies were conducted to gain better insights on the interactions between OPH and Ent or Fe-Ent. The present chapter describes experimental procedures and results obtained on various aspects of OPH interactions. Initial experiments were done to test if active site of OPH has any role in observed interactions between OPH and Ent/Fe-Ent. As active site alterations failed to affect OPH-Ent interactions, further investigations were done to test if there exists an alternate site in OPH to bind with Ent/Fe-Ent. The second chapter describes experimental procedures followed and results obtained during the course of investigation.

4.1 Objective specific methodology

4.1.1 Generation of OPH variants

The expression plasmid pUCOPH, encoding mature OPH (mOPH) from a constitutively expressed promoter, was used as a template. Complementary oligos having mutations at the desired position were designed (Table-4.1) and used for performing site-directed mutagenesis. Three expression plasmids were generated to encode OPH variants OPH^{D301A} (pMD301A), OPH^{D301N} (pMD301N), OPH^{K82A} (pMK82A). These plasmids were first transformed into *E. coli* strain, and the expression and stability of the OPH variants were assessed both by performing western blots and measuring OPH activity. After establishing their stability and activity they were purified and used to perform SPR analysis following the procedures described in previous chapter.

TABLE 4.1: List of primers used in this study

Primer Name	Sequence (5'	Description
D301A-FP	CGTTTCGAATGCGTGGCTGTTCG	Primers used to generate OPH variant
		OPH ^{D301A} by performing site directed
		mutagenesis. The codon introduced to
D301A-RP	AGGATTTGTTTCATGTAGCCTTGG	substitute aspartic acid found at position
		301 to alanine in OPH sequences is shown
		in bold case.
D301N-FP	CGTTTCGAATAACTGGCTGTTCG	Primers used to generate OPH variant
		OPH ^{D301N} by performing site directed
		mutagenesis. The codon introduced to
D301N-RP	AGGATTTGTTTCATGTAGCCTTGG	substitute aspartic acid found at position
		301 to asparagine in OPH sequences is
		shown in bold case.
K82A-FP	TCTAGCGGAAGCGGCTGTGAGAG	Primers used to generate OPH variant
	GATTG	OPH ^{K82A} by performing site directed
K82A-RP	GCTTTGCGGCTACCGAAG	mutagenesis. The codon introduced to
K02A-KI	GCTTGCGGCTACCGAAG	substitute lysine found at position 82 to
		alanine in OPH sequences is shown in bold
		case.

TABLE 4.2: List of plasmids used in this study

Plasmid	Description	Reference
name		
pUCOPH	Amp ^r , opd cloned in pUC19 vector under the control of	Mulbry and
	constitutive promoter.	Karns, 1989a
pMD301A	Amp ^r , Expression plasmid. The pUCOPH derivative. Codes for	
	OPH ^{D301A} .	This Study
pMD301N	Amp ^r , Expression plasmid. The pUCOPH derivative. Codes for	
	OPH ^{D301N} .	This Study
pMK82A	Amp ^r , Expression plasmid. The pUCOPH derivative. Codes for	This Study
	OPH ^{K82A} .	

TABLE 4.3: List of strains used in this study

Strain	Genotype or Phenotype	Reference
name		
	$\lambda supE44$, $\Delta lacU169$ ($\Delta 80$ lacZ $\Delta M15$) hsdR17 recA1 endA1 gyrA96 thi1 relA1	Hanahan <i>et al</i> , 1983

4.1.2 Site-Directed Mutagenesis (SDM)

Site-directed mutagenesis (SDM) was performed to generate *opd* variants coding for (OPH^{D301A}, OPH^{D301N}, OPH^{K82A}). SDM was performed by using Q5 SDM Kit (NEB Labs) by following manufacturers protocols using plasmid (pUCOPH) as a template. Briefly, the SDM was performed by using complementary oligonucleotide primers designed taking the sequence of *opd* gene into consideration (Table 4.1). The region of the *opd* gene containing the codon to be altered was identified and complementary oligos were designed by introducing the required alteration in the sequence of the primer. The sequence found upstream and downstream region of the codon to be altered remain perfect complements for *opd* gene. Plasmid pUCOPH (Table 4.2) was used as template. The *PfuTurbo* DNA polymerase was used in PCR reaction. The PCR product generated was treated with KLD enzyme mix consisting of Kinase, Ligase, DpnI. The KLD treated PCR product was transformed into the *E. coli* strain.

4.1.3 Generation of expression plasmid pMD301A

While generating OPH variants by SDM plasmid pUCOPH coding mature form of OPH (mOPH) was used as template. The OPH^{D301A} coding expression plasmid was generated by using primer pair D301A-FP/D301A-RP corresponding to the region of *opd* gene that specify aspartate at 301 position (Table-4.1). These primers were complementary to the *opd* region except that in the region that specifies 301 aspartate. At this position the GAC that codes for aspartate was changed to GCG to specify alanine in place of aspartate. PCR was performed for 30 cycles using pUCOPH as template using 93 $^{\circ}$ C as denaturing, 57 $^{\circ}$ C annelation and 72 $^{\circ}$ C as extension temperatures. The resulting PCR product was gel extracted and digested with DpnI to eliminate parent molecules. The DpnI resistant amplicons were transformed into *E. coli* DH5 α and insertion of desired mutation that substitutes aspartate to alanine is confirmed by sequencing the plasmid. The plasmid that contains GCG in place of GAC was designated as pMD301A was used for further studies. The pMD301A codes for OPH variant OPH^{D301A}.

4.1.4 Generation of expression plasmid pMD301N

While generating expression plasmid to code OPH^{D301N} the primer set D301N-FP/D301N-RP were used (Table-4.1). These primers were complementary to the *opd* region except in the region that specifies 301 aspartate. At this position the GAC that codes for aspartate was changed to AAC to substitute asparagine in place of aspartate. PCR was performed for 30 cycles using pUCOPH as template using 93°C as denaturing, 57°C annelation and 72°C as extension temperatures. The resulting PCR product was gel extracted and digested with DpnI to eliminate parent molecules. The DpnI resistant amplicons were transformed into *E. coli* DH5 α and insertion of desired mutation that substitutes aspartate to asparagine is confirmed by sequencing the plasmid. The plasmid that contains AAC in place of GAC was designated as pMD301N was used for further studies. The pMD301N codes for OPH variant OPH^{D301N}.

4.1.5 Generation of expression plasmid pMK82A

While generating expression plasmid to code OPH^{K82A} the primer set K82A-FP/ K82A-RP were used (Table-4.1). These primers were complementary to the *opd* region except in the region that specifies 82 lysine. At this position the AAG that codes for lysine was changed to GCG to substitute alanine in place of lysine. PCR was performed for 30 cycles using pUCOPH as template using 93°C as denaturing, 56°C annelation and 72°C as extension temperatures. The resulting PCR product was gel extracted and digested with DpnI to eliminate parent molecules. The DpnI resistant amplicons were transformed into *E. coli* DH5α and insertion of desired mutation that substitutes lysine to alanine is confirmed by sequencing the plasmid. The plasmid that contains GCG in place of AAG was designated as pMK82A was used for further studies. The pMK82A codes for OPH variant OPH^{K82A}.

4.1.6 Expression of OPH variants

The expression plasmids coding OPH variants pMD301A (OPH^{D301A}), pMD301N (OPH^{D301N}), pMK82A (OPH^{K82A}) were transformed independently into *E. coli* DH5α cells and grown in 10ml LB medium at 30°C for 16 h with shaking at 200 rpm. Cells were harvested at 6000 rpm for 5 min and the obtained cell pellet was dissolved in 1ml of lysis buffer (PBS pH 7.4, 5% glycerol, 150mM NaCl, 1mM PMSF, 50 μg lysozyme). After the suspension of cells in lysis buffer the contents were sonicated for 5 min to lyse the cells. The lysate was centrifuged

for 10 minutes at 13,000 rpm and the supernatant obtained was used to perform OPH activity and to detect OPH by performing western blot.

4.1.7 Measurement of Triesterase Activity

The triesterase activity of OPH and its variants was measured by following standard protocols described elsewhere (Chaudhry et al., 1988). Briefly, the reaction was carried out in a 1ml reaction mix containing 100μM of methyl parathion, 1μM of CoCl₂ in 50mM CHES buffer (pH9.0). The clear cell lysates prepared from cells expressing either OPH or its variants (10μg) were added to the reaction tubes and the contents were incubated at 37°C for 10 minutes. The formation of *p*-nitrophenol (PNP) was measured at 410nm and the activity was measured by calculating the amount of PNP released /mg of protein/minute (Chaudhry et al., 1988).

4.1.8 Purification of OPH variants

In the preceding chapter, the detailed protocols used for purification of OPH were described. The same procedures were followed for purification of OPH variants. Purification of OPH variants OPH^{D301A}, OPH^{D301N}, OPH^{K82A} were performed by following established protocols (Omburo et al., 1992). Fresh overnight culture of DH5 α containing expression plasmids pMD301A (OPH^{D301A}), pMD301N (OPH^{D301N}) and pMK82A (OPH^{K82A}) were independently inoculated in 3 L of terrific broth supplemented with 50 μ g/ml of ampicillin. After 12 hours an additional amount of 50 μ g/ml of ampicillin was added to the culture medium to maintain selection pressure for retaining the cultures with plasmid. After 36 hours, the culture was centrifuged at 8000 rpm for 10 minutes, to harvest the cells. Cell lysis, ammonium sulphate precipitation and purification by ion exchange, gel filtration chromatography experiments were done for purification of OPH variants strictly by following the procedures described for purification of wildtype OPH (Methods Section, Chapter-I).

4.1.9 Circular Dichroism (CD) Spectroscopy

CD spectra for OPH and its variants OPH^{D301A}, OPH^{D301N}, OPH^{K82A} were obtained using a Jasco J-810 spectropolarimeter (JAPAN) using a quartz cuvette with path-length of 0.2 cm in a nitrogen atmosphere at 25°C. Using either pure OPH (0.1 mg) or its variants in a clean quartz cuvette, three scans were performed at a rate of 50nm/min. The spectral data were recorded in the range of 190 to 270nm. The obtained spectra were overlaid to observe structural changes between wild type OPH and its variants.

4.1.10 Fluorescence emission measurements

Room temperature fluorescence emission spectra were recorded with a LS-55 Spectrofluorimeter (PerkinElmer Inc., USA) fitted with 1 cm quartz cuvettes at RT with a wavelength range of 300–450 nm with an excitation wavelength of 280 nm, and slit width of 5.0 nm for both excitation and emission. The sample temperature was kept constant at 25°C. The concentration of OPH variants OPH^{D301A}, OPH^{D301N} were fixed at 1μM, and the concentrations of ferric-enterobactin (Fe-Ent) dissolved in 0.01M sodium phosphate buffer (pH 7.4) was varied from 1 to 11μM. Three independent experiments were performed to obtain statistically significant data following procedures described in materials and methods section of chapter I.

4.2 Identification of Ent/Fe-Ent binding site- in silico predictions

4.2.1 Prediction and investigation of a potential secondary binding site

In order to investigate alternate site for binding to Fe-Ent targeted docking was performed for OPH by using Autodock4.2 (Morris et al., 2009). From the Protein Data Bank (PDB) the crystal structure of OPH homodimer (PDB Id:1EYW) bound with substrate analog triethyl phosphate was taken and the Ferric-Enterobactin 3D structure was retrieved from the crystal structure of a siderocalin- Fe-Ent complex (PDB Id:3CMP). While doing docking studies homodimer structure of OPH was used as a receptor and Fe-Ent structure was used as ligand. The substrate analogue was removed along with water molecules except for the one near at the Zn metal ion at the catalytic site. Thirty runs of docking were attempted using the genetic algorithm in AutoDock. The docking poses were analyzed using AutoDock Tools. Pymol was used for visualization of the docking poses.

4.3 Results & Discussion

After establishing OPH-Fe-Ent interactions, attempts were made to map Fe-Ent binding site in OPH. Since its binding to OPH is established, initially it was assumed that the active site of OPH would be serving as the binding site of Ent. If the proposed hypothesis is true if the active site architecture is altered there should be no interactions between OPH and Ent. In fact, the observed interactions should seize to exists between OPH variant having active site mutations and the Ent/Fe-Ent. While testing this proposition the active site architecture of the OPH was altered by substituting active site residue with amino acids having either simple or bulky side chains. Crystal structure of OPH is known and its active site is well established (Benning et al., 2001). In OPH at least five amino acids are part of OPH active site. Among

them four are histidine residues found at positions 55,57,201,230 and coordinate to keep Zn ions at the active site. Substitutions to these residues affect Zn binding to OPH and hence they were not changed. The active site aspartic acid (Asp³⁰¹) interacts with substrate and plays a critical role in hydrolysis of OP compounds (Benning et al., 2001). If substitutions are made to this active site aspartic acid, which has no role in keeping Zn ions at active site, it should not affect the overall structure of the protein, except catalytic activity. Such variants of OPH are expected to serve as good candidate molecules to test interactions with Ent/Fe-Ent and to ascertain the role of active site in interacting with OPH. Therefore, the active site architecture of OPH is altered by substituting active site aspartate with amino acids having small (alanine) and bulky (asparagine) side chains (Fig. 4.1).

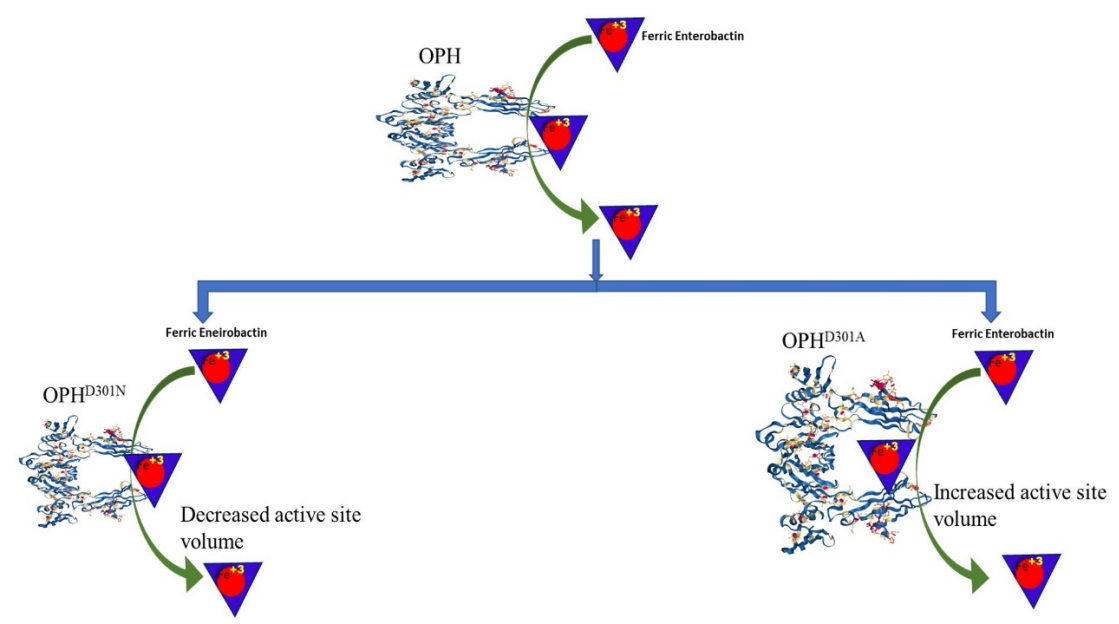


Fig. 4.1: Schematic diagram showing alteration of active site architecture by substituting active site aspartate with alanine and asparagine.

4.3.1 OPH with reduced active site volume (OPHD301N)

The active site aspartate was substituted with asparagine to create OPH variant with reduced active site volume. The insertion of the desired codon that specifies asparagine instead of aspartate was established by sequencing the expression plasmid, pMD301N generated by introducing AAC codon at nucleotide position 901 of *opd* gene. The substitution was validated by sequencing the plasmid pMD301N (Fig. 4.2. Panel A). The chromatogram clearly showed insertion of codon AAC in place of GAC in plasmid pMD301N. Such change clearly suggests substitution of aspartate with asparagine in OPH. After confirming substitution of Asp with Asn the OPH variant OPH^{D301N} was tested its stability and ability to perform triesterase activity

using methyl parathion as substrate. The stability of OPH^{D301N} was determined by performing western blot. The OPH^{D301N}, found to be stable like wildtype OPH (Fig. 4.2. Panel B & C). However, as expected the OPH^{D301N} has lost triesterase activity. As against 81.16μmole PNP/mg/min of specific activity obtained for wild type OPH, the OPH^{D301N} showed just 3.32μmole PNP/mg/min activity, clearly indicating loss of triesterase activity in OPH^{D301N} (Fig. 4.2. Panel D) (Tsai et al., 2012; Bigley et al., 2015).

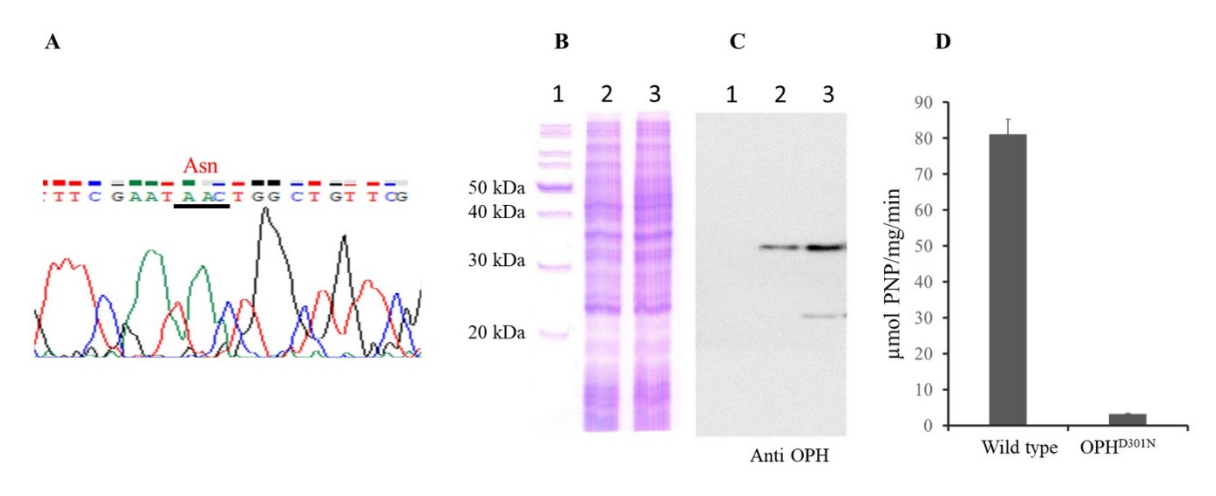


Fig. 4.2: Generation of OPH variant OPH^{D301N}. Panel A shows the chromatogram generated using plasmid pMD301N as a template. Insertion of codon AAC, which specifies asparagine, in place of GAC is underlined. Panel B and C shows the expression and subsequent detection of OPH^{D301N} in *E. coli* DH5α (pMD301N). The SDS-PAGE (12.5%) (Panel B) and corresponding western blot (Panel C) probed with anti-OPH antibodies shows stability of expressed OPH^{D301N}. Lane 1 shows the protein molecular weight marker. The protein extracts prepared from cells expressing OPH^{D301N} (Lane 2), and native OPH (Lane 3) show stable expression of OPH^{D301N}. The triesterase activity measured using methyl parathion as substrate for OPH and OPH^{D301N} is shown in panel D. Loss of triesterase activity for OPH^{D301N} clearly seen.

4.3.2 Purification of OPH variant (OPHD301N)

The purification of OPH^{D301N} was done following the methodology used to purify wild type OPH (vide chapter-1). The cell lysate prepared from *E. coli* DH5α (pMD301N) cells were subjected to ammonium sulphate (AS) precipitation. The pellet obtained from AS precipitation was dialyzed and passed through SP Sepharose column and the elution fractions were pooled and analyzed on a 12.5 % SDS-PAGE gel. As shown in SDS-PAGE the protein band that coincides the molecular mass of OPH was enriched in elution fractions (Fig. 4.3. Panel A Lanes 6-8). The fractions with enriched OPH^{D301N} were pooled and passed through DEAE Sepharose column. Most of the contaminating proteins have remained in the DEAE column as the SDS-PAGE clearly shows existence of pure protein that corresponds to the size of OPH^{D301N} (Fig. 4.3. Panel B). Although the DEAE purified OPH^{D301N} is purified to electrophoretic homogeneity and final round of purification was done by passing the DEAE

purified OPH^{D301N} through gel filtration column. The OPH^{D301N} came out of gel filtration column appears to be pure and hence was used for performing further experiments (Fig. 4.3. Panel C).

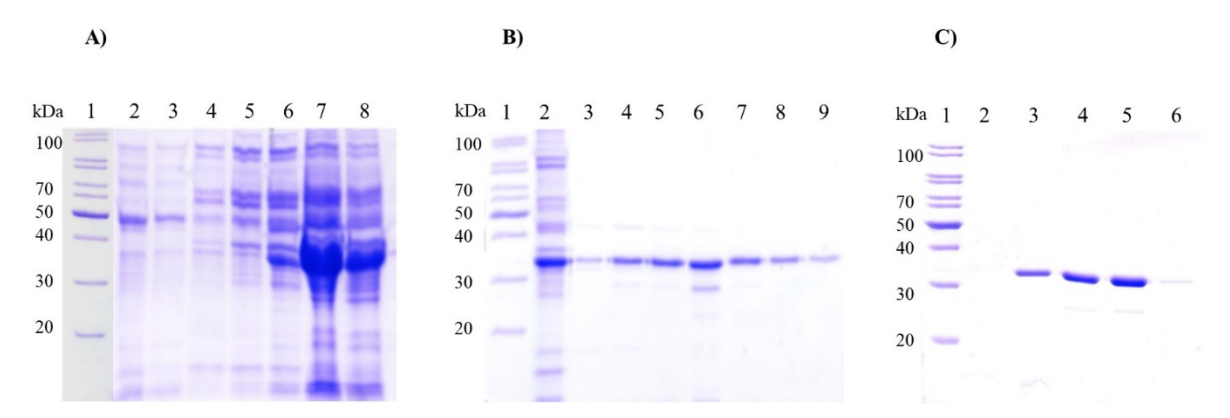


Fig. 4.3: Purification of OPH^{D301N}. Panel A, B & C represent SDS-PAGE (12.5%) used to determine the purity of OPH^{D301N} during different stages of purification. Panel A shows protein profile obtained during OPH^{D301N} purification using SP Sepharose column: lane 1 shows the protein molecular weight marker. Proteins found in AS fraction used as input are shown in lane 2. The protein profile obtained for flowthrough (lane 3), wash (lane 4) and elution fractions (lane 5-8) are shown in panel A. Panel B shows protein profile obtained for flowthrough fractions collected from DEAE Sepharose column (2-8) and native OPH loaded as size marker is shown in lane 9. The pure OPH^{D301N} obtained from gel filtrations column are shown in panel C.

4.3.3 OPH^{D301N} retains native conformation

The cell lysate expressing OPH^{D301N} failed to show triesterase activity. However, the western blots clearly showed existence of OPH^{D301N} in the cell lysate (Figure. 4.2. Panel C Lane 2). The loss of triesterase activity could also be either due to substitution of asparagine to active site aspartate or it may also be due to structural distortion due to amino acid substitution. Before proceeding to conduct further experiments on OPH^{D301N}-Fe-Ent interactions, the structural identity of OPH^{D301N} with wild type OPH was assessed by measuring Circular Dichroism (CD) spectrum for these two proteins. Interestingly, the CD spectrum obtained for OPH^{D301N} was identical to the CD spectrum obtained for wild type OPH. There were no deviations in the spectral properties of these two proteins (Fig. 4.4. Panel D). The protein stability as revealed by western blot and CD spectrum clearly suggest that the OPH^{D301N} is structurally identical to the wild type OPH except that it has lost triesterase activity due to substitution of active site aspartate with asparagine. The pure OPH^{D301N} was stored at -80°C and used for conducting further experiments.

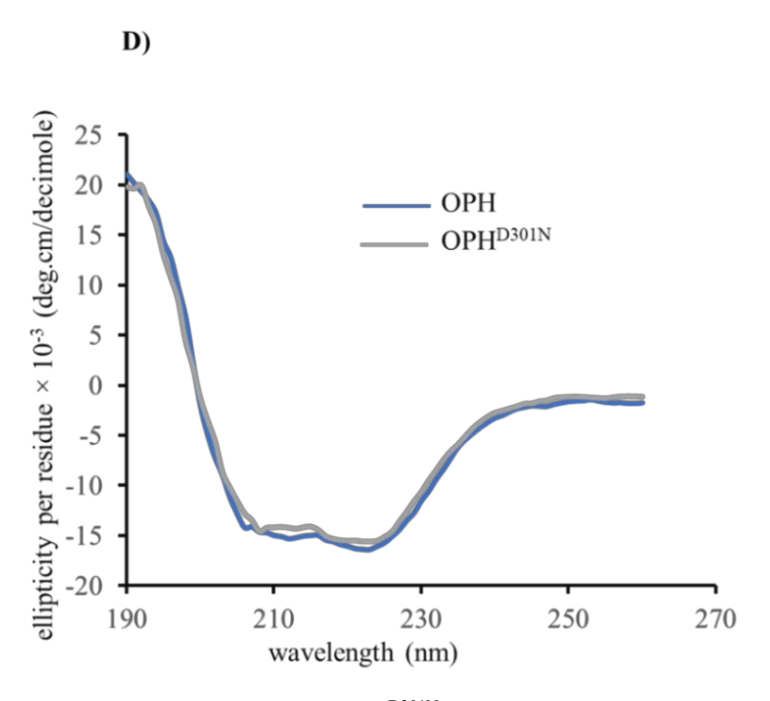


Fig. 4.4: CD spectra obtained for OPH (———) and OPH^{D301N} (———) are overlaid to show structural similarities between OPH and OPH^{D301N}.

4.3.4 OPH with increased active site volume (OPHD301A)

The active site aspartate was substituted with alanine to create OPH variant with increased active site volume. The insertion of the desired codon that specifies alanine instead of aspartate was successfully achieved by performing site directed mutagenesis following method described in methods section. The change in the sequence was confirmed by determining the sequence of expression plasmid, pMD301A. The chromatogram clearly shown insertion of GCG codon at nucleotide position 901 of opd gene by replacing the codon GAC found in wild type gene (Fig. 4.5. Panel A). The chromatogram clearly shows insertion of codon GCG in place of GAC in plasmid pMD301A. Such change clearly suggests substitution of alanine in place of aspartate found at position 301 in OPH. The cell lysates containing OPH^{D301A} were then used to perform triesterase activity using methyl parathion as substrate. As expected, the OPH^{D301A} failed to show triesterase activity (Fig. 4.5. Panel D), despite of showing its stability in cell lysate (Fig. 4.5. Panel B & C). As against 81.16µmole PNP/mg/min of specific activity obtained for wild type OPH, the OPH^{D301A} showed just 3.26µmole PNP/mg/min activity, clearly indicating loss of triesterase activity in OPH^{D301A} (Fig. 4.5. Panel D). Finally, before going to perform further studies using OPHD301A its overall structural identity with wild type OPH was established by overlying the CD spectra taken for these two proteins (Fig. 4.7. Panel D). Obtaining such spectra required pure OPHD301A. The following section describes purification strategies followed for obtaining pure OPH^{D301A}.

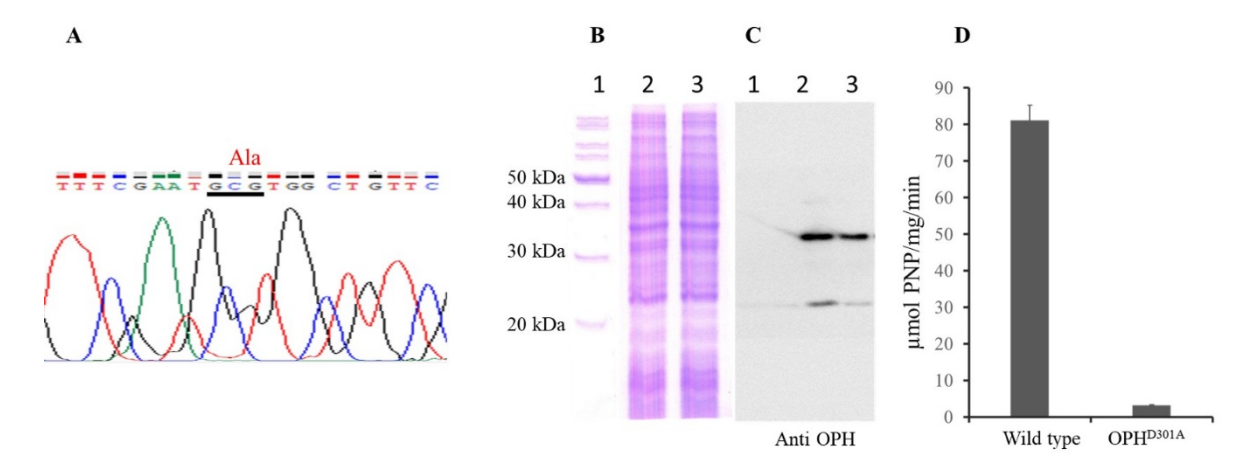


Fig. 4.5: Generation OPH^{D301A}. Panel A shows the chromatogram generated using plasmid pMD301A as a template. Insertion of codon GCG, which specifies alanine, in place of GAC is underlined. Panel B and C shows the expression and subsequent detection of OPH^{D301A} in *E. coli* DH5α (pMD301A). The SDS-PAGE (12.5%) (Panel B) and corresponding western blot (Panel C) probed with anti-OPH antibodies shows stability of expressed OPH^{D301A}. Lane 1 shows the protein molecular weight marker. The protein extracts prepared from cells expressing OPH^{D301A} (Lane 2), and native OPH (Lane 3) show stable expression of OPH^{D301A}. The triesterase activity measured using methyl parathion as substrate for OPH and OPH^{D301A} is shown in panel D. Loss of triesterase activity for OPH^{D301A}. clearly seen.

4.3.5 Purification of OPH variant (OPHD301A)

The purification of OPH^{D301A} was followed the methodology described in earlier chapter-1. The cell lysate prepared from *E. coli* DH5α (pMD301A) cells were subjected to ammonium sulphate (AS) precipitation. The pellet obtained from AS precipitation was dialyzed and passed through SP Sepharose column and the elution fractions were analyzed on a 12.5 % SDS-PAGE gel (Fig. 4.6. Panel A). The fractions enriched with OPH^{D301A} were pooled and passed through DEAE Sepharose column. The flowthrough fractions were collected and loaded on SDS-PAGE gel along with native OPH used as size marker (Fig. 4.6. Panel B). The OPH^{D301A} enriched fractions were passed through DEAE column appears to be equal to the size of native OPH. Most of the contaminating proteins were retained in the column. The eluted OPH^{D301A} was further through gel filtration column to obtain pure protein to be used for further experiments (Fig. 4.6. Panel C).

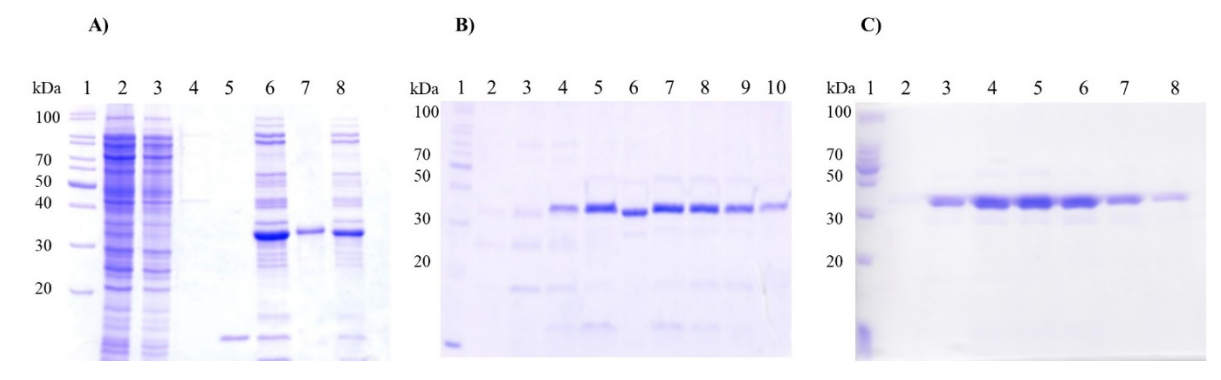


Fig. 4.6: Purification of OPH^{D301A}. Panel A, B & C represent SDS-PAGE (12.5%) used to determine the purity of OPH^{D301A} during different stages of purification. Panel A shows protein profile obtained during OPH^{D301A} purification using SP Sepharose column: lane 1 shows the protein molecular weight marker. Proteins found in AS fraction used as input are shown in lane 2. The protein profile obtained for flowthrough (lane 3), wash (lane 4) and elution fractions (lane 5-8) are shown in panel A. Panel B shows protein profile obtained for flowthrough fractions collected from DEAE Sepharose column (2-9) and native OPH loaded as size marker is shown in lane 10. The pure OPH^{D301A} obtained from gel filtrations column are shown in panel C.

4.3.6 Structural stability of OPHD301A

The loss of triesterase activity was clearly shown by assaying the cell lysate containing OPH^{D301A}. The expressed OPH^{D301A} was also stable as the western blots were done using anti-OPH antibodies have clearly shown the stability of the expressed protein (Fig. 4.5. Panel C). However, these two experiments fail to show if OPH^{D301A} retains the native conformation like wild type OPH. Therefore, the purified OPH^{D301A} was used to measure Circular Dichroism (CD) spectrum. The spectra obtained was then overlaid to observe structural changes in OPH^{D301A} (Fig. 4.7. Panel D). There was no deviation in the spectral properties of these two proteins (Fig.4.7. Panel D). The CD spectrum clearly suggests that the OPH^{D301A} is structurally identical to OPH, except that it has lost triesterase activity due to substitution of active site aspartate with alanine. The pure OPH^{D301A} was then used for conducting further studies to establish OPH-Fe-Ent interactions.

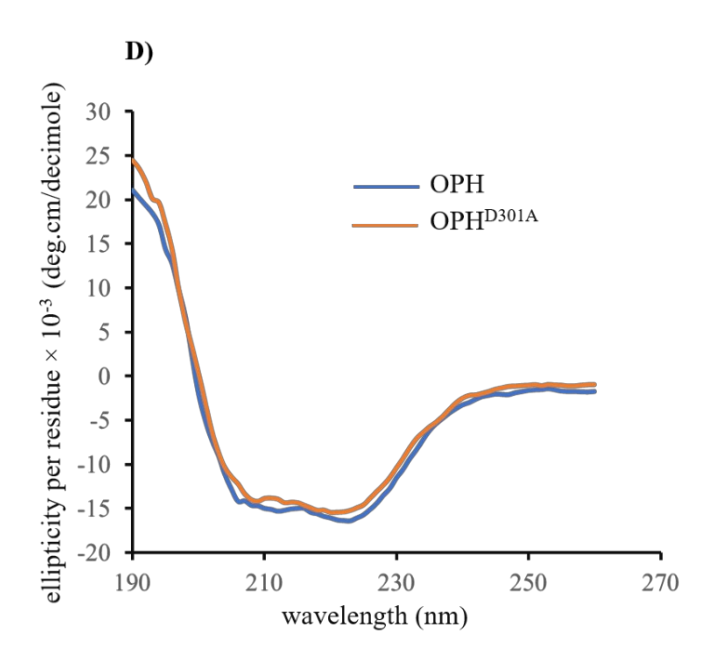


Fig. 4.7: CD spectra obtained for OPH (——) and OPH^{D301A} (——) are overlaid to show structural similarities between OPH and OPH^{D301A}.

4.3.7 Ent/Fe-Ent binding ability is independent of triesterase activity

After purification, the triesterase negative OPH variants were immobilized independently on CM7 sensor chip (GE Healthcare). Subsequently, the Fe-Ent prepared as described in chapter-I was passed ranging from $3.12\mu\text{M}$ to $100\mu\text{M}$ over CM7 chip immobilized either with OPH^{D301A} or OPH^{D301N} to obtain the binding response units. Interestingly, both OPH variants, OPH^{D301A}, OPH^{D301N} interacted with the Fe-Ent and the binding kinetics were equal to the wild type OPH. The association (k_a) and dissociation (k_d) rate constants between OPH^{D301A} and Fe-Ent were 1.46E+02 (1/Ms) and 8.94E-03(1/s) respectively and with the equilibrium constant dissociation (k_D) of 6.12E-05 M (Fig. 4.8. Panel A & B).

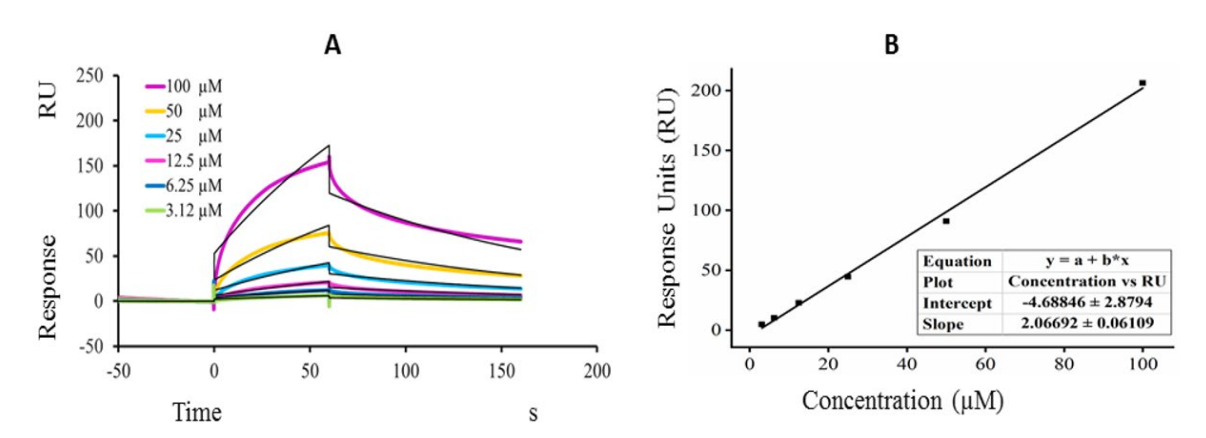


Fig. 4.8: OPH^{D301A} and Fe-Ent interactions. SPR analysis was done using Biocore T200. Sensorgrams generated at different time points by passing increased concentrations of Fe-Ent over CM7-sensor chip having immobilized OPH^{D301A}. Graph was plotted taking response units on 'Y' and time on 'X' axis (Panel A). Similar graph plated using response units versus Fe-Ent concentration is shown in (Panel B).

Whereas for OPH^{D301N}, the association (k_a) and dissociation (k_d) rate constants were 1.63E+02 (1/Ms) and 1.14E-02(1/s) respectively and with the equilibrium constant dissociation (K_D) of 6.97E-05 M (Fig. 4.9. Panel A & B). The binding kinetic clearly suggested that the Fe-Ent binding ability was totally independent of triesterase activity. The data also suggests that OPH doesn't involve its active site while interacting with Fe-Ent.

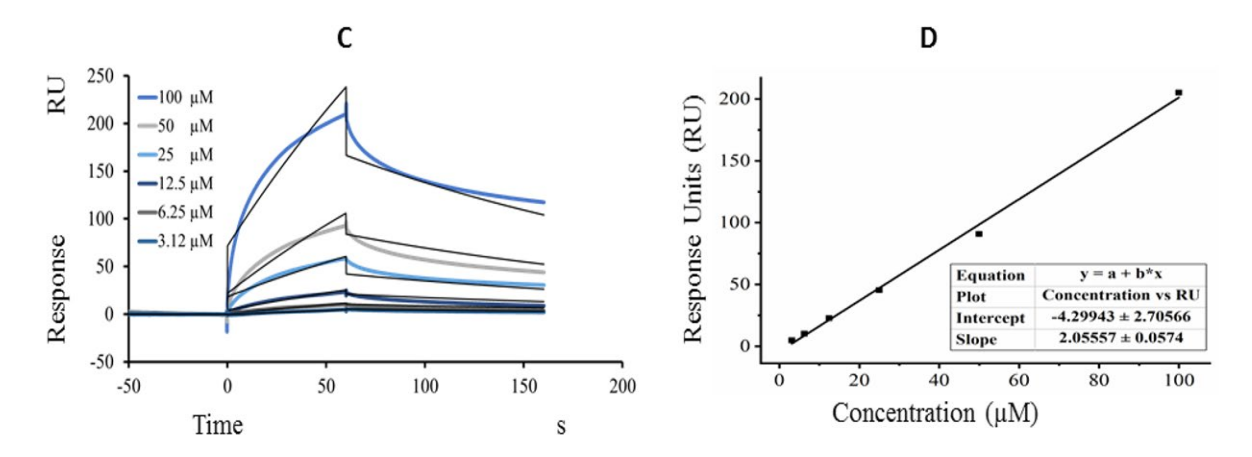


Fig. 4.9: OPH^{D301N} and Fe-Ent interactions. SPR analysis was done using Biocore T200. Sensorgrams generated at different time interval by passing increased concentrations of Fe-Ent over CM7-sensor chip having immobilized OPH^{D301N}. Graph was plotted taking response units on 'Y' and time on 'X' axis (Panel A). Similar graph plated using response units versus Fe-Ent concentration is shown in (Panel B).

4.3.8 Measurement of Fluorescence Emission Maximum

The supporting evidence on binding of OPH variants OPH^{D301N} and OPH^{D301A} to Fe-Ent was also obtained by measuring the intrinsic fluorescence emission maximum intensity of OPH variants OPH^{D301A} and OPH^{D301N} at different concentrations of Fe-Ent. Basically, the Fe-Ent show no fluorescence (Fig. 4.10. Panel A & B). However, when it was added to OPH variants OPH^{D301A} and OPH^{D301N} in increasing concentrations (0.001-0.011 mM) maximum fluorescence emission obtained at 335 nm was proportionately decreased (Fig. 4.10. Panel A & B). This observation clearly showed concentration dependent quenching of fluorescence. As in case of wild type OPH, a total quench in the fluorescence of OPH^{D301A} and OPH^{D301N} was observed at maximum concentrations of Fe-Ent. Further, a good linear relationship has been seen between concentration of Fe-Ent and fluorescence quenching of OPH and its variants (Fig. 4.10. Panel A & B). Likewise, the binding dissociation constants for Fe-Ent with OPH variants OPH^{D301A} and OPH^{D301N} show all most identity with the wild type OPH. (Table 4.4). Interestingly the kinetic values determined by using fluorescence emission showed very good correlation with binding kinetics determined by SPR data (Fig. 4.8. Panel B & Fig. 4.9. Panel

D). As described these independent studies involving SPR and fluorescence emission indicated existence of interactions between OPH variants OPH^{D301A} and OPH^{D301N} with Fe-Ent suggesting existence of alternate Fe-Ent binding site in OPH.

TABLE 4.4: The association and dissociation constants of OPH^{D301A} and OPH^{D301N} with Fe-Ent.

Sample	Ka	<i>K</i> d
OPH ^{D301A} -Fe Ent	2.32×10 ⁶ M ⁻¹	5.91716E-06 M ± 4.7655E-10 M
OPH ^{D301N} -Fe Ent	9.01×10 ⁵ M ⁻¹	1.10988E-06 M ± 5.2915E-11 M

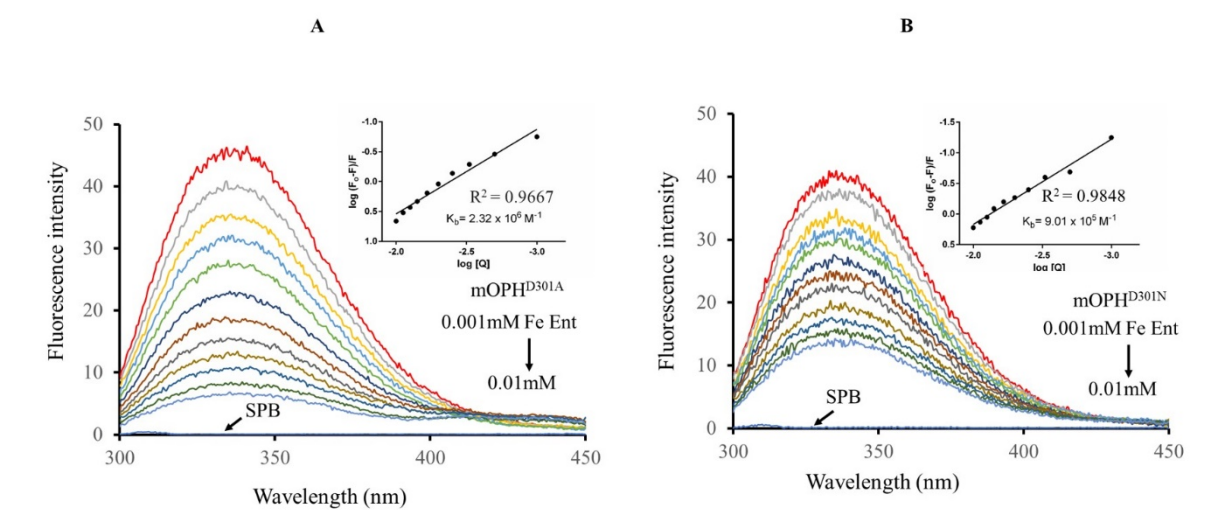


Fig. 4.10: Panels A and B show the fluorescence emission spectra taken for OPH variants OPH^{D301A} (A) and OPH^{D301N} (B) in presence of increasing concentrations (1 to 11 μ M) of ferric-enterobactin. The observed fluorescence quench with the increasing concentrations (1 to 11 μ M) of Fe-Ent is shown. The inset shows modified Stern–Volmer plots obtained by plotting Log [Q] values on X-axis and Log [dF/F] values on Y-axis. The slope of the plot indicates number of binding sites. The Y intercept gives log K values. The binding constant values were calculated from log K. Lack of fluorescence emission for buffer (SPB) containing Fe-Ent is shown with an arrow.

4.4 In silico prediction of Ent binding site

After showing that ferric enterobactin interaction was independent of triesterase activity of OPH, *in-silico* experiments were performed to gain preliminary information on existence of secondary binding site. The blind docking was performed for ferric enterobactin on OPH using AutoDock and obtained 7 different potential secondary binding sites. Among these seven predicted sites three potential binding sites withstood the predictions of PARS server (Panjkovich and Daura, 2014). Out of these three sites, two sites were identical to each other, situated on both of the monomers related

by the dimer symmetry, and the third one was at the dimer interface. The sites on the two monomers corresponded to the best binding energy (Fig. 4.11. Panel A). The best pose obtained from the docking study is stabilized by side chains of residues lysine (82) and arginine (85) placed between two of the three catechol rings through hydrogen bonding interactions as shown in Fig. 4.11. Panel B & C. Surprisingly, similar interactions were reported for xenosiderophores with Factor H binding protein (fHbp) of *Neisseria meningitides* (Veggi et al., 2012).

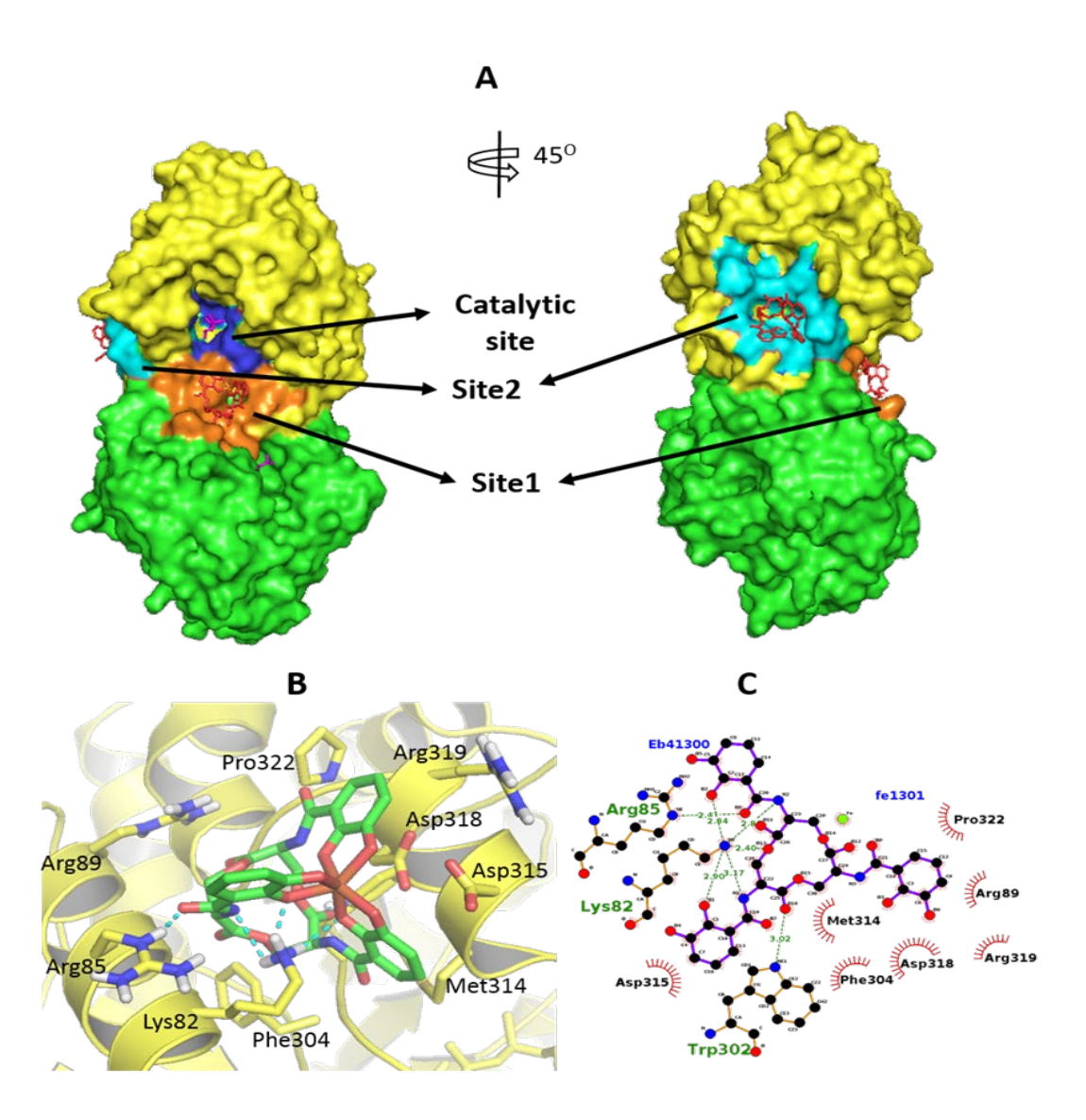


Fig. 4.11: The Fe-Ent binding site in OPH. Panel A shows the *in silico*-predicted enterobactin binding sites. Panels B and C shows the best pose obtained from the docking study after stabilizing the side chain residues lysine 82 and arginine 85 placed between two of the three catechol rings by hydrogen bonding interactions.

4.4.1 OPH variant OPH^{K82A} retains native structure and triesterase activity

The *in-silico* predicted enterobactin binding site was validated by generating OPH variants having mutations at Ent binding site. As shown in figure 4. 11 Panel C, lysine

found at position 82 is very critical for interacting with Ent. If this lysine is changed to alanine, the positive charge required to facilitate Ent interactions would not be there and it is expected to affect OPH interactions with Ent. Therefore, OPH variant was generated by substituting alanine in place of lysine. The insertion of codon, GCG that specifies alanine in the place of lysine in the sequence of opd gene was done by performing site directed mutagenesis. The inserted changes were then established by sequencing the DpnI resistant pUCOPH plasmid used as template while performing site directed mutagenesis. The plasmid that confirmed existence of, GCG codon in place of AAG in pMK82A at nucleotide position 244 of opd gene was taken and used for producing OPH^{K82A} and the expression plasmid was then designated as, pMK82A (Fig. 4.12. Panel A). The cell lysate prepared from E. coli (pMK82A) was used to test the stability and to test triesterase activity using methyl parathion as substrate. The stability of OPH^{K82A} was determined by performing western blot. The OPH^{K82A}, found to be stable like wildtype OPH (Fig. 4.12. Panel B & C). As expected, the lysine to alanine substitution at position 82, which is not closely located or part of active site did not affect the triesterase activity. The wild type OPH showed 81.16µmole PNP/mg/min of specific activity whereas, the OPH^{K82A} gave 79.6µmole PNP/mg/min activity under similar assay conditions, suggesting that OPH^{K82A} retained triesterase activity (Fig. 4.12. Panel D)

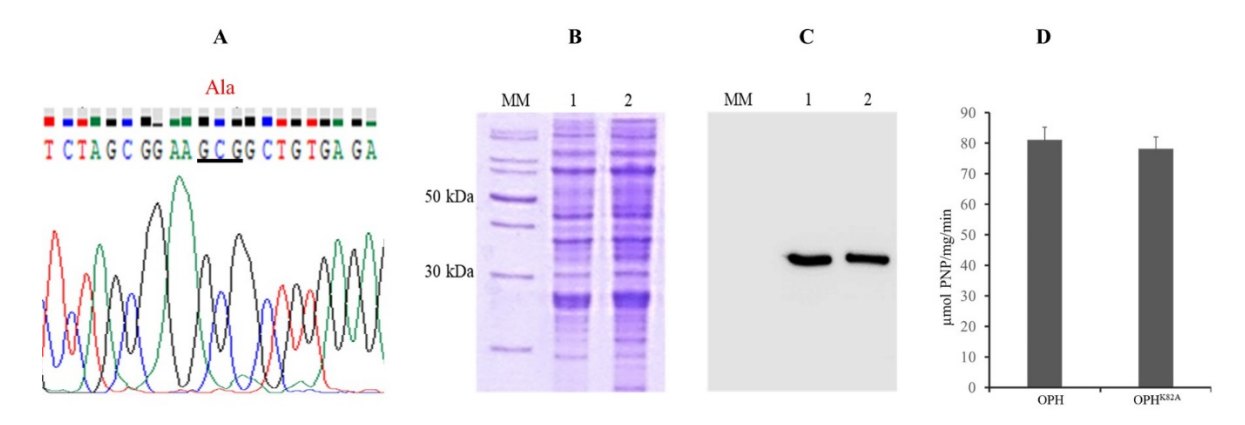


Fig. 4.12: Generation of OPH^{K82A}. Panel A shows the chromatogram generated using plasmid pMK82A as template. Change of codon from AAG to GCG is underlined. Panel B and C show SDS-PAGE (12.5%) and corresponding western blot probed with anti-OPH antibodies. Lane MM indicate lane loaded with protein molecular weight marker. The protein extracts prepared from cells expressing OPH^{K82A} and native OPH are loaded in lane 2 and 3 respectively. The triesterase activity of native OPH and OPH^{K82A} is shown in panel D.

4.4.2 Purification of OPH^{K82A}

The purification of OPH^{K82A} was done following procedures described elsewhere (chapter-I). The cell lysate prepared from E. coli DH5 α (pMK82A) cells was subjected to ammonium sulphate (AS) precipitation. The pellet obtained from AS precipitation

was dialyzed and passed through SP Sepharose column and the elution fractions were analyzed on a 12.5 % SDS-PAGE gel (Fig. 4.13. Panel A). The total fractions containing OPH activity were pooled and passed through DEAE Sepharose column. The flowthrough fractions were collected and loaded on SDS-PAGE gel along with native OPH, which served size control (Fig. 4.13. Panel B). The OPH^{K82A} protein from DEAE column appears to be equal to the size of native OPH were collected and the remaining contaminated proteins were eliminated by passing the partially pure OPH^{K82A} through gel filtration column. (Fig. 4.13. Panel C).

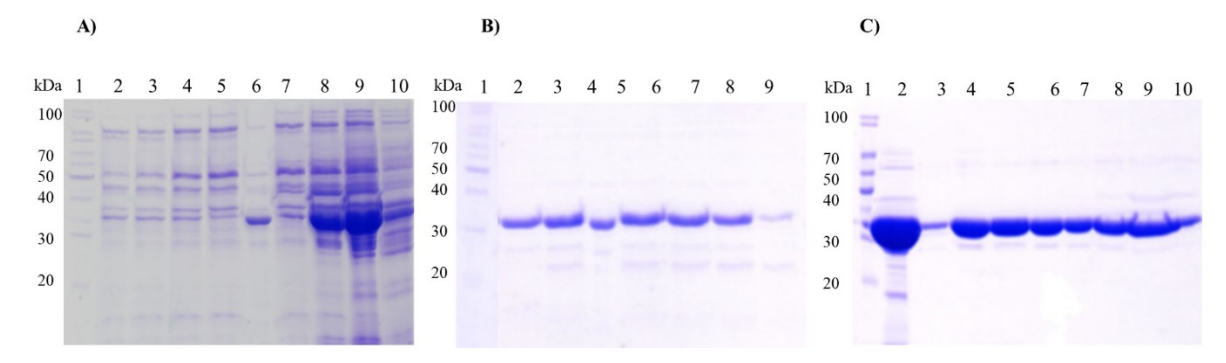


Fig. 4.13: Purification of OPH^{K82A}. Panel A, B & C represent 12.5 % SDS-PAGE used to determine the purity of OPH^{K82A} during different stages of purification. Panel A shows enrichment of OPH^{K82A} in elution fractions collected from SP Sepharose column: lane 1 shows the protein molecular weight marker. Proteins found in AS fraction used as input are seen in lane 2. Proteins found flowthrough (lane 3), wash (lane 4) and elution fractions (lane 5-10) are shown in Panel A. Proteins found in flowthrough fractions collected from DEAE Sepharose column was shown in panel B, lanes 2-8. The native OPH loaded as control is loaded in lane 9. The OPH positive peak fractions found in gel filtrations column are shown in panel C.

After purification of OPH^{K82A} CD spectrum was taken for OPH^{K82A} and it was overlaid with the similar spectra taken for wild type protein. Interestingly there was no difference between these two spectra suggesting that OPH^{K82A} shows structural identity to the wild type OPH (Fig. 4.14. Panel D). The protein stability as revealed by western blot and CD spectrum clearly suggest the OPH^{K82A} is structurally identical to OPH. After ascertaining structural features, the OPH^{K82A} protein was used to perform native PAGE and SPR to assess its ability to interact with Fe-Ent.

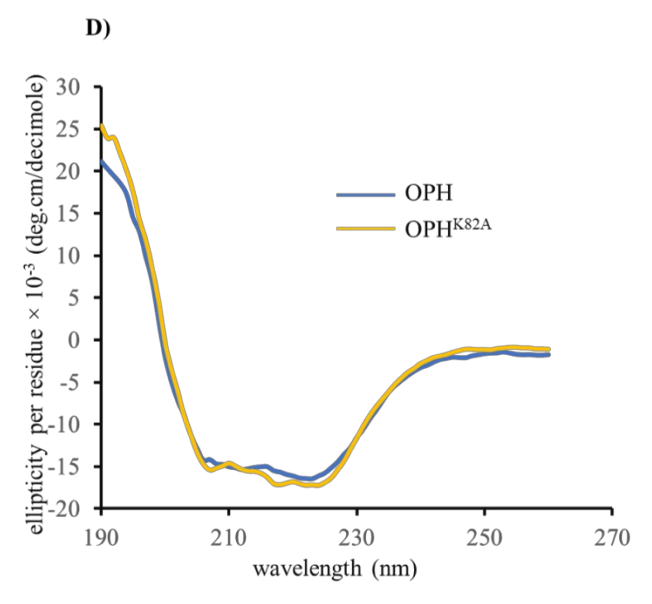


Fig. 4.14: CD spectra obtained for OPH (_____) and OPH^{K82A} (_____) are overlaid to show structural similarities between OPH and OPH^{K82A}.

4.4.3 Lysine residue is critical for interacting with Fe-Ent

Results described in earlier sections clearly suggest that the OPH^{K82A} is structurally similar to native OPH. It has also shown to retain triesterase activity like the wild type protein. The OPH^{K82A} was similar to wild type OPH, except that it doesn't contain lysine residue at predicted Ent binding site. Therefore, the pure OPH^{K82A} was used to perform both native PAGE and SPR to assess its interactions with Fe-Ent. Initially, the OPH^{K82A}-Fe-Ent interactions were studied using native PAGE. The purified OPH^{K82A} (10μM) was incubated with 100μM of Fe-Ent in 100mM sodium phosphate buffer (pH 8.0) and left at RT for 20 minutes. The complex formation was then analyzed by performing BNPAGE as described in methods section. There was no difference in mobility pattern of OPH in BNPAGE. Both OPH^{K82A} and OPH^{K82A} incubated with Fe-Ent showed similar mobility pattern (Fig. 4.15. Panel A Lane 2 & 3), suggesting that there was no formation OPH^{K82A}- Fe-Ent complex. There was no faster migrating band, typically generated due to formation of OPH-Fe-Ent, when Fe-Ent was incubated with wild type OPH (Fig. 3.5. Panel B Lane 2 & 3).

While generating secondary evidence on Fe-Ent and OPH^{K82A} interactions SPR was also performed using pure OPH^{K82A} immobilized on CM7 sensor chip (GE Healthcare). The Fe-Ent concentrations ranging from $3.12\mu M$ to $100\mu M$ were passed over OPH^{K82A}-CM7 chip to obtain the binding response units. Interestingly the sensorgram obtained has shown no response units, suggesting lysine, found at secondary binding site was critical

for interacting with Fe-Ent (Fig. 4.15. Panel B). The data generated from BNPAGE and SPR clearly supported *in-silico* predictions which suggested existence of a secondary binding site in OPH.

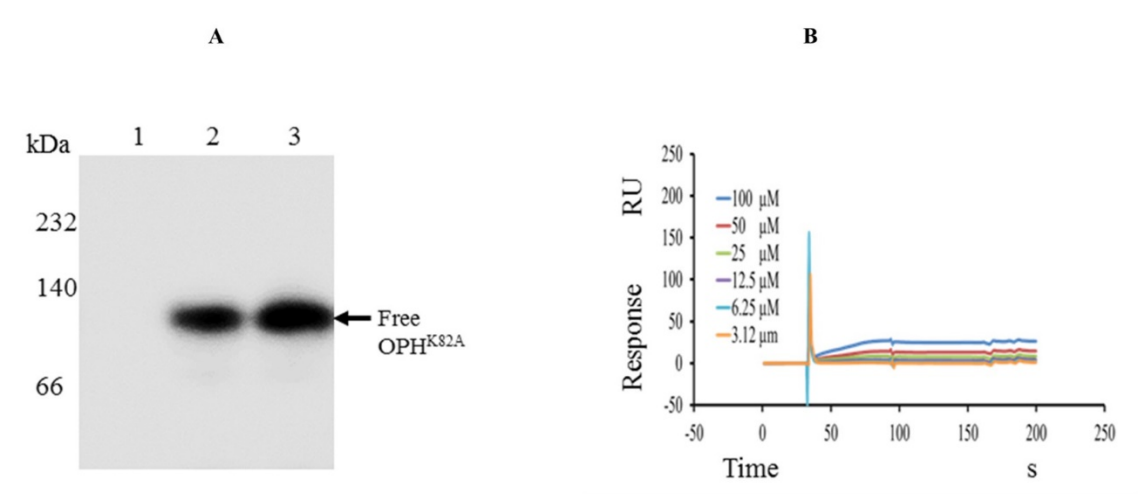


Fig. 4.15: OPH^{K82A}-Fe-Ent interactions. Panel A shows the western blot of BNPAGE developed using anti-OPH antibodies. The OPH^{K82A} and OPH^{K82A} incubated with Fe-Ent was loaded in lanes 2 and 3 respectively. There was no difference in the mobility pattern of OPH^{K82A} in lanes loaded either with OPH^{K82A} or with OPH^{K82A} incubated with Fe-Ent. SPR analysis was done using Biocore T200. Sensorgrams generated at different time interval by passing increased concentrations of Fe-Ent over CM7-sensor chip having immobilized OPH^{K82A}. Graph was plotted taking response units on 'Y' and time on 'X' axis (Panel B).

4.5 Discussion

Previous chapter described existence of interactions between OPH and Fe-Ent. However, experimental evidence gained in the previous chapter is not enough to identify precise Fe-Ent interaction site in OPH. The crystal structure is known for OPH and the active site that contributes for triesterase activity is well defined (Benning et al., 1994; Benning et al., 2001). Its crystal structure both for free OPH and for the OPH-inhibitor complex is also available (Benning et al., 2000). The amino acid residues that form active site and catalytic mechanism involved in hydrolysis of third ester linkage found in OP insecticides is very well elucidated (Fig. 1.1). Until our lab has shown existence of OPH as part of Ton-complex, OPH was identified only with degradation of OP-insecticides (Gudla et al., 2019). Due to its unique catalytic properties and broad substrate range the OPH has been extensively engineered to develop nerve gas detection and decontamination strategies (LeJeune et al., 1998; Prokop et al., 2006; Singh and Walker, 2006; Karpouzas and Singh 2006; Theriot and Grunden, 2011 & Bigley and Raushel 2012). Taking its catalytic rate towards certain OP insecticides released about 75 years ago into environment, into account it is proposed that the OPH is evolved to counter the toxic effects of OP-insecticide residues accumulated in soil (Dumas et al., 1989; Singh et al., 1999 & Siddavattam et al., 2003). However, after seeing its association with outer membrane transport components a new picture started emerging on the physiological role of OPH. More particularly, its involvement in outer membrane appears to be obvious as its membrane targeting is dependent on its association with outer membrane transport components ExbB/ExbD (Gudla et al., 2019). During the process of finding a physiological role our lab considered its role in iron uptake for obvious reasons. A hypothesis was made implicating OPH in transport of Fe-Ent considering its intrinsic properties. Its weak lactonase activity is hypothesized to have a role in iron uptake. Unfortunately, the proposed hypothesis was proved wrong as the experiments described in first chapter failed to show Ent hydrolase activity to OPH. However, the experiments conducted gave an indication on its interaction with Fe-Ent. The experiments performed here have proved beyond reasonable doubt, about existence of interactions between OPH-Fe-Ent. The OPH variants with active alterations affected triesterase activity but not Fe-Ent binding activity of OPH suggesting existence of secondary binding site for Fe-Ent in OPH. Both in silico predictions and in vitro studies have shown existence of secondary binding site OPH. What physiological significance these interactions have? How do they contribute for transport of Fe-Ent across outer membrane? These are some of the questions answered in next chapter. The evidence gained through the experiments described in present chapter conclusively show specific interactions between OPH and Fe-Ent.

Chapter-III

Role of triesterase and Ent binding activities of OPH in iron uptake

The experiments described in the previous chapter clearly demonstrated interactions between Fe-Ent and OPH and its triesterase negative variants OPHD301A, OPHD301N and OPHK82A. All though OPH^{D301A} and OPH^{D301N} interacted with OPH like wild type OPH, the Fe-Ent failed to bind to OPH^{K82A} and supported bioinformatic predictions described in Chapter II. The primary aim in generating OPH variants was to identify exact Ent binding site and to evaluate triesterase and Ent binding activities of OPH in iron acquisition. Our lab has demonstrated OPH role in iron acquisition by reconstituting *Sphingobium fuliginis* TonB dependent transport (sfTonBDT) system in E. coli. This pioneering study has established OPH interactions with Ton-complex components ExbB/ExbD and TonB and showed OPH containing sfTonBDT system enhanced iron uptake in E. coli cells. In this chapter further experiments were conducted to answer the key questions pertaining to OPH dependent enhanced iron uptake. As described in previous chapters the OPH has, in addition to an active site contributing for triesterase activity, contains secondary Ent binding site. It is not clear if either or both of these activities contribute for OPH dependent enhanced iron uptake. While answering these questions the stTonBDT system was reconstituted by including OPH variants that are defective in triesterase activity (OPH^{D301A}, OPH^{D301N}) or Ent binding activity and performed iron uptake experiments. The experimental procedures followed and results obtained during iron uptake studies are discussed in this chapter.

5.1 Objective specific methodology

TABLE 5.1: List of plasmids used in this study

Plasmid	Description	Reference
name		
pOPHV400	Cm ^r , AviTag coding sequence was inserted as XhoI and HindIII fragment inframe of <i>opd</i> gene of pSM5, codes for OPH ^{CAviTag}	Parthasarathy et al., 2016
pMS5	Cm ^r , Expression plasmid. Codes preOPH ^{6xHis} . Generated by cloning <i>opd</i> gene amplified from pPHYS400 in pMMB206 as EcoRI and HindIII fragment.	Siddavattam et al., 2003
pGS6	Amp ^r , Expression plasmid. Generated by cloning <i>exbBD</i> operon in pGS5 as EcoRI and SacI fragment. The <i>exbBD</i> operon is taken from pGS23. Codes for TonB ^{C6His} and ExbB ^{NFLAG} /ExbD ^{CMyc} .	Gudla et al., 2019
pGS25	Km ^r , The T7 promoter driven expression plasmid. Generated by cloning <i>tbdT</i> in pGS2C. The <i>tbdt</i> amplified from <i>Sphingobium fuliginis</i> ATCC 27551 is cloned as <i>Nco</i> I and <i>Xho</i> I fragment. Codes for TBDT ^{C6xHis} .	Ramurthy Gudla Thesis
pPD301A	Cm ^r , Expression plasmid. The pOPHV400 derivative. Codes for preOPH ^{D301A}	This Study

pPD301N	Cm ^r , Expression plasmid. The pOPHV400 derivative. Codes	
	for preOPH ^{D301N}	This Study
pPK82A	Cm ^r , Expression plasmid. The pOPHV400 derivative. Codes	
_	for preOPH ^{K82A}	This Study
pGS19	Km ^r , Expression plasmid. Generated by cloning <i>exbD</i> gene	
	of Sphingobium fuliginis ATCC 27551 in pGS2N. Codes for	
	ExbD ^{N6His} .	Gudla et al., 2019

TABLE 5.2: List of strains used in this study

Strain name	Genotype or Phenotype	Reference
	$\lambda sup E44$, $\Delta lac U169$ ($\Delta 80~lac Z\Delta M15$) $hsd R17~rec A1$	
E. coli DH5α	endA1 gyrA96 thi1 relA1	Hanahan et al, 1983
Sphingopyxis wildii	Sm ^r , PmB ^r , opd ⁺	Serdar et al., 1982
Sphingopyxis wildii		
DS010	Sm ^r , Tc ^r , PmB ^r , opd ^r (opd::tet)	Gorla et al., 2009
Arctic express	E. coli B F-ompThsdS $(r_B m_B)$ dcm tet gal endA hte	Agilent
1	(cpn10 cpn60 Gent')	Technologies
<i>E coli</i> K-12 MG1655	Wild type strain, F-, λ -, rph -1	Blattner et al., 1997
		Ramurthy Gudla
E. coli GS027	Gm ^r . Generated by deleting exbD and <i>tonB</i> . <i>E. coli</i> Arctic express - $\Delta exbD$, $\Delta tonB$.	Thesis
	Gm ^r , Amp ^r Km ^r . Cells having reconstituted	Ramurthy Gudla
E. coli GS029	s/TonBDT system (pGS6+pGS25)	Thesis
	Gm ^r , Amp ^r Km ^r . Cm ^r . Cells having reconstituted	Ramurthy Gudla
E. coli GS030	syTonBDT system with OPH (pGS6+pGS25+pOPHV400)	Thesis
	Gm ^r , Amp ^r Km ^r . Cm ^r . Cells having reconstituted	
E. coli GS031	s/TonBDT system with preOPH ^{D301A} (pGS6+pGS25+	This study
L. con Goosi	pPD301A)	11113 Study
	Gm ^r , Amp ^r Km ^r . Cm ^r . Cells having reconstituted s/TonBDT system with preOPH ^{D301N} (pGS6+pGS25+	
E. coli GS032	pPD301N) (pO30+pO323+	This study

TABLE 5.3: List of primers used in this study

Primer	Sequence (5' → 3')	Description
Name		
RG13 FP	AAA <u>CCATGG</u> AAATGGGTATGGGAAAGTTTGC	Forward primer used to amplify tbdt from S. fuliginis. The NcoI site appended to facilitate cloning is underlined. (Ramurthy Gudla Thesis)

RG13 RP	AAA <u>CTCGAG</u> CCAGGCCTTTGAGACGGTG	Reverse primer used to amplify
		tbdt from S. fuliginis. The XhoI
		site appended to facilitate
		cloning is underlined.
		(Ramurthy Gudla Thesis)

5.1.1 Interactions of OPH variants with ExbD-Pull-down assays

The E. coli Arctic express (pGS19) cells expressing ExbDN6xHis was independently co-transformed with expression plasmids coding OPH variants pMD301A (OPH^{D301A}), pMD301N (OPH^{D301N}), pMK82A (OPH^{K82A}) and these E. coli Arctic express cells were grown in 10ml LB medium at 37°C till the culture reached to mid log phase. Coexpression of OPH variants and ExbD were induced with 1mM IPTG (Gudla et al., 2019). The cells were allowed to grow at 30°C for 16 h with shaking at 200 rpm. Cells were harvested at 6000 rpm for 10 min and the obtained cell pellet was washed with wash buffer (PBS pH 7.4, 5% glycerol, 150mM NaCl). The washed cell pellet was dissolved in 5ml of lysis buffer (PBS pH 7.4, 5% glycerol, 150mM NaCl, 1mM PMSF) and 50 µg lysozyme was added before lysing the cells by sonication for 15 min (20 sec ON and 40 sec OFF). The lysate was centrifuged for 30 minutes at 15,000 rpm. The clear supernatant was mixed with Ni-NTA magnetic beads (50µl) from (Thermo Fisher Scientific, India) and incubated for overnight at 4°C with rotation and the collected beads were washed with wash buffer for 3 to 4 times. The washed magnetic beads were mixed with 2x SDS-PAGE sample dye and boiled for 8 min before analyzing on SDS-PAGE (12.5 %) gel. The western blots were performed to detect OPH and ExbD^{N6xHis} by using ant-OPH and anti-His antibodies respectively. The cell lysates were prepared independently from E. coli Arctic express cells expressing OPHD301A, OPHD301N, OPHK82A and ExbD^{N6xHis} treated in a similar manner and used as controls.

5.1.2 Generation of preOPH variants

While reconstituting syTonBDT with OPH variants should be generated with signal sequence. The OPH variants used for studying interactions with Ent were derived from mOPH (mature form of OPH expressed by deletion signal peptide). The plasmids coding mOPH variants cannot be used for reconstitution experiments. Therefore, the preOPH variants, preOPH^{D301A}, preOPH^{D301N} and preOPH^{K82A} were generated by performing site-directed mutagenesis (SDM) following the procedure described in (Methods Section, Chapter-II). The plasmid pOPHV400, encoding preOPH^{CAviTag} was used as a template while generating variants (precursor form of OPH). The complementary oligos (the same oligos used for

generating mature form of variants OPH shown in chapter-II, Table-4.1) used for SDM. Three expression plasmids were generated to encode OPH variants pPD301A, (preOPH^{D301A}), pPD301N (preOPH^{D301N}), pPK82A (preOPH^{K82A}). After establishing their stability and activity, the subcellular localization of OPH variants were studied. For that, the plasmid (pGS19) (encoding ExbD^{N6xHis} protein) having *E. coli* cells were transformed with plasmids pPD301A, pPD301N or pPK82A. The co-expression, subcellular fractionation and detection of ExbD^{N6xHis} and OPH variants were performed following procedures (Gudla et al., 2019).

5.1.3 Generation of expression plasmid pPD301A

While generating OPH variants by SDM, the plasmid pOPHV400 coding precursor form of OPH (preOPH) was used as a template. The preOPHD301A coding expression plasmid was generated by using primer pair D301A-FP/D301A-RP (used earlier for generating OPHD301A, Chapter-II, Table-4.1) corresponding to the region of *opd* gene that specify aspartate at 301 position. PCR was performed for 30 cycles using pOPHV400 as a template using a similar program used for generation of plasmid pMD301A mentioned (Methods Section, Chapter-II). The insertion of the desired mutation that substitutes aspartate to alanine is confirmed by sequencing the plasmid. The plasmid that contains GCG in place of GAC was designated as pPD301A was used for further studies. The pPD301A codes for OPH variant preOPHD301A.

5.1.4 Generation of expression plasmid pPD301N

While generating OPH variants by SDM, the plasmid pOPHV400 coding precursor form of OPH (preOPH) was used as a template. The preOPH^{D301N} coding expression plasmid was generated by using primer pair D301N-FP/D301N-RP (used earlier for generating OPH^{D301N}, Chapter-II, Table-4.1) corresponding to the region of *opd* gene that specify aspartate at 301 position. PCR was performed for 30 cycles using pOPHV400 as a template using a similar program used for generation of plasmid pMD301N mentioned (Methods Section, Chapter-II). The insertion of the desired mutation that substitutes aspartate to asparagine is confirmed by sequencing the plasmid. The plasmid that contains AAC in place of GAC was designated as pPD301N was used for further studies. The pPD301N codes for OPH variant preOPH^{D301N}.

5.1.5 Generation of expression plasmid pPK82A

While generating OPH variants by SDM, the plasmid pOPHV400 coding precursor form of OPH (preOPH) was used as a template. The preOPH^{K82A} coding expression plasmid was generated by using primer pair K82A-FP/ K82A -RP (used earlier for generating OPH^{K82A}, Chapter-II, Table-4.1) corresponding to the region of *opd* gene that specify lysine at 82 position. PCR was performed for 30 cycles using pOPHV400 as a template using a similar program used for generation of plasmid pPK82A mentioned (Methods Section, Chapter-II). The insertion of the desired mutation that substitutes lysine to alanine is confirmed by sequencing the plasmid. The plasmid that contains GCG in place of AAG was designated as pPK82A was used for further studies. The pPK82A codes for OPH variant preOPH^{K82A}.

5.2 Expression of OPH variants

The expression plasmids coding OPH variants pPD301A (preOPH^{D301A}), pPD301N (preOPH^{D301N}), pPK82A (preOPH^{K82A}) were transformed independently into *E. coli* DH5α cells. These cultures were grown up to mid log phase in 10 ml LB medium and induced with 1mM IPTG. The cells were allowed to grow at 30°C for 16 h with shaking at 200 rpm. The supernatant was obtained by following procedure described in (Methods Section, Chapter-II) and used to perform OPH activity and to detect OPH by performing western blot. The triesterase activity of OPH and its variants was measured by following standard protocols described elsewhere (Chaudhry et al., 1988).

5.2.1 Co-expression of preOPH D301A and ExbD N6xHis and subcellular localization of preOPH D301A

The *E. coli* GS027 (pGS19) cells were co-transformed with plasmid pPD301A and induced with 1mM IPTG by following standard procedure described in general methods and the subcellular localization of the induced cultures was done (Gorla et al., 2009). The cytoplasm and membrane fractions were analyzed on SDS-PAGE (12.5%) and the presence of preOPH^{D301A} was detected by performing western blots using anti-OPH antibodies.

5.2.2 Co-expression of pre OPH^{D301N} and $ExbD^{N6xHis}$ and subcellular localization of pre OPH^{D301N}

The *E. coli* GS027 (pGS19) cells were co-transformed with plasmid pPD301N and induced with 1mM IPTG by following standard procedure described in general methods and the

subcellular localization of the induced cultures was done (Gorla et al., 2009). The cytoplasm and membrane fractions were analyzed on SDS-PAGE (12.5%) and the presence of preOPH^{D301N} was detected by performing western blots using anti-OPH antibodies.

5.2.3 Co-expression of preOPH K82A and ExbD N6xHis and subcellular localization of preOPH K82A

The *E. coli* GS027 (pGS19) cells were co-transformed with plasmid pPK82A and induced with 1mM IPTG by following standard procedure described in general methods and the subcellular localization of the induced cultures was done (Gorla et al., 2009). The cytoplasm and membrane fractions were analyzed on SDS-PAGE (12.5%) and the presence of preOPH^{K82A} was detected by performing western blots using anti-OPH antibodies.

5.3 Reconstitution of sfTonBDT system with OPH variants

Previously in our laboratory generated the *E. coli* GS027 (the *exbD* and *tonB* double mutant) and reconstituted stTonBDT system. The E. coli GS029 (pGS6+pGS25), expressing s/ExbBNFLAG, s/ExbDCMyc, s/TonBC6xHis, and s/TBDTC6xHis was used to transform independently with expression plasmids coding OPH variants pPD301A (preOPHD301A), pPD301N (preOPHD301N). The resulting strains were designated as E. coli GS031 (pGS6+pGS25+pPD301A) and E. coli GS032 (pGS6+pGS25+pPD301N). The overnight cultures of these were inoculated and grown in 10 ml LB broth at 37°C with shaking at 200 rpm till the mid log phase (0.5 OD) and induced the stTonBDT components by adding 1mM IPTG. The induced cultures were grown at 18°C with shaking at 200 rpm. The cells were harvested and the obtained cells pellet was resuspended, washed two times with iron free minimal media. Finally, the cells were resuspended in 0.02µg/ml of Fe (Iron limiting) minimal media. For acclimatization of these cultures under iron limiting conditions, cells were allowed to grow for 12h at 18°C with shaking at 180 rpm and to keep the stTonBDT components 0.5mM IPTG was supplemented. The cells were harvested and 0.05 OD of cells were resuspended in 0.02µg/ml of Fe containing minimal media and by adding 0.5mM IPTG. To facilitate the survival growth of cells antibiotics were kept at low concentration (ampicillin 50µg, chloramphenicol 10µg and 10µg kanamycin) and growth was recorded every 2h at 600 nm. The TonBDT null mutant of E. coli GS027, E. coli GS029 (pGS6+pGS25) cells without OPH and E. coli GS030 (pGS6+pGS25+pOPHV400) cells having s/TonBDT system with OPH were grown under similar manner and used as controls.

5.3.1 Preparation of ⁵⁵Fe-enterobactin

The stock solution of Enterobactin (Ent) (Sigma-Aldrich, USA) was prepared by dissolving 1 mg of Ent in 150 μl DMSO. The stock solution was store at -20°C until further use. For the preparation ⁵⁵Fe-enterobactin, 5 μl of ⁵⁵Fe was taken from 0. 2 μmol of ⁵⁵Fe stock (American Radiolabeled Chemicals, MO, USA; specific activity of 10.18 mCi / mg) and added into the sterile eppendorf tube containing 3 μl of enterobactin from the stock solution and incubated at RT for 5 min. The contents were made up to 50 μl with HEPES buffer (pH 7.3) and by passing it through a Sephadex G-25 column the free ⁵⁵Fe was trapped in a column and the ⁵⁵Fe-enterobactin was collected in the flowthrough by centrifuging the column at 1000 rpm The radioactivity was determined by pipetting 2 μl into 5 ml of scintillation fluid [1, 4 – bis (5-phenyl-2-oxazolyl) benzene and 2,5 - diphenyloxazole] and measuring it in a Perkin Elmer Tri-Carb 2910TR scintillation counter.

5.3.2 Uptake of ⁵⁵Fe-enterobactin

The TonBDT null mutant of E. coli GS027 and SfTonBDT system reconstituted without OPH E. coli GS029 (pGS6+pGS25), with OPH E. coli GS030 (pGS6+pGS25+pOPHV400) or its variants preOPHD301A E. coli GS031 (pGS6+pGS25+pPD301A), preOPHD301N E. coli GS032 (pGS6+pGS25+pPD301N) were initially grown to mid log phase in a 50 ml flask containing iron-sufficient medium (10 µg/ml of Fe) and the expression of SfTonBDT components was then induced with 1mM IPTG for three hours. After induction, the cells were centrifuged at 6000 rpm for 5 min. The cell pellet was collected and washed twice with the iron-free minimal salt medium. The cells were resuspended in an equal volume of 0.02µg/ml of Fe containing iron limiting medium. The expression of STOnBDT components were induced by adding 1mM IPTG at 18°C for 12 hours. After induction, cells were harvested and extensively washed within iron-free minimal media. Finally, the redissolved cells were taken to get the 1.0 OD (A_{600nm}) of cells by using a spectrophotometer, which is equivalent to $8x10^8$ cells/ml. The ⁵⁵Fe-enterobactin (equivalent to 178 µmol of ⁵⁵Fe) was added to the cell suspension and incubated at 37°C for 2 hours with moderate shaking (120 rpm). Then the cells were again centrifuged at 6000 rpm for 5 min and to remove the free ⁵⁵Fe the cell pellet was extensively washed with 0.1M LiCl₂ followed by two washes with cold iron-free minimal media. Before going for scintillation counting the pellet was dried and transferred into 5ml of scintillation fluid. The amount of iron (55Fe) found in cell pellet was counted as described above.

A similar strategy was followed while measuring iron uptake in *S. wildii* and *S. wildii* DS010 except that the cells were grown in a minimal medium (vide General methods) that support the growth of these cells (Matzanke et al., 1986; Parthasarathy et al., 2016).

5.4 Results & Discussion

As stated before, the primary aim of the study is to assess the role of triesterase and Ent binding activities of OPH in OPH dependent enhanced iron uptake. In order to gain experimental evidence, the syTonBDT has to be reconstituted in E. coli TonBDT (TonB dependent transport system) negative mutants. Before proceeding to reconstitute syTonBDT in E. coli TonBDT negative mutants, it is necessary to know if the OPH variants are interacting with Ton-complex components ExbD and TonB. Further the OPH variants ability to target membranes in presence of ExbB/ExbD has to be established. Therefore prior to reconstitution of syTonBDT system with OPH variants experiments were conducted to ascertain their ability to interact with Ton-complex components and to target membrane like wildtype OPH, in presence of ExbB/ExbD.

5.4.1 OPH variant OPH^{D301A} interacts with ExbD

The OPH and ExbD interactions are critical for membrane targeting of OPH in E. coli (Gudla et al., 2019). Therefore, pulldown assays were conducted to ascertain interactions between OPH variants and ExbD. Initially, the cell lysate prepared from E. coli Arctic express (pGS19+pMD301A) cells expressing $ExbD^{N6xHis}$ and OPH^{D301A} were used to perform pulldown assays using Ni-NTA magnetic beads. The cell lysate, flowthrough, wash and elution fractions were collected and analyzed on 12.5 % SDS-PAGE gel. The western blots were probed with either anti-His or anti-OPH antibodies to detect ExbD^{N6xHis} and OPH^{D301A} (Fig. 5.1. Panel I & II). The ExbD^{N6xHis} and OPH^{D301A} were seen in cell lysate (CL) and flowthrough (FT) (Fig. 5.1. Panel I & Panel II Lanes 1, 2). These proteins were not detected in wash fractions (W) (Fig. 5.1. Panel I & Panel II Lane 3). In principle, in elution fraction collected from Ni-NTA magnetic beads should show only ExbD^{N6xHis} specific signal. Interestingly in addition to ExbDN6xHis specific signal a signal specific to OPHD301A was also noticed suggesting interactions between ExbDN6xHis and OPHD301A (Fig. 5.1. Panel I & Panel II Lane 4). These results clearly show that the mutations in active site (substitution of active site aspartate to alanine) failed to influence interactions between OPHD301A and ExbDN6xHis. Strengthening the observations, the elution fractions collected from the beads incubated with cell lysates expressing only OPH^{D301A} didn't bind to Ni-NTA magnetic (Fig. 5.1. Panel II Lane 5). This results clearly suggest existence of specific interactions between OPH^{D301A} and ExbD^{N6xHis}.

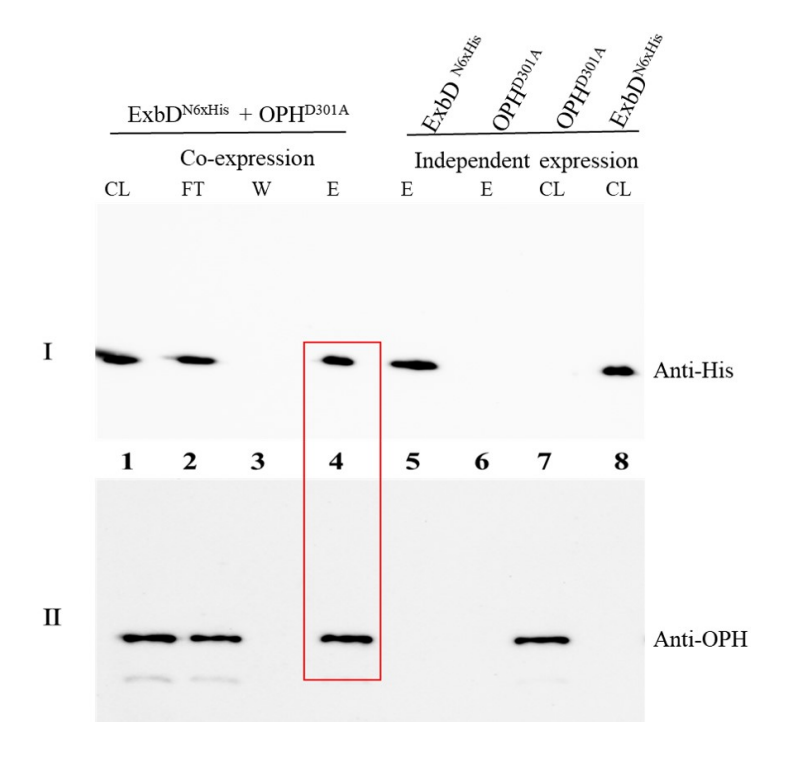


Fig. 5.1: Interactions between OPH^{D301A} and ExbD^{N6xHis}. Pull down assays performed by using cell lysates prepared from *E. coli* Arctic express cells co-expressing ExbD^{N6xHis} and OPH^{D301A} (co-expression) Lanes 1 to 4 and pulldown assays performed for the cell lysates prepared from the cells expressing ExbD^{N6xHis} and OPH^{D301A} independently are shown in lanes 5 to 8. The cell lysate used as input (CL), flowthrough (FT), wash (W), E (elution fraction) were collected and analyzed on 12. 5 % SDS-PAGE and western blots were performed using either anti-His antibodies (I) or anti-OPH antibodies (II) to detect ExbD^{N6xHis} and OPH^{D301A}.

5.4.2 OPH variant OPH^{D301N} interacts with ExbD

The OPH and ExbD interactions are critical for membrane targeting of OPH in *E. coli* (Gudla et al., 2019). Therefore, pulldown assays were conducted to ascertain interactions between OPH^{D301N} and ExbD. Initially, the cell lysate prepared from *E. coli* Arctic express (pGS19+pMD301N) cells expressing ExbD^{N6xHis} and OPH^{D301N} were used to perform pulldown assays using Ni-NTA magnetic beads. The cell lysate, flowthrough, wash and elution fractions were collected and analyzed on 12.5 % SDS-PAGE gel. The western blots were probed with either anti-His or anti-OPH antibodies to detect ExbD^{N6xHis} and OPH^{D301N} (Fig. 5.2. Panel I & II). The ExbD^{N6xHis} and OPH^{D301N} were seen in cell lysate (CL) and flowthrough (FT) (Fig. 5.2. Panel I & Panel II Lanes 1, 2). These proteins were not detected in wash fractions (W) (Fig. 5.1. Panel I & Panel II Lane 3). In principle, in elution fraction collected from Ni-NTA magnetic beads should show only ExbD^{N6xHis} specific signal. Interestingly in addition to ExbD^{N6xHis} specific signal a signal specific to OPH^{D301N} was also noticed suggesting interactions between ExbD^{N6xHis} and OPH^{D301N} (Fig. 5.1. Panel I & Panel II Lane 4). These results clearly show that the mutations in active site (substitution of active site aspartate to

asparagine) failed to influence interactions between OPH^{D301N} and ExbD^{N6xHis}. Strengthening the observations, the elution fractions collected from the beads incubated with cell lysates expressing only OPH^{D301N} didn't bind to Ni-NTA magnetic (Fig. 5.1. Panel II Lane 5). This results clearly suggest existence of specific interactions between OPH^{D301N} and ExbD^{N6xHis}.

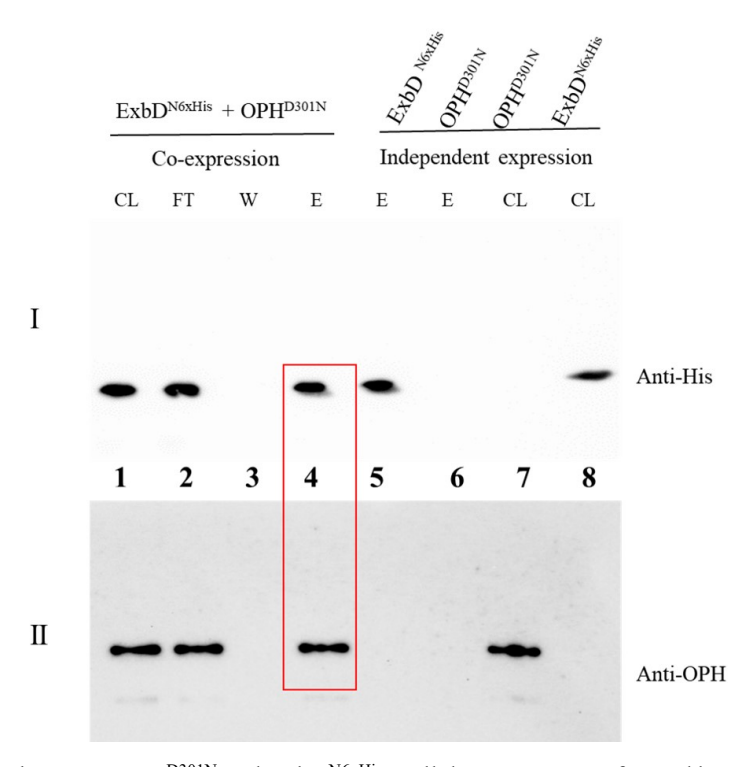


Fig. 5.2: Interactions between OPH^{D301N} and ExbD^{N6xHis}. Pull down assays performed by using cell lysates prepared from $E.\ coli$ Arctic express cells co-expressing ExbD^{N6xHis} and OPH^{D301N} (co-expression) Lanes 1 to 4 and pulldown assays performed for the cell lysates prepared from the cells expressing ExbD^{N6xHis} and OPH^{D301N} independently are shown in lanes 5 to 8. The cell lysate used as input (CL), flowthrough (FT), wash (W), E (elution fraction) were collected and analyzed on 12. 5 % SDS-PAGE and western blots were performed using either anti-His antibodies (I) or anti-OPH antibodies (II) to detect ExbD^{N6xHis} and OPH^{D301N}.

5.4.3 Generation of OPH variants with signal sequence (preOPHD301A and preOPHD301N)

In order to study the membrane localization of triesterase negative OPH variants, signal sequence is required for membrane targeting. For that the plasmid (pOPHV400) having N-terminal signal sequences used as a template. The expression plasmids pPD301A and pPD301N were generated and the substitution was validated by sequencing the plasmids (Fig. 5.3 Panel A & Panel B). The chromatogram clearly shows the insertion of codon GCG in place of GAC in plasmid pPD301A (Fig. 5.3. Panel A) and whereas in plasmid pPD301N the insertion of codon AAC in place of GAC (Fig. 5.3. Panel B). After confirming the substitution of Asp with Ala and Asn the OPH variants preOPH^{D301A} and preOPH^{D301N} were tested for stability by performing western blot and ability to perform triesterase activity as described (Methods Section, Chapter-II). Both the variants were found to be stable like wildtype OPH (Fig. 5.3.

Panel C & D). However, as expected, the preOPH^{D301A} and preOPH^{D301N} have shown no triesterase activity (Fig. 5.3. Panel D).

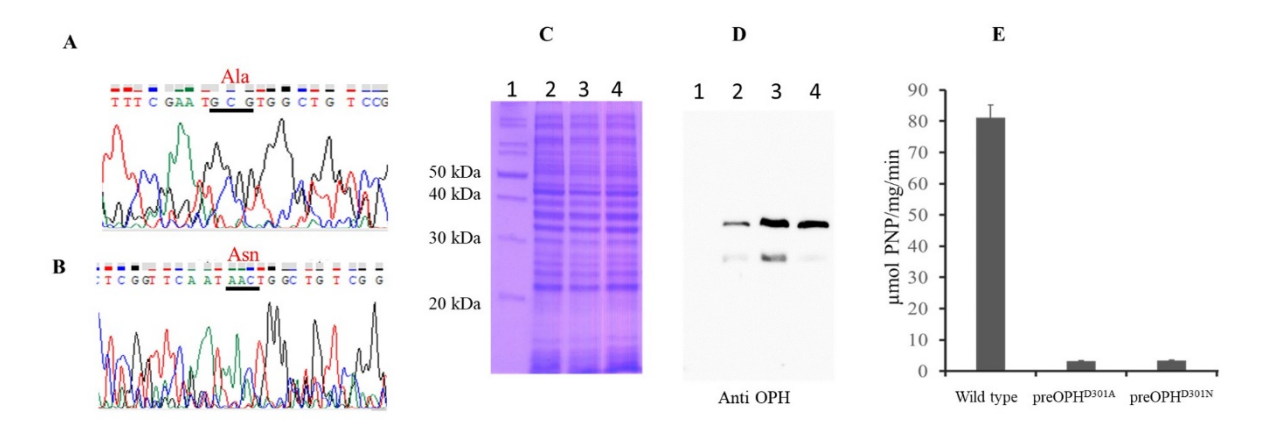


Fig. 5.3: Generation of preOPH variants preOPH^{D301A} and preOPH^{D301N}. Panel A shows the chromatograms generated using plasmid pPD301A as a template. Change of codon from GAC to GCG is shown with an underline. Panel B shows the chromatograms generated using plasmid pPD301N as a template and change of codon from GAC to AAC is shown with an underline. Panel C and D shows the expression and subsequent detection of preOPH^{D301A} and preOPH^{D301N} in *E. coli* DH5α (pPD301A), *E. coli* DH5α (pPD301N) cells. The SDS-PAGE (12.5%) (Panel C) and corresponding western blot (Panel D) probed with anti-OPH antibodies shows the stability of expressed preOPH^{D301A} and preOPH^{D301N}. Lane 1 shows the protein molecular weight marker. The protein extracts prepared from cells expressing preOPH^{D301A} (Lane 2), preOPH^{D301N} (Lane 3) and native OPH (Lane 4) show stable expression of preOPH^{D301A} and preOPH^{D301N}. The triesterase activity measured using methyl parathion as a substrate for OPH, preOPH^{D301A} and preOPH^{D301N} is shown in panel E. Loss of triesterase activity for preOPH^{D301A} and preOPH^{D301N} clearly seen.

5.4.4 OPH variants target to the membrane in the presence of ExbD

Previously our laboratory has shown interaction of OPH with PMF component ExbD and the OPH, ExbD interactions are critical for membrane targeting of OPH in *E. coli* (Gudla et al., 2019). Based on these observations the subcellular localization of triesterase esterase negative OPH variants preOPH^{D301A} and preOPH^{D301N} were examined in the presence of ExbD. Since OPH variants shown interactions with ExbD further experiments were done to see if OPH variants targets membrane in presence of ExbD. The *E. coli* GS027 (pGS19) cells were transformed independently with the plasmids pPD301A and pPD301N. These cells coexpressing ExbD^{N6xHis} + preOPH^{D301A} and ExbD^{N6xHis} + preOPH^{D301N} were then fractionated into cytoplasm, membrane and their subcellular localizations were determined by performing the western blots probed with anti-OPH antibodies. Interestingly, both the OPH variants preOPH^{D301A} and preOPH^{D301N} got processed and successfully targeted to the membrane in the presence of ExbD^{N6xHis} (Fig. 5.4. Panel C & D Lane M). Therefore, reconstitution of s/TonBDT system was possible with preOPH^{D301A}, preOPH^{D301N} in *E. coli*. The *E. coli* GS027 (pGS19+

pOPHV400) co-expressing ExbD^{N6xHis} + preOPH served as a control (Fig. 5.4 Panel B Lane M).

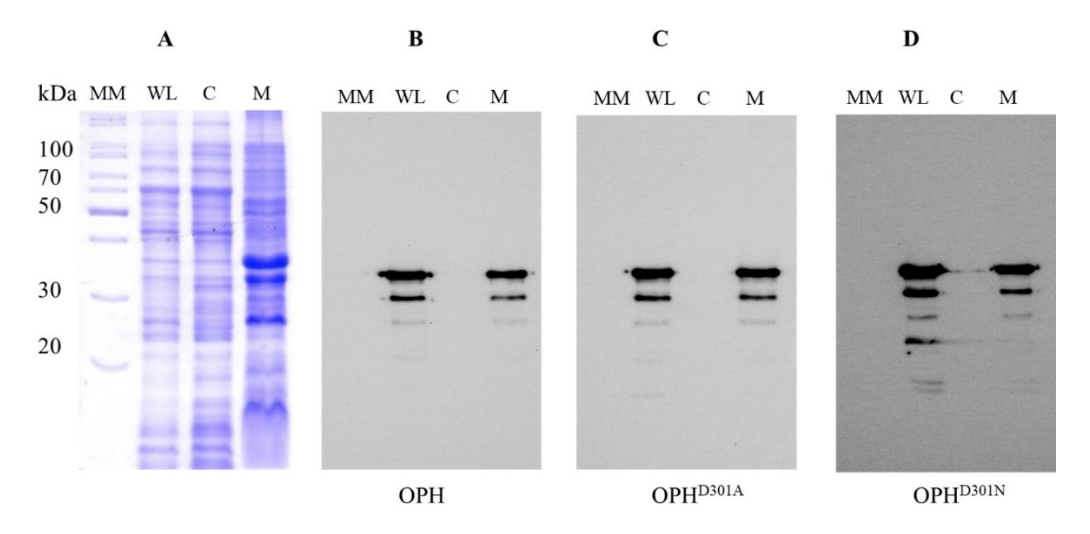


Fig. 5.4: Membrane localization of OPH variants (preOPH^{D301A} and preOPH^{D301N}). Panel A shows the (12.5%) SDS-PAGE. Panel B to D shows western blot analysis performed for the whole cell lysate (WL), cytoplasmic (C) and membrane (M) proteins extracted from *E. coli* GS027 cells co-expressing ExbD^{N6xHis} + preOPH (Panel B), ExbD^{N6xHis} + preOPH^{D301A} (Panel C), ExbD^{N6xHis} + preOPH^{D301N} (Panel D) by probing with anti-OPH antibodies to detect OPH, OPH^{D301A}, OPH^{D301A} respectively. MM stands for molecular weight marker.

5.4.5 OPH^{K82A} fails to interact with ExbD

Results described in earlier sections show that the OPH variants OPH^{D301A} and OPH^{D301N} interact with ExbD and target in its presence like wild type OPH to the membrane. The results clearly showed that there exists no difference between wildtype OPH and its variants with respect to ExbD interactions and membrane targeting. After ascertaining the interaction behavior of triesterase negative mutants with ExbD further experiments were done to know the interaction between ExbD and OPH^{K82A}. Pulldown assays were performed using cell lysates prepared from E. coli Arctic express (pGS19+pMK82A) cells expressing ExbD^{N6xHis} and OPH^{K82A}. The lysate was incubated with Ni-NTA magnetic beads as described in materials and methods section. The cell lysate, flowthrough, wash and elution fractions were collected and analyzed on 12.5 % SDS-PAGE gel. The western blots were probed with either anti-His or anti-OPH antibodies to detect ExbDN6xHis and OPHK82A (Fig. 5.5. Panel I & II). The ExbD^{N6xHis} and OPH^{K82A} were seen in cell lysate (CL) and flowthrough (FT) (Fig. 5.5. Panel I & Panel II Lanes 1, 2). These proteins were not detected in wash fractions (W) (Fig. 5.5. Panel I & Panel II Lane 3). If interactions exist between OPH^{K82A} and ExbD^{N6xHis} in elution fraction collected from Ni-NTA magnetic beads should indicate existence of signals specific to both ExbD^{N6xHis} and OPH^{K82A}. Surprisingly, in elution fraction only ExbD^{N6xHis} specific signal was detected. There was no signal specific to OPHK82A suggesting lack of interactions between ExbD^{N6xHis} and OPH^{K82A} (Fig. 5.5. Panel I & Panel II Lane 4). These results clearly show that the mutation in Ent binding site (substitution of Ent binding site lysine to alanine) has negative impact on OPH^{K82A} and ExbD^{N6xHis} interactions. Strengthening the observations, the elution fractions collected from the beads incubated with cell lysates expressing only OPH^{K82A} didn't bind to Ni-NTA magnetic beads (Fig. 5.5. Panel II Lane 5). This results clearly suggest inability of OPH^{K82A} to interact with ExbD^{N6xHis}.

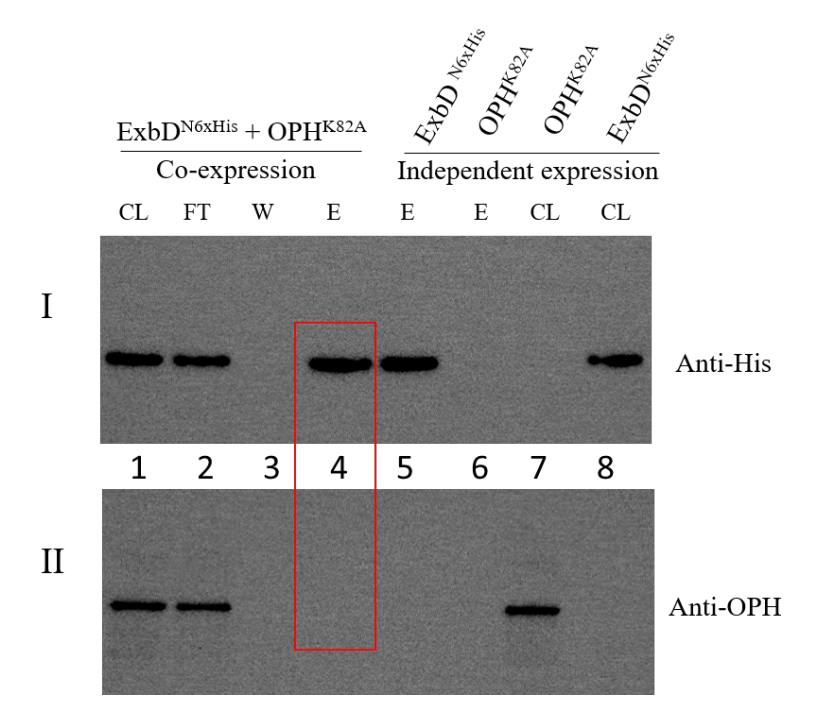


Fig. 5.5: Interactions between OPH^{K82A} and ExbD^{N6xHis}. Pull down assays performed by using cell lysates prepared from *E. coli* Arctic express cells co-expressing ExbD^{N6xHis} and OPH^{K82A} (co-expression) Lanes 1 to 4 and pulldown assays performed for the cell lysates prepared from the cells expressing ExbD^{N6xHis} and OPH^{K82A} independently are shown in lanes 5 to 8. The cell lysate used as input (CL), flowthrough (FT), wash (W), E (elution fraction) were collected and analyzed on 12. 5 % SDS-PAGE and western blots were performed using either anti-His antibodies (I) or anti-OPH antibodies (II) to detect ExbD^{N6xHis} and OPH^{K82A}. The red box indicates absence of OPH^{K82A} in elution fraction collected from Ni-NTA magnetic beads.

5.4.6 The preOPH^{K82A} retains native structure and triesterase activity

Reconstitution s/TonBDT with Ent negative OPH, OPH^{K82A} requires an expression plasmid coding preOPH^{K82A}. Therefore, such plasmid was generated by performing site-directed mutagenesis using pOPHV400 as a template. The expression plasmid pPK82A was generated and the lysine to alanine substitution was validated by sequencing the plasmid pPK82A (Fig. 5.6. Panel A). The chromatogram clearly showed the insertion of codon GCG in place of AAG in plasmid pPK82A (Fig. 5.6. Panel A). After confirming the substitution of Lys with Ala the preOPH variant preOPH^{K82A} its stability was assessed by performing western blot and

measuring triesterase activity (Methods Section, Chapter-II). The western blot and triesterase assay clearly indicated both stability and activity of preOPH^{K82A}. It is shown to be stable and that the alanine substitution did not affect the activity of OPH (Fig. 5.6. Panel C & D).

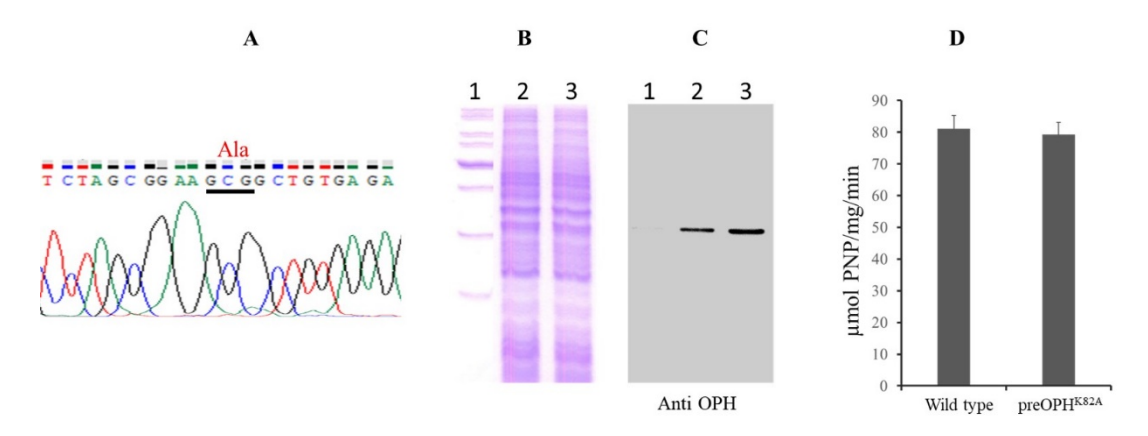


Fig. 5.6: Generation of preOPH^{K82A}. Panel A shows the chromatogram generated using plasmid pPK82A as template. Change of codon from AAG to GCG is underlined. Panels B and C show SDS-PAGE (12.5%) and corresponding western blot probed with anti-OPH antibodies. Lane 1 indicate the protein molecular weight marker. The protein extracts prepared from *E. coli* cells expressing preOPH^{K82A} and native OPH are loaded in lane 2 and 3 respectively. The triesterase activity of native OPH and preOPH^{K82A} is shown in panel D.

5.4.7 preOPH^{K82A} fails to target to the membrane

The pulldown experiment described in earlier sections clearly shown the inability of OPH^{K82A} to interact with ExbD^{N6xHis}. Further experiments were conducted examine if preOPH^{K82A} targets membrane in presence of ExbD like wild type OPH. The *E. coli* GS027 (pGS19) cells were co-transformed with the plasmid pPK82A to co-express ExbD^{N6xHis} + preOPH^{K82A}. The cells expressing these two proteins were fractionated into cytoplasm, membrane and the subcellular localization of preOPH^{K82A} was determined by performing western blot using anti-OPH antibodies. Surprisingly, most of the preOPH^{K82A} remained in cytoplasm (Fig. 5.7. Panel C Lane C). and not targeted to the membrane (Fig. 5.7. Panel C Lane M). It appears that the formation of complex between OPH and Ton components is required prior to their targeting to the membrane. Since preOPH^{K82A} fails to target membrane even in the presence of ExbD reconstitute *sy*TonBDT with OPH^{K82A} was not possible in *E. coli* cells.

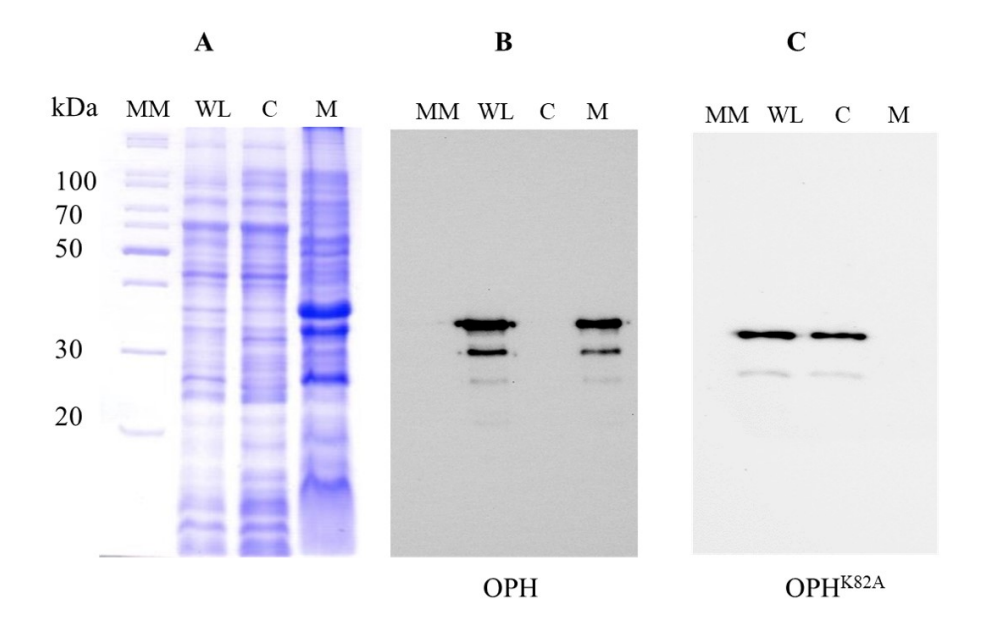


Fig. 5.7: Membrane localization of preOPH^{K82A}. Panel A shows the (12.5%) SDS-PAGE. Panel B to C shows western blot analysis performed for the whole cell lysate (WL), cytoplasmic (C) and membrane (M) proteins extracted from *E. coli* GS027 cells co-expressing ExbD^{N6xHis} + preOPH (Panel B), ExbD^{N6xHis} + preOPH^{K82A} (Panel C) by probing with anti-OPH antibodies to detect OPH, OPH^{K82A}. MM stands for molecular weight marker.

5.5 Both triesterase and Ent binding activities are critical for increased iron uptake

Previously our laboratory has shown the increased growth and iron uptake of E. coli GS030 (pGS6+pGS25+pOPHV400) cells having sfTonBDT system with OPH. However, it was not clear if the observed enhancement in growth and iron uptake was associated with triesterase or Ent binding activity or on both of these properties of OPH. The E. coli GS29 cells were therefore used to reconstitute sfTonBDT system with OPH variants that failed to show triesterase activity (preOPHD301A and preOPHD301N). The E. coli GS031 cells having with (pGS6+pGS25+ pPD301A) or E. coli GS032 cells (pGS6+pGS25+ pPD301N) were then grown under iron limiting conditions along with TonBDT negative GS027, complemented with StTonBDT system without OPH (GS029) and with OPH (GS030) used as controls. As seen in Fig. 5.8 there was no growth in iron limiting medium in E. coli GS27 cells, generated by deleting TonB and ExbD. As shown before there was difference in growth pattern between E. coli cells having sfTonBDT with (GS30) and without (GS029) cells. The GS30 cells have shown better growth than GS029 cells. Most strikingly the E. coli GS031 and E. coli GS032 cells growth pattern was comparable to the growth profile of GS029 cells having sfTonBDT without OPH. It clearly states that the triesterase negative mutants are not contributing for better growth and better iron uptake. (Fig. 5.8).

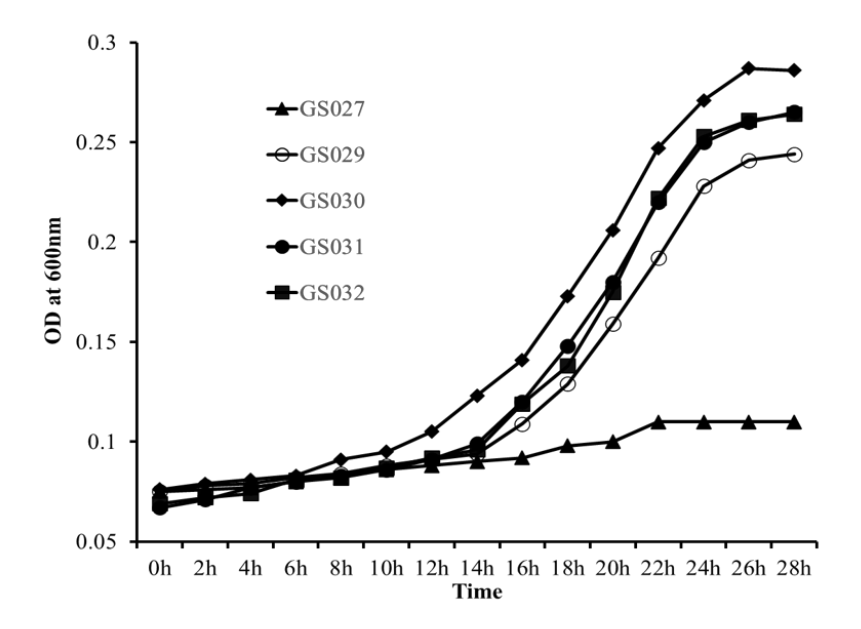


Fig. 5.8: Growth curve showing the growth pattern of *E. coli* GS27 cells complemented with _{s/}TonBDT system reconstituted with OPH and its variants in a minimal medium containing Fe-Ent as sole source of iron. Showing the growth of GS027 cells (♣), GS029 cells having reconstituted _{s/}TonBDT system without OPH (pGS6+pGS25) cells with (♣), GS030 (pGS6+pGS25+pOPHV400) cells with OPH (♣), GS031 (pGS6+pGS25+ pPD301A) cells with OPH^{D301A} (♣) and GS031 (pGS6+pGS25+ pPD301N) cells with OPH^{D301N}(♣).

The growth behavior clearly suggested influence of tristerase activity on growth of *E. coli* GS027 cells. The cells reconstituted with syTonDBT with wildtype OPH have shown better growth when compared to their counterparts generated either without OPH or with OPH variants OPH^{D301A}, OPH^{D301N}. These cultures were further used to know if the differential growth behavior is due to decreased iron uptake. The cell grown under iron limiting conditions were incubated for two hours in a medium containing pure ⁵⁵Feenterobactin as sole source of iron. Surprisingly the OPH dependent enhanced iron uptake was not seen in cells having syTonBDT system reconstituted with preOPH^{D301A} and preOPH^{D301N}. The GS031 retained 35,812 picomoles of ⁵⁵Fe having syTonBDT with preOPH^{D301A} and the GS032 cells with preOPH^{D301N} showed 24995 picomoles of iron (Fig. 5.9. Lane 4, 5). Whereas in GS030 cells having with wild type OPH showed accumulation of 46,545 picomoles of iron (Fig. 5.9. Lane 3). These results clearly suggested that the aspartate (301) present at the active site is critical for OPH dependent enhanced iron uptake.

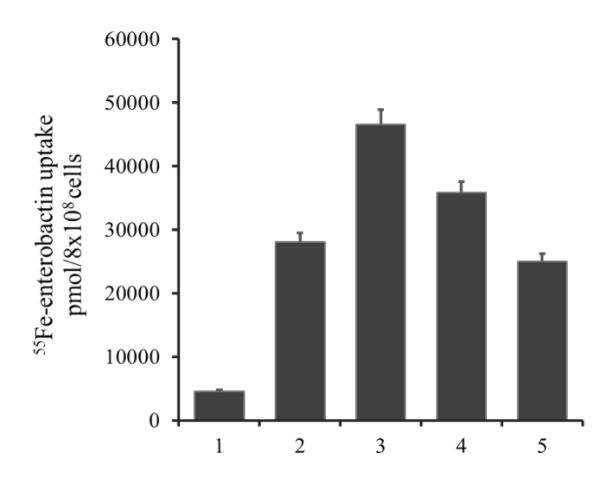


Fig. 5.9: Iron Uptake. Amount of ⁵⁵Fe accumulated in *E. coli* GS027 cells (1) having reconstituted _{S/}TonBDT system without OPH (2) and with OPH (3) and its variants preOPH^{D301A} (GS031) (4), preOPH^{D301N} (GS032) (5). TonBDT negative GS027 cells (1) and its counterparts with reconstituted TonBDT system with OPH and its variants were grown in iron limiting conditions before incubating for 2 hours with ⁵⁵Fe-Ent

5.6 The opd negative mutants of S. wildii show retarded growth in iron limiting medium

The results described in earlier sections clearly show influence of OPH in iron uptake using E. coli as model system. Further experiments were carried out to find out influence of OPH in wild type S. fuliginis. Our laboratory has made several attempts to create opd-negative mutant of S. fuliginis by using standard procedures (Gorla et al., 2009) and is unsuccessful in generating opd-negative strain of S. fuliginis. Previously our laboratory generated the opd-negative mutant of sphingopyxis wildii and showed loss of OPH activity. These cells designated as S. wildii DS010 were used to conduct various experiments pertaining to membrane targeting of OPH (Gorla et al., 2009). Identical opd genes exist both in S. fuliginis and S. wildii (Mulbry et al., 1987). Therefore, the opd negative strains of S. wildii were used to test OPH role in Fe-Ent dependent iron uptake. Initially both the opd negative and positive cells of S. wildii were grown in iron-sufficient medium (10 μg/ml of Fe) and then shifted to iron limiting conditions of (0.02µg/ml of Fe) containing iron limiting medium for acclimatization of the cells. The growth was monitored for every 6 hours and the opd mutant of S. wildii showed retarded growth when compared to the wild type cells (Fig. 5.10 Panel A). The similar growth pattern was observed in E. coli GS029 cells having sfTonBDT system without OPH (Fig. 5.8. Panel A). After studying the growth behavior, performed the iron uptake assay by incubating the equal number of cells in the iron limiting medium with ⁵⁵Fe-Ent for two hours to see the accumulation of ⁵⁵Fe in opd positive and opd negative background. Interestingly, nearly 31586 picomoles of iron was found in wild type cells as against 11497 picomoles found in opd negative mutants (Fig. 5.10. Panel B). these results clearly indicate a role for OPH in Fe-Ent mediated iron uptake in *S. wildii*.

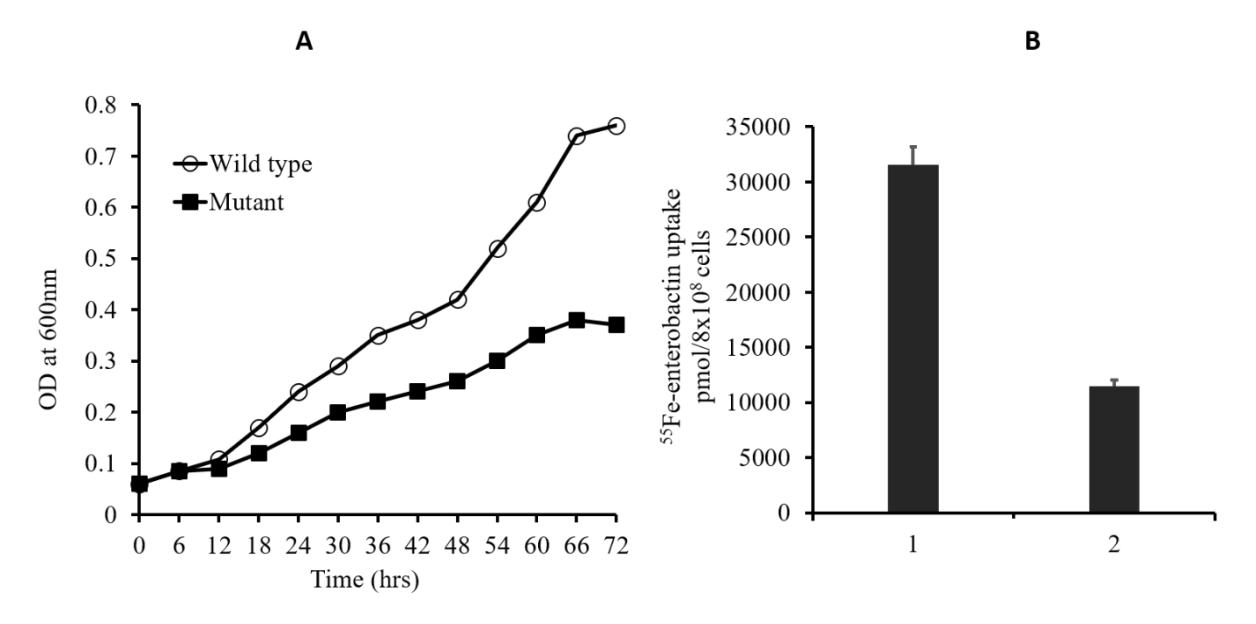


Fig. 5.10: Growth curve and uptake of ⁵⁵Fe by *S. wildii* cells. Growth pattern was monitored in cells grown in iron limiting minimal medium. Panel A shows the growth of wild type *S. wildii* (♣) and *opd* negative *S. wildii* DS010 (♣) cells under iron limiting conditions. Panel B shows uptake of ⁵⁵Fe by *S. wildii* (1), *S. wildii* DS010 (2) cells when incubated in ⁵⁵Fe-enterobactin containing minimal medium for two hours at 30°C.

5.7 Discussion

TonB dependent transport system is involved in transport of iron complexes, vitamin B₁₂ and Heme, Nickel complexes through energy-transducing membranes (Schauer et al., 2008; Noinaj et al., 2010). In Gram-negative bacteria, ferric iron bound to siderophores translocate across outer membrane to reach periplasmic space using TonB-dependent transport (TBDTs) system (Schauer et al., 2008). Enterobactin is one of the major iron chelating siderophore synthesized and secreted into environment by a variety of Gram-negative bacteria grown under iron limiting conditions. Once released it chelates ferric iron to form Fe-Ent complex. The Fe-Ent interacts specifically with an outer membrane transporter TBDT. The translocation of Fe-Ent complex into periplasmic space requires energy. Outer membrane is deprived of energy source. The required energy source is obtained from the inner membrane associated Ton-complex. The Ton complex contains PMF components ExbB/ExbD and energy transducer TonB. The TonB harvests energy from PMF component and transduces it to TBDT by interacting with its periplasmically located N-terminal region of the transporter called TonB box (Krewulak and Vogal, 2011). After translocation into periplasmic space the bound iron has to be released from Fe-Ent. Interactions between ferric iron and Ent are very strong affinity (K

= 10⁵² M⁻¹) (Carrano and Raymond, 1979) and release of ferric iron from Fe-Ent requires additional enzymatic or non-enzymatic steps. Enzymatic step involves an esterase located either in cytoplasm or in periplasm (Brickman et al.,1992; Lin et al., 2005). Enterobactin is a cyclic trilactone, where three 2, 3-dihydroxybenzoylserine residues are linked through an ester linkage (Raymond et al., 2003). These esterases hydrolyze the trilactone ring facilitating the release of ferric iron bound strongly to Ent. Alternatively, the Fe³⁺ ions held firmly with Ent through octahedral coordination by the six hydroxyl groups of the three catecholates are reduced to weaken the reactions. The Ent exists in deprotonated form at neutral pH (Harris et al., 1979; Lee et al., 1985) with a net charge of -3 and is highly favourable for formation of Fe-Ent complex. This association between Ent and ferric iron can be weakened when Fe-Ent is protonated (Abergel et al., 2006).

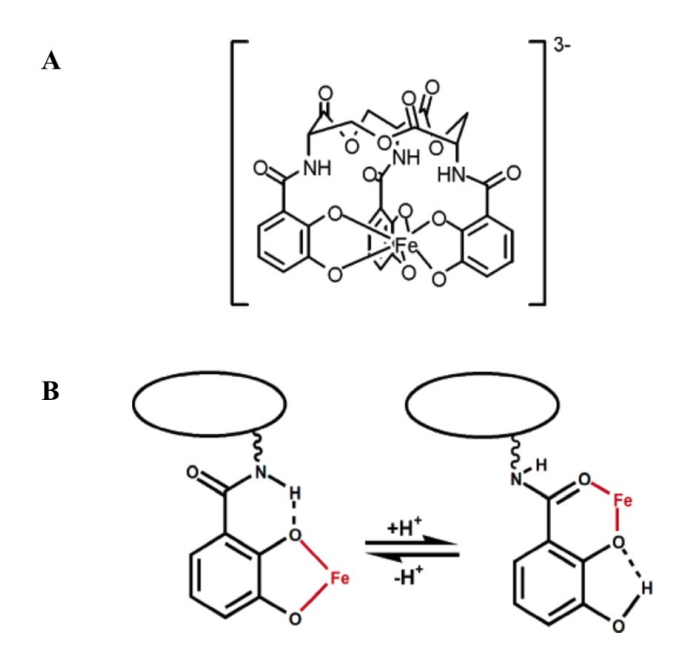


Fig. 5.11: Panel A shows the Ferric-enterobactin (Fe-Ent) structure (top) and Panel B shows the coordination shift from catecholate (bottom left) to salicylate (bottom right) upon protonation (Abergel et al., 2006).

Physiologically the non-enzymatic process of releasing ferric iron from Ent is advantageous to cell. Unlike in enzymatic process, where Ent is cleaved soon after transport of every single ferric ion in to periplasmic space, the non-enzymatic process involves only oxidation and reduction mechanisms. There is no destruction for Ent molecule and it can be recycled for transporting ferric iron from the environment. The OPH association with PMF components ExbB/ExbD and energy transducer TonB, appears to promote reduction of Fe-Ent. In a mechanism yet to be deciphered the OPH is contributing for the reduction process. Since the *E. coli* cells having sfTonBDT system with triesterase negative OPH variants failed to show

enhanced iron uptake, the role of active site which contains binuclear metal center cannot be ignored. A model depicting the role of OPH is given below to show possible role of OPH in enhanced iron uptake.

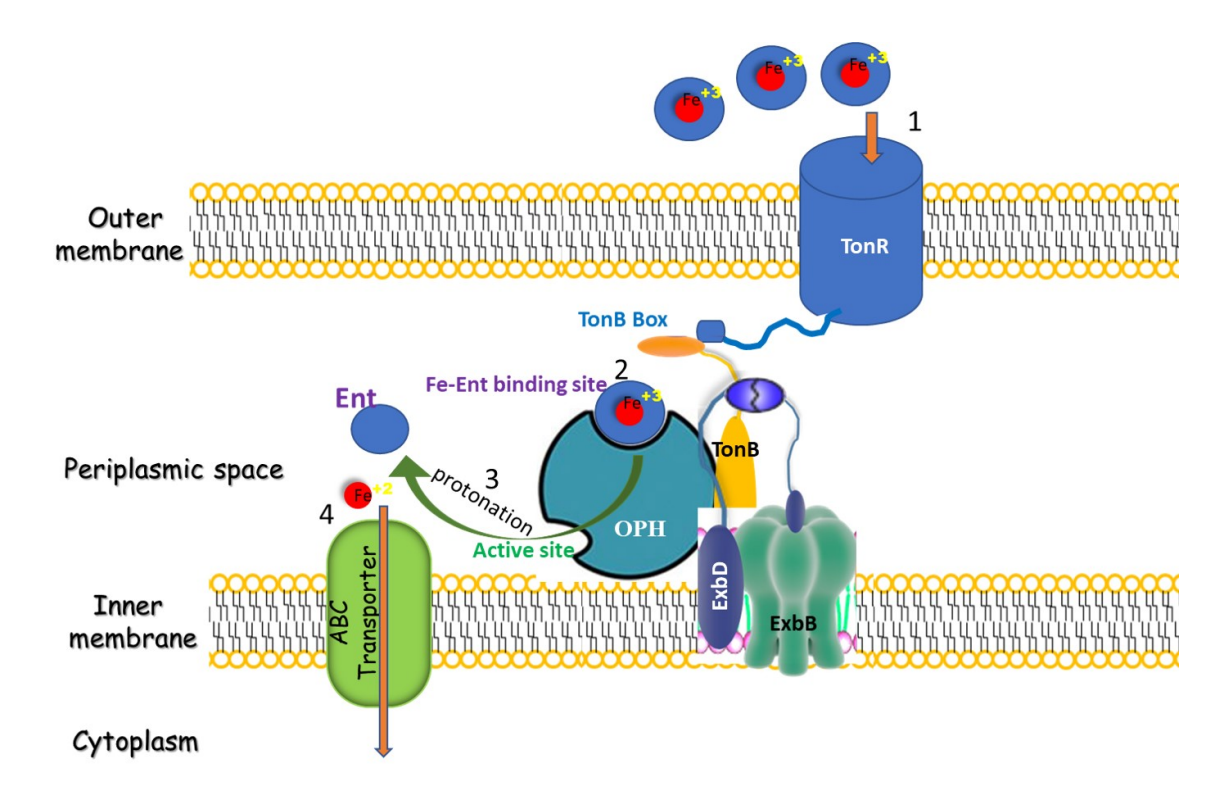
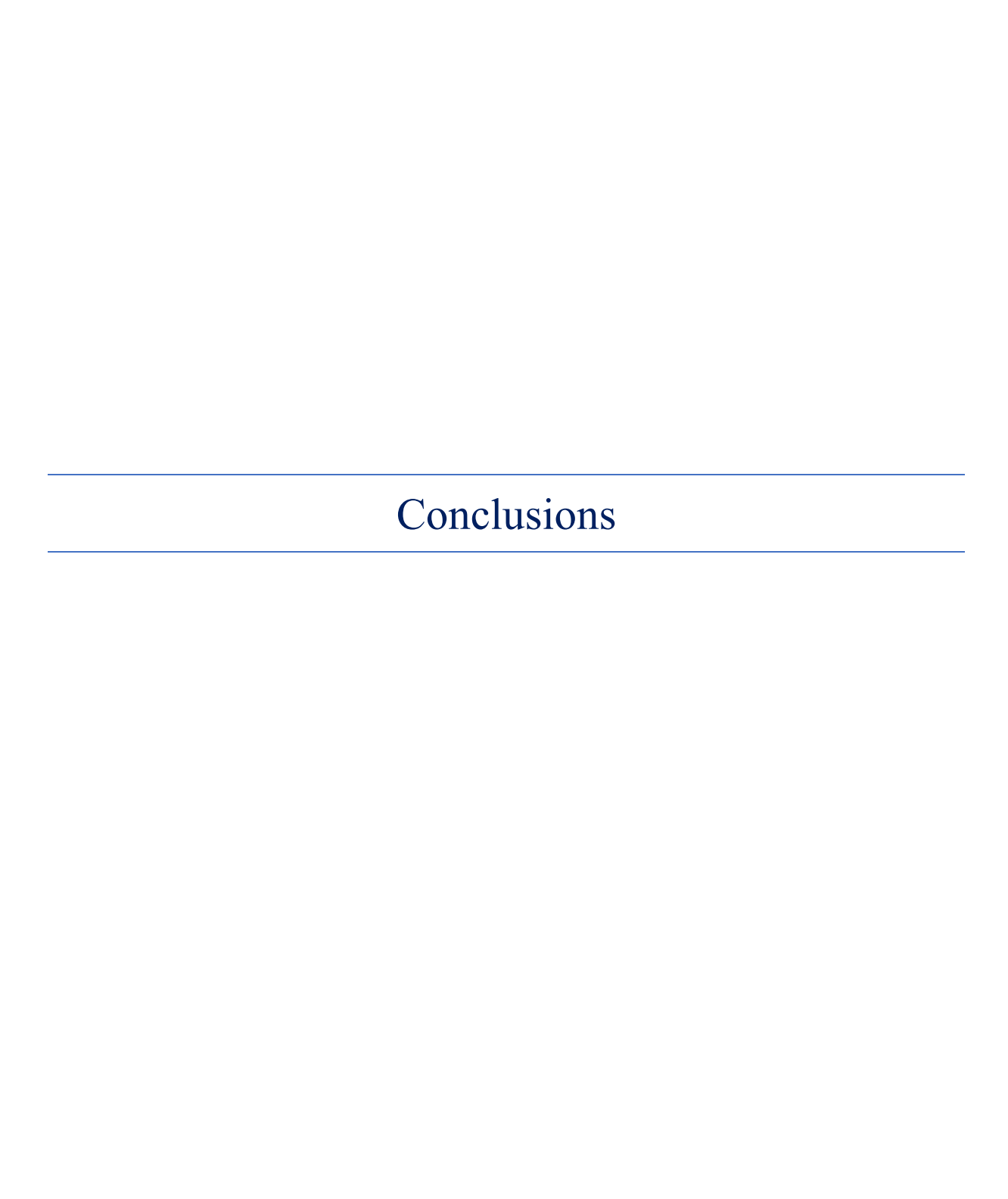


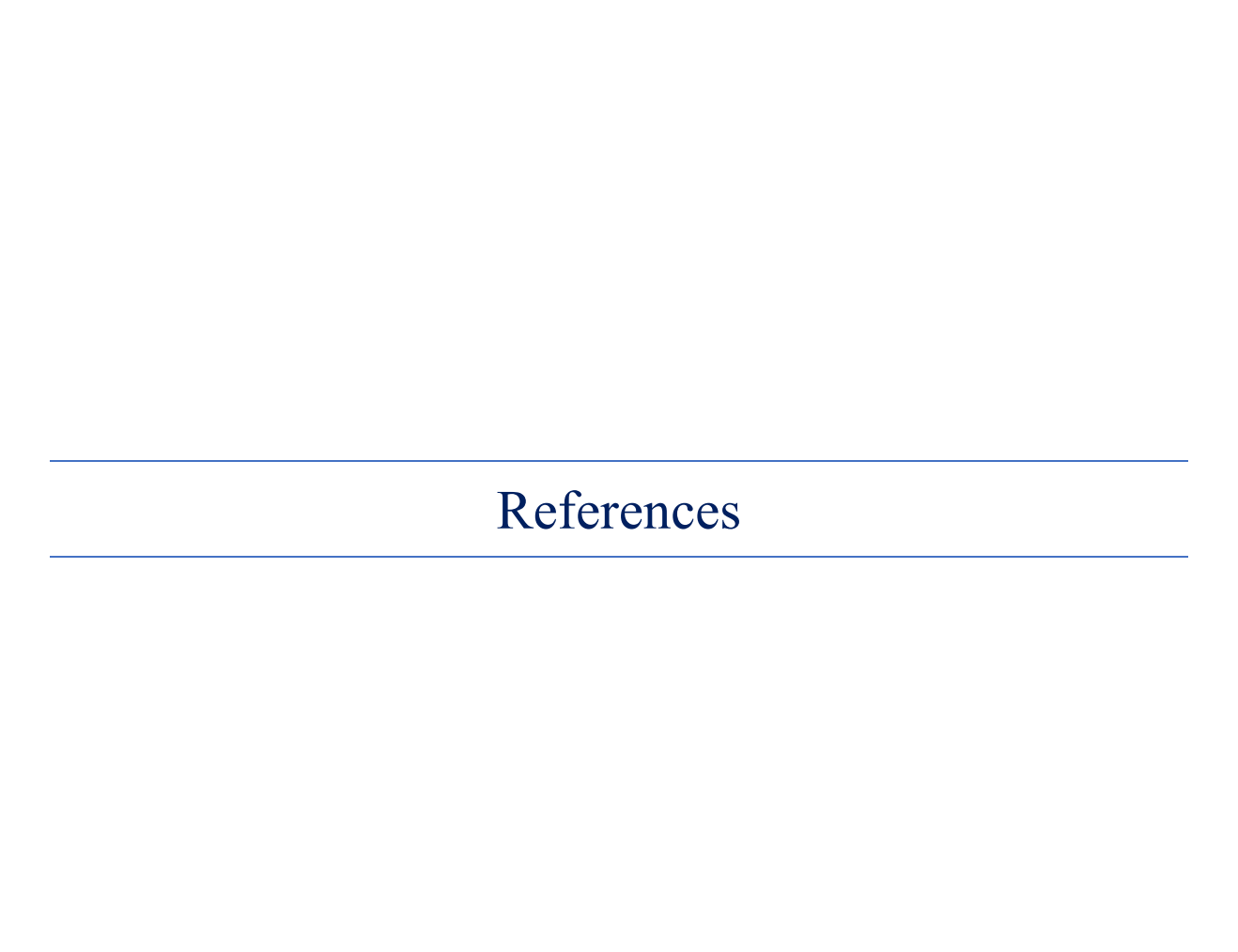
Fig. 5.12: Proposed model showing the role of OPH in protonation of Fe-Ent. Stage 1 indicates translocation of Fe-Ent into periplasmic space through TBDT. The Fe-Ent bound to the Fe-Ent binding site of OPH is shown in stage 2. The protonation of Fe-Ent complex through binuclear metal center located in the active site present in OPH is shown in stage 3 and transport of ferrous ions into cytoplasm through ABC transporter is shown in stage 4.



6. Conclusions

The work described in the theses was initiated to find the role of OPH in outer membrane transport. Ever since our lab reported association of OPH with inner membrane associated Toncomplex (ExbB/ExbD and TonB), the lab has been working to establish its physiological role. The Ton-complex is part of TonBDT system, specialized in transport of nutrients across the energy deprived outer membrane. Its involved in transport of nutrients like iron complexes, vitamin B₁₂ and Heme, Nickel complexes is well established. While exploring to identify logic behind OPH association with Ton-complex a number of hypothetical possibilities were considered. Out of these hypothetical options the proposition involving OPH role in transport of Fe-Ent was appealing due to following reasons. The Fe³⁺ ions bind Ent very strongly. After transport to the periplasmic space the bound Fe³⁺ ions need to be released from Ent either by destruction of lactone ring of Ent or by reducing the Fe-Ent complex. OPH has promiscuous lactonase activity and hydrolyzes quorum quenching signaling molecule, homoserine lactone. Since Ent is a cyclic trilactone, in this study detailed investigations were made to assess if Ent serves as substrate for OPH. The experiments described in the first chapter failed to show any Ent hydrolase activity to OPH. The analytical tools such as TLC and HPLC failed to show existence of Ent hydrolytic activity for OPH. As iron uptake studies and growth properties assessed in OPH negative background (opd null strain of Sphingophyxis wildii) clearly indicated a positive role for OPH in iron uptake, an attempt was made to examine if OPH has a role in reductive release of iron from Fe-Ent complex. Research work described in second chapter clearly demonstrated specific interactions between OPH and Ent. In fact, OPH bound more strongly to Fe-Ent than to enterobactin (Ent). Involving elegant bioinformatic tools and experimental design existence of a secondary Fe-Ent binding site was identified in OPH. A lysine residue found at secondary binding site is shown playing a critical role in establishing interactions between OPH and Fe-Ent. The SPR analysis and fluorescent emission spectra described in the second chapter clearly showed existence of specific interactions between OPH-Ent. The role of lysine, identified at the Ent binding site played a critical role in establishing interactions between OPH and Fe-Ent. Interestingly the Fe-Ent/OPH interactions influenced iron uptake in E. coli. The TonBDT negative E. coli strains used to reconstitute SfTonBDT and successfully reconstituted syTonBDT both with wild type OPH and with OPH^{D301A}, OPH^{D301N}. The iron uptake studies described in third chapter revealed influence of Ent binding site of OPH on iron uptake. Interestingly, the OPH^{K82A} failed to interact with Ton-complex components and hence it remained in the cytoplasm. In the absence of membrane targeting,

reconstitution of syTonBDT was not possible with OPH^{K82A}. However, the *E. coli* cells having syTonBDT with wildtype OPH clearly demonstrated OPH dependent enhanced iron uptake in *E. coli* cells. The overall experimental evidences gained in this study proved the role of OPH, hitherto known for its involvement in degradation of organophosphate insecticides, in outer membrane transport, particularly in iron uptake.



- 1. Abergel, R. J., J. A. Warner, D. K. Shuh and K. N. Raymond (2006). "Enterobactin protonation and iron release: structural characterization of the salicylate coordination shift in ferric enterobactin." J Am Chem Soc 128(27): 8920-8931.
- 2. Abergel, R. J., A. M. Zawadzka, T. M. Hoette and K. N. Raymond (2009). "Enzymatic hydrolysis of trilactone siderophores: where chiral recognition occurs in enterobactin and bacillibactin iron transport." J Am Chem Soc 131(35): 12682-12692.
- **3.** Afriat, L., C. Roodveldt, G. Manco and D. S. Tawfik (2006). "The latent promiscuity of newly identified microbial lactonases is linked to a recently diverged phosphotriesterase." Biochemistry 45(46): 13677-13686.
- **4.** Afriat-Jurnou, L., C. J. Jackson and D. S. Tawfik (2012). "Reconstructing a missing link in the evolution of a recently diverged phosphotriesterase by active-site loop remodeling." Biochemistry 51(31): 6047-6055.
- **5.** Alami, M., I. Luke, S. Deitermann, G. Eisner, H. G. Koch, J. Brunner and M. Muller (2003). "Differential interactions between a twin-arginine signal peptide and its translocase in Escherichia coli." Mol Cell 12(4): 937-946.
- **6.** Azam, S., S. Parthasarathy, C. Singh, S. Kumar and D. Siddavattam (2019). "Genome Organization and Adaptive Potential of Archetypal Organophosphate Degrading Sphingobium fuliginis ATCC 27551." Genome Biol Evol 11(9): 2557-2562.
- 7. Barrett, C. M. and C. Robinson (2005). "Evidence for interactions between domains of TatA and TatB from mutagenesis of the TatABC subunits of the twin-arginine translocase." Febs j 272(9): 2261-2275.
- **8.** Benning, M. M., S. B. Hong, F. M. Raushel and H. M. Holden (2000). "The binding of substrate analogs to phosphotriesterase." J Biol Chem 275(39): 30556-30560.
- 9. Benning, M. M., J. M. Kuo, F. M. Raushel and H. M. Holden (1994). "Three-dimensional structure of phosphotriesterase: an enzyme capable of detoxifying organophosphate nerve agents." Biochemistry 33(50): 15001-15007.
- **10.** Benning, M. M., H. Shim, F. M. Raushel and H. M. Holden (2001). "High resolution X-ray structures of different metal-substituted forms of phosphotriesterase from Pseudomonas diminuta." Biochemistry 40(9): 2712-2722.
- **11.** Berks, B. C. (1996). "A common export pathway for proteins binding complex redox cofactors?" Mol Microbiol 22(3): 393-404.

- **12.** Berks, B. C. (2015). "The twin-arginine protein translocation pathway." Annu Rev Biochem 84: 843-864.
- **13.** Berks, B. C., T. Palmer and F. Sargent (2003). "The Tat protein translocation pathway and its role in microbial physiology." Adv Microb Physiol 47: 187-254.
- **14.** Berks, B. C., T. Palmer and F. Sargent (2005). "Protein targeting by the bacterial twinarginine translocation (Tat) pathway." Curr Opin Microbiol 8(2): 174-181.
- **15.** Berks, B. C., F. Sargent and T. Palmer (2000). "The Tat protein export pathway." Mol Microbiol 35(2): 260-274.
- **16.** Bigley, A. N., M. F. Mabanglo, S. P. Harvey and F. M. Raushel (2015). "Variants of Phosphotriesterase for the Enhanced Detoxification of the Chemical Warfare Agent VR." Biochemistry 54(35): 5502-5512.
- **17.** Bigley, A. N. and F. M. Raushel (2013). "Catalytic mechanisms for phosphotriesterases." Biochim Biophys Acta 1834(1): 443-453.
- 18. Blattner, F. R., G. Plunkett, 3rd, C. A. Bloch, N. T. Perna, V. Burland, M. Riley, J. Collado-Vides, J. D. Glasner, C. K. Rode, G. F. Mayhew, J. Gregor, N. W. Davis, H. A. Kirkpatrick, M. A. Goeden, D. J. Rose, B. Mau and Y. Shao (1997). "The complete genome sequence of Escherichia coli K-12." Science 277(5331): 1453-1462.
- **19.** Bogsch, E. G., F. Sargent, N. R. Stanley, B. C. Berks, C. Robinson and T. Palmer (1998). "An essential component of a novel bacterial protein export system with homologues in plastids and mitochondria." J Biol Chem 273(29): 18003-18006.
- **20.** Bolhuis, A. (2002). "Protein transport in the halophilic archaeon Halobacterium sp. NRC-1: a major role for the twin-arginine translocation pathway?" Microbiology 148(Pt 11): 3335-3346.
- **21.** Brickman, T. J. and M. A. McIntosh (1992). "Overexpression and purification of ferric enterobactin esterase from Escherichia coli. Demonstration of enzymatic hydrolysis of enterobactin and its iron complex." J Biol Chem 267(17): 12350-12355.
- 22. Carrano, C. J. and K. N. Raymond (1979). "Ferric ion sequestering agents. 2. Kinetics and mechanism of iron removal from transferrin by enterobactin and synthetic tricatechols." Journal of the American Chemical Society 101(18): 5401-5404.
- **23.** Celia, H., N. Noinaj, S. D. Zakharov, E. Bordignon, I. Botos, M. Santamaria, T. J. Barnard, W. A. Cramer, R. Lloubes and S. K. Buchanan (2016). "Structural insight into the role of the Ton complex in energy transduction." Nature 538(7623): 60-65.

- **24.** Chaddock, A. M., A. Mant, I. Karnauchov, S. Brink, R. G. Herrmann, R. B. Klosgen and C. Robinson (1995). "A new type of signal peptide: central role of a twin-arginine motif in transfer signals for the delta pH-dependent thylakoidal protein translocase." Embo j 14(12): 2715-2722.
- **25.** Chaudhry, G., A. Ali and W. Wheeler (1988). "Isolation of a methyl parathion-degrading Pseudomonas sp. that possesses DNA homologous to the opd gene from a Flavobacterium sp." Appl. Environ. Microbiol. 54(2): 288-293.
- **26.** Creighton, A. M., A. Hulford, A. Mant, D. Robinson and C. Robinson (1995). "A monomeric, tightly folded stromal intermediate on the delta pH-dependent thylakoidal protein transport pathway." J Biol Chem 270(4): 1663-1669.
- **27.** de Keyzer, J., C. van der Does and A. J. Driessen (2003). "The bacterial translocase: a dynamic protein channel complex." Cell Mol Life Sci 60(10): 2034-2052.
- **28.** De Leeuw, E., I. Porcelli, F. Sargent, T. Palmer and B. C. Berks (2001). "Membrane interactions and self-association of the TatA and TatB components of the twin-arginine translocation pathway." FEBS Lett 506(2): 143-148.
- **29.** DeLisa, M. P., P. Samuelson, T. Palmer and G. Georgiou (2002). "Genetic analysis of the twin arginine translocator secretion pathway in bacteria." J Biol Chem 277(33): 29825-29831.
- **30.** Dumas, D. P., S. R. Caldwell, J. R. Wild and F. M. Raushel (1989). "Purification and properties of the phosphotriesterase from Pseudomonas diminuta." J Biol Chem 264(33): 19659-19665.
- **31.** Dumas, D. P., J. R. Wild and F. M. Raushel (1990). "Expression of Pseudomonas phosphotriesterase activity in the fall armyworm confers resistance to insecticides." Experientia 46(7): 729-731.
- **32.** Eijlander, R. T., J. D. Jongbloed and O. P. Kuipers (2009). "Relaxed specificity of the Bacillus subtilis TatAdCd translocase in Tat-dependent protein secretion." J Bacteriol 191(1): 196-202.
- **33.** Elias, M., J. Dupuy, L. Merone, L. Mandrich, E. Porzio, S. Moniot, D. Rochu, C. Lecomte, M. Rossi, P. Masson, G. Manco and E. Chabriere (2008). "Structural basis for natural lactonase and promiscuous phosphotriesterase activities." J Mol Biol 379(5): 1017-1028.

- **34.** Elias, M. and D. S. Tawfik (2012). "Divergence and convergence in enzyme evolution: parallel evolution of paraoxonases from quorum-quenching lactonases." J Biol Chem 287(1): 11-20.
- **35.** Ferguson, A. D. and J. Deisenhofer (2004). "Metal import through microbial membranes." Cell 116(1): 15-24.
- **36.** Folschweiller, N., I. J. Schalk, H. Celia, B. Kieffer, M. A. Abdallah and F. Pattus (2000). "The pyoverdin receptor FpvA, a TonB-dependent receptor involved in iron uptake by Pseudomonas aeruginosa (review)." Mol Membr Biol 17(3): 123-133.
- **37.** Furrer, J. L., D. N. Sanders, I. G. Hook-Barnard and M. A. McIntosh (2002). "Export of the siderophore enterobactin in Escherichia coli: involvement of a 43 kDa membrane exporter." Mol Microbiol 44(5): 1225-1234.
- **38.** Gorla, P., J. P. Pandey, S. Parthasarathy, M. Merrick and D. Siddavattam (2009). "Organophosphate hydrolase in Brevundimonas diminuta is targeted to the periplasmic face of the inner membrane by the twin arginine translocation pathway." J Bacteriol 191(20): 6292-6299.
- **39.** Greenwood, K. T. and R. K. Luke (1978). "Enzymatic hydrolysis of enterochelin and its iron complex in Escherichia Coli K-12. Properties of enterochelin esterase." Biochim Biophys Acta 525(1): 209-218.
- **40.** Gudla, R., G. V. Konduru, H. A. Nagarajaram and D. Siddavattam (2019). "Organophosphate hydrolase interacts with Ton components and is targeted to the membrane only in the presence of the ExbB/ExbD complex." FEBS Lett 593(6): 581-593.
- **41.** Hanahan, D. (1983). "Studies on transformation of Escherichia coli with plasmids." J Mol Biol 166(4): 557-580.
- **42.** Harper, L. L., C. S. McDaniel, C. E. Miller and J. R. Wild (1988). "Dissimilar plasmids isolated from Pseudomonas diminuta MG and a Flavobacterium sp. (ATCC 27551) contain identical opd genes." Appl Environ Microbiol 54(10): 2586-2589.
- 43. Harris, W. R., C. J. Carrano, S. R. Cooper, S. R. Sofen, A. E. Avdeef, J. V. McArdle and K. N. Raymond (1979). "Coordination chemistry of microbial iron transport compounds. 19. Stability constants and electrochemical behavior of ferric enterobactin and model complexes." Journal of the American Chemical Society 101(20): 6097-6104.
- **44.** Held, K. G. and K. Postle (2002). "ExbB and ExbD do not function independently in TonB-dependent energy transduction." J Bacteriol 184(18): 5170-5173.

- **45.** Hider, R. C. and X. Kong (2010). "Chemistry and biology of siderophores." Nat Prod Rep 27(5): 637-657.
- **46.** Higgs, P. I., R. A. Larsen and K. Postle (2002). "Quantification of known components of the Escherichia coli TonB energy transduction system: TonB, ExbB, ExbD and FepA." Mol Microbiol 44(1): 271-281.
- **47.** Hu, Y., E. Zhao, H. Li, B. Xia and C. Jin (2010). "Solution NMR structure of the TatA component of the twin-arginine protein transport system from gram-positive bacterium Bacillus subtilis." J Am Chem Soc 132(45): 15942-15944.
- **48.** Jack, R. L., F. Sargent, B. C. Berks, G. Sawers and T. Palmer (2001). "Constitutive expression of Escherichia coli tat genes indicates an important role for the twin-arginine translocase during aerobic and anaerobic growth." J Bacteriol 183(5): 1801-1804.
- **49.** James, L. C. and D. S. Tawfik (2001). "Catalytic and binding poly-reactivities shared by two unrelated proteins: The potential role of promiscuity in enzyme evolution." Protein Sci 10(12): 2600-2607.
- **50.** Karpishin, T. B. and K. N. Raymond (1992). "The First Structural Characterization of a Metal–Enterobactin Complex: [V (enterobactin)] 2–." Angewandte Chemie International Edition in English 31(4): 466-468.
- **51.** Karpouzas, D. G. and B. K. Singh (2006). "Microbial degradation of organophosphorus xenobiotics: metabolic pathways and molecular basis." Adv Microb Physiol 51: 119-185.
- **52.** Kawahara, K., A. Tanaka, J. Yoon and A. Yokota (2010). "Reclassification of a parathione-degrading Flavobacterium sp. ATCC 27551 as Sphingobium fuliginis." J Gen Appl Microbiol 56(3): 249-255.
- **53.** Khersonsky, O. and D. S. Tawfik (2010). "Enzyme promiscuity: a mechanistic and evolutionary perspective." Annu Rev Biochem 79: 471-505.
- **54.** Killmann, H., G. Videnov, G. Jung, H. Schwarz and V. Braun (1995). "Identification of receptor binding sites by competitive peptide mapping: phages T1, T5, and phi 80 and colicin M bind to the gating loop of FhuA." J Bacteriol 177(3): 694-698.
- **55.** Krewulak, K. D. and H. J. Vogel (2008). "Structural biology of bacterial iron uptake." Biochim Biophys Acta 1778(9): 1781-1804.
- **56.** Krewulak, K. D. and H. J. Vogel (2011). "TonB or not TonB: is that the question?" Biochem Cell Biol 89(2): 87-97.

- **57.** Laemmli, U. K. (1970) Cleavage of structural proteins during the assembly of the head of bacteriophage T4. Nature. 227(5259): 680–685.
- **58.** Lawlor, K. M. and S. M. Payne (1984). "Aerobactin genes in Shigella spp." J Bacteriol 160(1): 266-272.
- **59.** Lee, P. A., D. Tullman-Ercek and G. Georgiou (2006). "The bacterial twin-arginine translocation pathway." Annu Rev Microbiol 60: 373-395.
- **60.** LeJeune, K. E., J. R. Wild and A. J. Russell (1998). "Nerve agents degraded by enzymatic foams." Nature 395(6697): 27-28.
- **61.** Liang, L., H. A. Tajmir-Riahi and M. Subirade (2008). "Interaction of beta-lactoglobulin with resveratrol and its biological implications." Biomacromolecules 9(1): 50-56.
- **62.** Lin, H., M. A. Fischbach, D. R. Liu and C. T. Walsh (2005). "In vitro characterization of salmochelin and enterobactin trilactone hydrolases IroD, IroE, and Fes." J Am Chem Soc 127(31): 11075-11084.
- **63.** Loomis, L. D. and K. N. Raymond (1991). "Solution equilibria of enterobactin and metal-enterobactin complexes." Inorganic Chemistry 30(5): 906-911.
- **64.** Maki-Yonekura S, Matsuoka R, Yamashita Y, et al. Hexameric and pentameric complexes of the ExbBD energizer in the Ton system [published correction appears in Elife. 2018 May 04;7:]. *Elife*. 2018;7:e35419. Published 2018 Apr 17. doi:10.7554/eLife.35419.
- **65.** Matzanke, B. F., D. J. Ecker, T. S. Yang, B. H. Huynh, G. Muller and K. N. Raymond (1986). "Escherichia coli iron enterobactin uptake monitored by Mossbauer spectroscopy." J Bacteriol 167(2): 674-680.
- **66.** Miethke, M. and M. A. Marahiel (2007). "Siderophore-based iron acquisition and pathogen control." Microbiol Mol Biol Rev 71(3): 413-451.
- 67. Mori, H., E. J. Summer and K. Cline (2001). "Chloroplast TatC plays a direct role in thylakoid (Delta)pH-dependent protein transport." FEBS Lett 501(1): 65-68.
- **68.** Morris, G. M., R. Huey, W. Lindstrom, M. F. Sanner, R. K. Belew, D. S. Goodsell and A. J. Olson (2009). "AutoDock4 and AutoDockTools4: Automated docking with selective receptor flexibility." J Comput Chem 30(16): 2785-2791.

- **69.** Mould, R. M. and C. Robinson (1991). "A proton gradient is required for the transport of two lumenal oxygen-evolving proteins across the thylakoid membrane." J Biol Chem 266(19): 12189-12193.
- **70.** Mujahid, M., C. Sasikala and V. Ramana Ch (2011). "Production of indole-3-acetic acid and related indole derivatives from L-tryptophan by Rubrivivax benzoatilyticus JA2." Appl Microbiol Biotechnol 89(4): 1001-1008.
- **71.** Mulbry, W. W. and J. S. Karns (1989a). "Parathion hydrolase specified by the Flavobacterium opd gene: relationship between the gene and protein." J Bacteriol 171(12): 6740-6746.
- **72.** Mulbry, W. W. and J. S. Karns (1989b). "Purification and characterization of three parathion hydrolases from gram-negative bacterial strains." Appl Environ Microbiol 55(2): 289-293.
- **73.** Mulbry, W. W., J. S. Karns, P. C. Kearney, J. O. Nelson, C. S. McDaniel and J. R. Wild (1986). "Identification of a plasmid-borne parathion hydrolase gene from Flavobacterium sp. by southern hybridization with opd from Pseudomonas diminuta." Appl Environ Microbiol 51(5): 926-930.
- **74.** Muller, M. and R. B. Klosgen (2005). "The Tat pathway in bacteria and chloroplasts (review)." Mol Membr Biol 22(1-2): 113-121.
- **75.** Munnecke, D. M. and D. P. Hsieh (1974). "Microbial decontamination of parathion and p-nitrophenol in aqueous media." Appl Microbiol 28(2): 212-217.
- **76.** Noinaj, N., M. Guillier, T. J. Barnard and S. K. Buchanan (2010). "TonB-dependent transporters: regulation, structure, and function." Annu Rev Microbiol 64: 43-60.
- 77. Oates, J., C. M. Barrett, J. P. Barnett, K. G. Byrne, A. Bolhuis and C. Robinson (2005). "The Escherichia coli twin-arginine translocation apparatus incorporates a distinct form of TatABC complex, spectrum of modular TatA complexes and minor TatAB complex." J Mol Biol 346(1): 295-305.
- **78.** O'Brien, I. G., G. B. Cox and F. Gibson (1971). "Enterochelin hydrolysis and iron metabolism in Escherichia coli." Biochim Biophys Acta 237(3): 537-549.
- **79.** O'Brien, I. G. and F. Gibson (1970). "The structure of enterochelin and related 2,3-dihydroxy-N-benzoylserine conjugates from Escherichia coli." Biochim Biophys Acta 215(2): 393-402.

- **80.** Omburo, G. A., J. M. Kuo, L. S. Mullins and F. M. Raushel (1992). "Characterization of the zinc binding site of bacterial phosphotriesterase." J Biol Chem 267(19): 13278-13283.
- **81.** Orriss, G. L., M. J. Tarry, B. Ize, F. Sargent, S. M. Lea, T. Palmer and B. C. Berks (2007). "TatBC, TatB, and TatC form structurally autonomous units within the twin arginine protein transport system of Escherichia coli." FEBS Lett 581(21): 4091-4097.
- **82.** Osborne, A. R., T. A. Rapoport and B. van den Berg (2005). "Protein translocation by the Sec61/SecY channel." Annu Rev Cell Dev Biol 21: 529-550.
- **83.** Palmer, T. and B. C. Berks (2012). "The twin-arginine translocation (Tat) protein export pathway." Nat Rev Microbiol 10(7): 483-496.
- **84.** Palmer, T., F. Sargent and B. C. Berks (2005). "Export of complex cofactor-containing proteins by the bacterial Tat pathway." Trends Microbiol 13(4): 175-180.
- **85.** Pandeeti, E. V. P., Chakka, D., Pandey, J. P., and Siddavattam, D. (2011). Indigenous organophosphate-degrading (opd) plasmid pCMS1 of Brevundimonas diminuta is self-transmissible and plays a key role in horizontal mobility of the opd gene. Plasmid, 65(3), 226-231.
- **86.** Pandeeti, E. V., T. Longkumer, D. Chakka, V. R. Muthyala, S. Parthasarathy, A. K. Madugundu, S. Ghanta, S. R. Medipally, S. C. Pantula, H. Yekkala and D. Siddavattam (2012). "Multiple mechanisms contribute to lateral transfer of an organophosphate degradation (opd) island in Sphingobium fuliginis ATCC 27551." G3 (Bethesda) 2(12): 1541-1554.
- **87.** Panjkovich, A. and X. Daura (2014). "PARS: a web server for the prediction of Protein Allosteric and Regulatory Sites." Bioinformatics 30(9): 1314-1315.
- **88.** Parthasarathy, S., S. Azam, A. Lakshman Sagar, V. Narasimha Rao, R. Gudla, H. Parapatla, H. Yakkala, S. Ghanta Vemuri and D. Siddavattam (2017). "Genome-Guided Insights Reveal Organophosphate-Degrading Brevundimonas diminuta as Sphingopyxis wildii and Define Its Versatile Metabolic Capabilities and Environmental Adaptations." Genome Biol Evol 9(1): 77-81.
- **89.** Parthasarathy, S., H. Parapatla, A. Nandavaram, T. Palmer and D. Siddavattam (2016). "Organophosphate Hydrolase Is a Lipoprotein and Interacts with Pi-specific Transport System to Facilitate Growth of Brevundimonas diminuta Using OP Insecticide as Source of Phosphate." J Biol Chem 291(14): 7774-7785.

- **90.** Parthasarathy, S., H. Parapatla and D. Siddavattam (2017). "Topological analysis of the lipoprotein organophosphate hydrolase from Sphingopyxis wildii reveals a periplasmic localisation." FEMS microbiology letters 364(19).
- **91.** Perry, R. D. and C. L. San Clemente (1979). "Siderophore synthesis in Klebsiella pneumoniae and Shigella sonnei during iron deficiency." J Bacteriol 140(3): 1129-1132.
- **92.** Poelarends, G. J., H. Serrano, W. H. Johnson, Jr. and C. P. Whitman (2005). "Inactivation of malonate semialdehyde decarboxylase by 3-halopropiolates: evidence for hydratase activity." Biochemistry 44(26): 9375-9381.
- **93.** Pohlschroder, M., K. Dilks, N. J. Hand and R. Wesley Rose (2004). "Translocation of proteins across archaeal cytoplasmic membranes." FEMS Microbiol Rev 28(1): 3-24.
- **94.** Pollack, J. R., B. N. Ames and J. B. Neilands (1970). "Iron transport in Salmonella typhimurium: mutants blocked in the biosynthesis of enterobactin." J Bacteriol 104(2): 635-639.
- **95.** Posey, J. E. and F. C. Gherardini (2000). "Lack of a role for iron in the Lyme disease pathogen." Science 288(5471): 1651-1653.
- **96.** Postle, K. and R. A. Larsen (2007). "TonB-dependent energy transduction between outer and cytoplasmic membranes." Biometals 20(3-4): 453-465.
- **97.** Prokop, Z., F. Oplustil, J. DeFrank and J. Damborsky (2006). "Enzymes fight chemical weapons." Biotechnol J 1(12): 1370-1380.
- **98.** Punginelli, C., B. Maldonado, S. Grahl, R. Jack, M. Alami, J. Schroder, B. C. Berks and T. Palmer (2007). "Cysteine scanning mutagenesis and topological mapping of the Escherichia coli twin-arginine translocase TatC Component." J Bacteriol 189(15): 5482-5494.
- **99.** Raushel, F. M. (2002). "Bacterial detoxification of organophosphate nerve agents." Curr Opin Microbiol 5(3): 288-295.
- **100.** Raushel, F. M. and H. M. Holden (2000). "Phosphotriesterase: an enzyme in search of its natural substrate." Adv Enzymol Relat Areas Mol Biol 74: 51-93.
- **101.** Raymond, K. N. and C. J. Carrano (1979). "Coordination chemistry and microbial iron transport." Accounts of Chemical Research 12(5): 183-190.
- **102.** Raymond, K. N., E. A. Dertz and S. S. Kim (2003). "Enterobactin: an archetype for microbial iron transport." Proc Natl Acad Sci U S A 100(7): 3584-3588.

- **103.** Robinson, C. and A. Bolhuis (2004). "Tat-dependent protein targeting in prokaryotes and chloroplasts." Biochim Biophys Acta 1694(1-3): 135-147.
- **104.** Roodveldt, C. and D. S. Tawfik (2005). "Shared promiscuous activities and evolutionary features in various members of the amidohydrolase superfamily." Biochemistry 44(38): 12728-12736.
- **105.** Rose, R. W., T. Bruser, J. C. Kissinger and M. Pohlschroder (2002). "Adaptation of protein secretion to extremely high-salt conditions by extensive use of the twin-arginine translocation pathway." Mol Microbiol 45(4): 943-950.
- **106.** Sambrook, J., & Russell David, W. (1989). Molecular cloning: a laboratory manual. Vol. 3: Cold spring harbor laboratory press.
- **107.** Samantarrai, D., A. Lakshman Sagar, R. Gudla and D. Siddavattam (2020). "TonB-Dependent Transporters in Sphingomonads: Unraveling Their Distribution and Function in Environmental Adaptation." Microorganisms 8(3).
- **108.** Sargent, F., U. Gohlke, E. De Leeuw, N. R. Stanley, T. Palmer, H. R. Saibil and B. C. Berks (2001). "Purified components of the Escherichia coli Tat protein transport system form a double-layered ring structure." Eur J Biochem 268(12): 3361-3367.
- **109.** Sargent, F., N. R. Stanley, B. C. Berks and T. Palmer (1999). "Sec-independent protein translocation in Escherichia coli. A distinct and pivotal role for the TatB protein." J Biol Chem 274(51): 36073-36082.
- **110.** Schagger, H. and G. von Jagow (1991). "Blue native electrophoresis for isolation of membrane protein complexes in enzymatically active form." Anal Biochem 199(2): 223-231.
- **111.** Schauer, K., B. Gouget, M. Carriere, A. Labigne and H. de Reuse (2007). "Novel nickel transport mechanism across the bacterial outer membrane energized by the TonB/ExbB/ExbD machinery." Mol Microbiol 63(4): 1054-1068.
- **112.** Schauer, K., D. A. Rodionov and H. de Reuse (2008). "New substrates for TonB-dependent transport: do we only see the 'tip of the iceberg'?" Trends Biochem Sci 33(7): 330-338.
- **113.** Sean Peacock, R., A. M. Weljie, S. Peter Howard, F. D. Price and H. J. Vogel (2005). "The solution structure of the C-terminal domain of TonB and interaction studies with TonB box peptides." J Mol Biol 345(5): 1185-1197.

- 114. Serdar, C. M., D. T. Gibson, D. M. Munnecke and J. H. Lancaster (1982). "Plasmid Involvement in Parathion Hydrolysis by Pseudomonas diminuta." Appl Environ Microbiol 44(1): 246-249.
- **115.** Sethunathan, N. and T. Yoshida (1973). "A Flavobacterium sp. that degrades diazinon and parathion." Can J Microbiol 19(7): 873-875.
- 116. Siddavattam, D., S. Khajamohiddin, B. Manavathi, S. B. Pakala and M. Merrick (2003). "Transposon-like organization of the plasmid-borne organophosphate degradation (opd) gene cluster found in Flavobacterium sp." Appl Environ Microbiol 69(5): 2533-2539.
- **117.** Siddavattam, D., H. Yakkala and D. Samantarrai (2019). "Lateral transfer of organophosphate degradation (opd) genes among soil bacteria: mode of transfer and contributions to organismal fitness." J Genet 98.
- **118.** Singh, B. K. (2009). "Organophosphorus-degrading bacteria: ecology and industrial applications." Nat Rev Microbiol 7(2): 156-164.
- **119.** Singh, B. K., R. C. Kuhad, A. Singh, R. Lal and K. K. Tripathi (1999). "Biochemical and molecular basis of pesticide degradation by microorganisms." Crit Rev Biotechnol 19(3): 197-225.
- **120.** Singh, B. K. and A. Walker (2006). "Microbial degradation of organophosphorus compounds." FEMS Microbiol Rev 30(3): 428-471.
- **121.** Somara, S. and D. Siddavattam (1995). "Plasmid mediated organophosphate pesticide degradation by Flavobacterium balustinum." Biochem Mol Biol Int 36(3): 627-631.
- **122.** Strauch, E. M. and G. Georgiou (2007). "Escherichia coli tatC mutations that suppress defective twin-arginine transporter signal peptides." J Mol Biol 374(2): 283-291.
- **123.** Theriot, C. M. and A. M. Grunden (2011). "Hydrolysis of organophosphorus compounds by microbial enzymes." Appl Microbiol Biotechnol 89(1): 35-43.
- **124.** Tsai, P. C., N. Fox, A. N. Bigley, S. P. Harvey, D. P. Barondeau and F. M. Raushel (2012). "Enzymes for the homeland defense: optimizing phosphotriesterase for the hydrolysis of organophosphate nerve agents." Biochemistry 51(32): 6463-6475.
- **125.** Tuckman, M. and M. S. Osburne (1992). "In vivo inhibition of TonB-dependent processes by a TonB box consensus pentapeptide." J Bacteriol 174(1): 320-323.
- **126.** Veggi, D., M. A. Gentile, F. Cantini, P. Lo Surdo, V. Nardi-Dei, K. L. Seib, M. Pizza, R. Rappuoli, L. Banci, S. Savino and M. Scarselli (2012). "The factor H binding protein

- of Neisseria meningitidis interacts with xenosiderophores in vitro." Biochemistry 51(46): 9384-9393.
- **127.** Weiner, J. H., P. T. Bilous, G. M. Shaw, S. P. Lubitz, L. Frost, G. H. Thomas, J. A. Cole and R. J. Turner (1998). "A novel and ubiquitous system for membrane targeting and secretion of cofactor-containing proteins." Cell 93(1): 93-101.
- **128.** Wickner, W., A. J. Driessen and F. U. Hartl (1991). "The enzymology of protein translocation across the Escherichia coli plasma membrane." Annu Rev Biochem 60: 101-124.
- **129.** Wiener, M. C. (2005). "TonB-dependent outer membrane transport: going for Baroque?" Curr Opin Struct Biol 15(4): 394-400.
- **130.** Yang, H., P. D. Carr, S. Y. McLoughlin, J. W. Liu, I. Horne, X. Qiu, C. M. Jeffries, R. J. Russell, J. G. Oakeshott and D. L. Ollis (2003). "Evolution of an organophosphate-degrading enzyme: a comparison of natural and directed evolution." Protein Eng 16(2): 135-145.
- 131. Yew, W. S., J. Akana, E. L. Wise, I. Rayment and J. A. Gerlt (2005). "Evolution of enzymatic activities in the orotidine 5'-monophosphate decarboxylase suprafamily: enhancing the promiscuous D-arabino-hex-3-ulose 6-phosphate synthase reaction catalyzed by 3-keto-L-gulonate 6-phosphate decarboxylase." Biochemistry 44(6): 1807-1815.
- **132.** Zeng, X., Y. Mo, F. Xu and J. Lin (2013). "Identification and characterization of a periplasmic trilactone esterase, Cee, revealed unique features of ferric enterobactin acquisition in Campylobacter." Mol Microbiol 87(3): 594-608.



Organophosphate Hydrolase Is a Lipoprotein and Interacts with P_i-specific Transport System to Facilitate Growth of *Brevundimonas diminuta* Using OP Insecticide as Source of Phosphate*

Received for publication, January 11, 2016, and in revised form, February 7, 2016 Published, JBC Papers in Press, February 9, 2016, DOI 10.1074/jbc.M116.715110

Sunil Parthasarathy^{‡1}, Hari Parapatla[‡], Aparna Nandavaram[‡], Tracy Palmer[§], and Dayananda Siddavattam^{‡2} From the [‡]Department of Animal Biology, School of Life Sciences, University of Hyderabad, Hyderabad, 500 046, India and the [§]Division of Molecular Microbiology, College of Life Sciences, University of Dundee, United Kingdom

Organophosphate hydrolase (OPH), encoded by the organophosphate degradation (opd) island, hydrolyzes the triester bond found in a variety of organophosphate insecticides and nerve agents. OPH is targeted to the inner membrane of Brevundimonas diminuta in a pre-folded conformation by the twin arginine transport (Tat) pathway. The OPH signal peptide contains an invariant cysteine residue at the junction of the signal peptidase (Spase) cleavage site along with a well conserved lipobox motif. Treatment of cells producing native OPH with the signal peptidase II inhibitor globomycin resulted in accumulation of most of the pre-OPH in the cytoplasm with negligible processed OPH detected in the membrane. Substitution of the conserved lipobox cysteine to serine resulted in release of OPH into the periplasm, confirming that OPH is a lipoprotein. Analysis of purified OPH revealed that it was modified with the fatty acids palmitate and stearate. Membrane-bound OPH was shown to interact with the outer membrane efflux protein TolC and with PstS, the periplasmic component of the ABC transporter complex (PstSACB) involved in phosphate transport. Interaction of OPH with PstS appears to facilitate transport of P_i generated from organophosphates due to the combined action of OPH and periplasmically located phosphatases. Consistent with this model, opd null mutants of B. diminuta failed to grow using the organophosphate insecticide methyl parathion as sole source of phosphate.

Membrane-associated organophosphate hydrolase (OPH)³ hydrolyzes the triester bond found in a variety of organophos-

phate insecticides and nerve agents (1, 2). The 39-kDa monomer requires Zn^+ ions as cofactor (3). OPH is encoded by the *opd* (organophosphate degrading) gene found on dissimilar plasmids and the *opd* gene has recently been shown to be a part of an integrative mobilizable element (IME) (4). Due to the mobile nature of the *opd* island, identical *opd* genes are found among bacterial strains isolated from different geographical regions (4, 5). Although its physiological substrate is unknown, OPH hydrolyzes paraoxon at a rate approaching the diffusion limit (k_{cat}/K_m 10^8 M^{-1} s⁻¹) (6). Considering its catalytic efficiency and broad substrate range, it has been assumed that OPH has evolved to degrade organophosphate (OP) insecticides accumulated in agricultural soils (7). Structural analysis shows that OPH contains a TIM barrel-fold as seen in most of the members of amidohydrolase superfamily proteins (8).

OPH associates with cell membranes and membrane-associated OPH has been purified from a number of sources (3, 9–13). Analysis of the amino acid sequences of OPH proteins indicates that all of them contain a predicted signal peptide harboring a well defined twin-arginine (Tat) motif. Twin-arginine signal peptides serve to target proteins to the twin-arginine protein transport (Tat) pathway, which translocates folded proteins across the bacterial cytoplasmic membrane (14). Proteinase K treatment confirmed that OPH is exported to the periplasmic side of the inner membrane in Brevundimonas diminuta and dependence on the Tat pathway was demonstrated because substitution of the invariant arginine residues of the Tat signal peptide affected both processing and localization of OPH (15). However, the mechanism by which OPH is anchored to the inner membrane and the physiological role of OPH are currently unclear. In this report we demonstrate that OPH is a lipoprotein and that it plays an essential role in the acquisition of phosphate from OP insecticides.

Experimental Procedures

Media, Strains, and Plasmids—Strains and plasmids used in the present work are shown in Table 1. Primers used for PCR amplification and site-directed mutagenesis are listed in Table 2. B. diminuta cultures were grown either in LB medium or in HEPES minimal medium. HEPES minimal medium was pre-

dase;DDM,n-dodecyl β -D-maltoside;Tricine,N-[2-hydroxy-1,1-bis(hydroxy-methyl)ethyl]glycine; IMAC, immobilized-metal affinity chromatography; BN-PAGE, blue native-PAGE.



^{*} This work was supported in part by the Department of Biotechnology, Govt. of India (to D. S. Laboratory). Department of Animal Biology was supported by the DST-FIST (Department of Science and Technology–Fund for Improvement of S&T Infrastructure), and the School of Life Sciences, University of Hyderabad is supported by DBT-CREBB/BUILDER (Department of Biotechnology–Centre for Research and Education in Biology and Biotechnology/Boost to University Interdisciplinary Life Science Departments for Education and Research). The authors declare that they have no conflicts of interest with the contents of this article.

¹ Supported by a Shantha Biotechnics Junior Research Fellowship (JRF) and Commonwealth Split-Site Fellowships, British Council, UK.

² To whom correspondence should be addressed: Dept. of Animal Biology, School of Life Sciences, University of Hyderabad, Prof. C. R. Rao Rd., Gachibowli, Hyderabad 500 046, India. Tel.: 91-40-23134578; Fax: 91-40-23010120/145; E-mail: sdsl@uohyd.ernet.in.

³ The abbreviations used are: OPH, organophosphate hydrolase; OP, organophosphate insecticides; Tat, Twin arginine transport; SPase, signal pepti-



doi: 10.1093/femsle/fnx187

Advance Access Publication Date: 31 August 2017 Research Letter

RESEARCH LETTER - Environmental Microbiology

Topological analysis of the lipoprotein organophosphate hydrolase from *Sphingopyxis wildii* reveals a periplasmic localisation

Sunil Parthasarathy, Hari Parapatla and Dayananda Siddavattam*

Department of Animal Sciences, School of Life Sciences, University of Hyderabad, C. R. Rao Road, Gachibowli, Hyderabad 500 046, India

*Corresponding author: Department of Animal Biology, School of Life Sciences, University of Hyderabad, C. R. Rao Road, Gachibowli, Hyderabad 500 046, India. Tel: +91-40-23134578; E-mail: sdsl@uohyd.ernet.in

One sentence summary: The inner-membrane topology of organophosphate hydrolase in Sphingopyxis wildii. Editor: Aleiandra Bravo

ABSTRACT

Organophosphate hydrolase (OPH) is a membrane-associated lipoprotein. It translocates across the inner membrane via the twin-arginine transport pathway and remains anchored to the periplasmic face of the inner membrane through a diacylglycerol moiety linked to the invariant cysteine residue found at the junction of a SpaseII cleavage site. Due to the existence of a transmembrane helix at the C-terminus of the mature OPH, an inner-membrane topology was predicted suggesting the C-terminus of OPH is cytoplasmic. The predicted topology was validated by generating OPH variants either fused in-frame with β -lactamase or with unique cysteine residues. Sphingopyxis wildii cells expressing OPH variants with Bla fused at the N-terminal, C-terminal or central regions all grew in the presence of ampicillin. Supporting the β -lactamase reporter assay, the OPH variants having unique cysteine residues at different strategic locations were accessible to the otherwise membrane-impermeant PEG-Mal (methoxypolyethylene glycol maleimide) revealing that, with the exception of the lipoprotein anchor, the entire OPH is in the periplasmic space.

Keywords: organophosphate hydrolase (OPH); membrane topology; membrane transport; phosphate acquisition

INTRODUCTION

Phosphotriesterases (PTEs) have been isolated from a variety of organophosphate (OP) degrading soil bacteria. They hydrolyse structurally dissimilar OP insecticides and nerve agents (Dumas et al. 1989). The organophosphate hydrolase (OPH) of Brivundimonas diminuta, recently reclassified as Sphingopyxis wildii, is one of the well-characterised PTEs (Parthasarathy et al. 2017). It is a membrane-associated metalloenzyme and requires Zn ions as cofactor. OPH contains a signal peptide typically seen in membrane-associated lipoproteins. It contains an invariant cysteine residue at the junction of the signal peptide-cleavage site. The OPH anchors to the periplasmic face of the inner mem-

brane through a diacyl glycerol linked to the invariant cysteine residue (Parthasarathy et al. 2016). The signal peptide of OPH also contains a twin-arginine transport (Tat) motif typically seen in proteins that target/translocate across the inner membrane in a pre-folded conformation. The OPH variants having substitutions to the invariant arginines failed to target the inner membrane (Gorla et al. 2009). The periplasmically located OPH exists as part of multiprotein complex. It interacts with the components of phosphate-specific transport (Pst) system, ABC transporters and efflux pump AcrZ/ToIC (Parthasarathy et al. 2016). Based on these interactions, the OPH has been implicated in acquisition of phosphate from OP compounds.

Received: 19 July 2017; Accepted: 30 August 2017

© FEMS 2017. All rights reserved. For permissions, please e-mail: journals.permissions@oup.com

Genome-Guided Insights Reveal Organophosphate-Degrading *Brevundimonas diminuta* as *Sphingopyxis wildii* and Define Its Versatile Metabolic Capabilities and Environmental Adaptations

Sunil Parthasarathy^{1,†}, Sarwar Azam^{2,†}, Annapoorni Lakshman Sagar¹, Veera Narasimha Rao², Ramurthy Gudla¹, Hari Parapatla¹, Harshita Yakkala¹, Sujana Ghanta Vemuri¹, and Dayananda Siddayattam^{1,*}

Accepted: November 5, 2016

Abstract

The complete genome sequence of *Brevundimonas diminuta* represented a chromosome (~4.15 Mb) and two plasmids (pCMS1 and pCMS2) with sizes of 65,908 and 30,654 bp, respectively. The sequence of the genome showed no significant similarity with the known bacterial genome sequences, instead showed weak similarity with the members of different genera of family, Sphingomonadaceae. Contradicting existing taxonomic position, the core genome-guided phylogenetic tree placed *B. diminuta* in the genus Sphingopyxis and showed sufficient genome-to-genome distance warranting a new species name. Reflecting the strains ability to grow in harsh environments, the genome-contained genetic repertoire required for mineralization of several recalcitrant man-made aromatic compounds.

Key words: biodegradation, aromatic compound degradation, biotransformation, Sphingomonadales.

Introduction

The safe disposal of neurotoxic organophosphate (OP) residues has attracted the attention of several microbiologists. Bacterial strains possessing organophosphate hydrolase (OPH) activity have been isolated from sewage and soil samples (Munnecke and Hsieh 1974). Using conventional taxonomic tools, the isolated OP-degrading bacterial strains have been placed in the genus, Pseudomonas (Munnecke and Hsieh 1974). However, when the genus *Pseudomonas* was reclassified, bacterial strains that were previously named as Pseudomonas diminuta and Pseudomonas vesicularis were moved to a separate genus known as Brevundimonas. Accordingly, the P. diminuta MG was renamed Brevundimonas diminuta MG (Segers et al. 1994). In this study, we generated the complete genome sequence of B. diminuta MG and report several interesting features pertaining to its taxonomy, evolution, and degradation potential.

Results and Discussion

A total of 6.8 Gbp data was generated to assemble the complete genome of B. diminuta. The scaffold level assembly contained 28 scaffolds with N50 of 1,786,567 bp. These scaffolds were further merged to obtain three super scaffolds using data generated from a mate-pair library. The super scaffolds were circularized by manually generating sequence for the DNA, amplified using primers specific to the right and left flanks of the assembled scaffold sequences. The largest super scaffold with a length of 4,147,822 bp is regarded as the chromosome sequence of B. diminuta (fig. 1A). The other two scaffolds gave circular DNA molecules with a size of 65,908 bp (fig. 1B) and 30,654 bp (fig. 1C), respectively. The 65,908 bp circular sequence matched perfectly with the physical map and partial sequence of pCMS1, a previously reported indigenous plasmid of B. diminuta (Pandeeti et al. 2011). However, the second circular DNA showed no complete similarity to any other

© The Author(s) 2016. Published by Oxford University Press on behalf of the Society for Molecular Biology and Evolution.

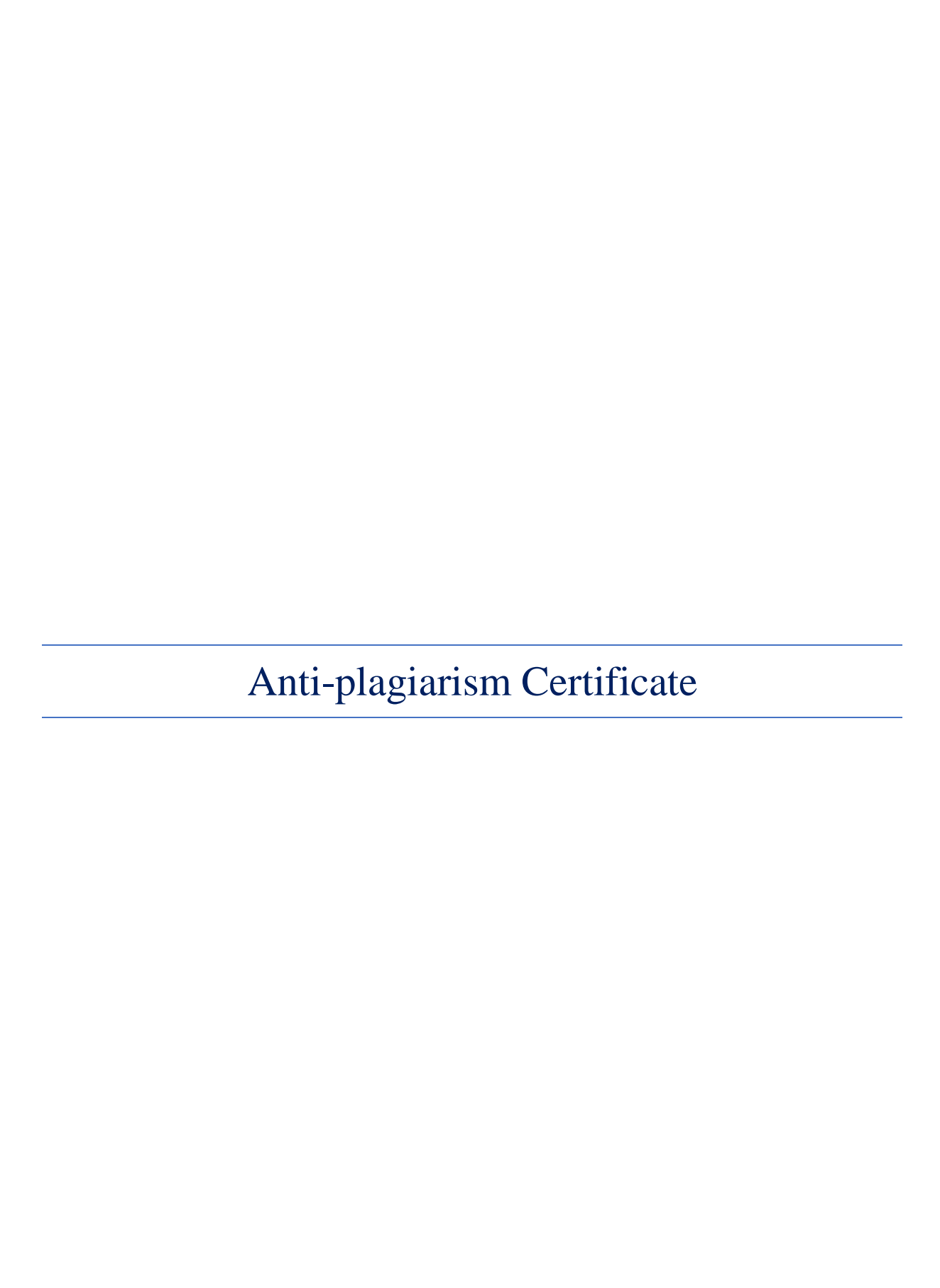
This is an Open Access article distributed under the terms of the Creative Commons Attribution Non-Commercial License (http://creativecommons.org/licenses/by-nc/4.0/), which permits non-commercial re-use, distribution, and reproduction in any medium, provided the original work is properly cited. For commercial re-use, please contact journals.permissions@oup.com

¹Department of Animal Biology, School of Life Sciences, University of Hyderabad, Hyderabad, India

²National Institute of Animal Biotechnology, Hyderabad, India

[†]These authors contributed equally to this work.

^{*}Corresponding authors: E-mails: sdsl@uohyd.ernet.in; siddavattam@gmail.com.



Four component Ton-Complex in Sphingobium fuliginis ATCC 27551: Role of Organophosphate hydrolase in transport of Ferric Enterobactin

by Hari Parapatla

Submission date: 10-Jun-2020 01:32PM (UTC+0530)

Submission ID: 1341196851

File name: HARI -Thesis for plagiarism-converted.pdf (423.3K)

Word count: 18630

Character count: 100950

Four component Ton-Complex in Sphingobium fuliginis ATCC 27551: Role of Organophosphate hydrolase in transport of Ferric Enterobactin

	Jiobaotiii				
ORIGINA	ALITY REPORT				
90 SIMILA	% ARITY INDEX	5% INTERNET SOURCES	7% PUBLICATIONS	4% STUDENT PAPERS	
PRIMAR	RY SOURCES				_
1	febs.onlin	nelibrary.wiley.co	om	2	%
2	structure organoph	ash Pandey. "mf modulates the tr nosphate hydrola r Biology Report	ranslation of se (OPH) in E	1	%
3	www.jbc. Internet Source			<1	%
4	www.tan	dfonline.com		<1	%
5	Hampapa Dayanan hydrolase targeted	y Gudla, Gurupra athalu Adimurty I da Siddavattam. e interacts with T to the membrane bB/ExbD comple	Nagarajaram, "Organophos on componer only in the p	sphate its and is resence	%

Miguel Á. Valderrama-Gómez, Rebecca A. Schomer, Michael A. Savageau, Rebecca E. Parales. "TaxisPy: A Python-based software for the quantitative analysis of bacterial chemotaxis", Journal of Microbiological Methods, 2020

Publication

32	d-nb.info Internet Source	<1%
33	Submitted to University of Birmingham Student Paper	<1%
34	Submitted to National University of Singapore Student Paper	<1%
35	"Microbial Transport Systems", Wiley, 2001	<1%
36	bmcmicrobiol.biomedcentral.com Internet Source	<1%
37	www.embopress.org Internet Source	<1%

Exclude quotes

On

On

Exclude matches

< 14 words

Exclude bibliography